Universität Rostock Traditio et Innovatio

Verification of nonclassicality in phase space

Dissertation

zur Erlangung des akademischen Grades
doctor rerum naturalium (Dr. rer. nat.)
der Mathematisch-Naturwissenschaftlichen Fakultät
der Universität Rostock

vorgelegt von
Thomas Kiesel, geb. am 07.02.1983 in Wismar
aus Rostock

Rostock, 29. Juni 2011

urn:nbn:de:gbv:28-diss2011-0145-7

Gutachter: Prof. Dr. Werner Vogel, Universität Rostock
Prof. Dr. John Klauder, University of Florida
Prof. Dr. Adam Miranowicz, University Poznań

Tag der Verteidigung: 12. Oktober 2011

Abstract

Nonclassicality has been introduced to examine the question whether experimental observations can be explained within a classical physical theory. In quantum optics, it is defined as the failure of the so-called Glauber-Sudarshan quasiprobability to be interpreted as a classical probability density. Although this definition has been accepted for several decades, there has been a lack of simple and complete criteria to check whether a given quantum state of light is nonclassical. In this thesis, the experimental use of some nonclassicality criteria is examined. Then, so-called nonclassicality quasiprobabilities are introduced, which allow a complete investigation of nonclassicality of an arbitrary quantum state in a simple manner. Their theoretical background is carefully elaborated, and their use is demonstrated with experimental data. Finally, some issues of the relation between nonclassicality and the special effect of entanglement are discussed, again with the application of experimental measurements.

Zusammenfassung

Der Begriff der Nichtklassizität wurde eingeführt, um Antworten auf die Frage zu finden, ob bestimmte experimentelle Ergebnisse noch mit einer klassischen physikalischen Theorie erklärt werden können. In der Quantenoptik ist Nichtklassizität dadurch definiert, dass die sogenannte Glauber-Sudarshan Quasiverteilung nicht mehr die Eigenschaften einer klassischen Wahrscheinlichkeitsverteilung erfüllt. Obwohl dieses Phänomen bereits seit einigen Jahrzehnten diskutiert wird, fehlten immer noch einfache Kriterien, mit denen man die Frage der Nichtklassizität für einen gegebenen Quantenzustand des Lichts vollständig beantworten kann. In der vorliegenden Dissertation werden einige Kriterien für Nichtklassizität auf ihre experimentelle Anwendbarkeit untersucht. Dann werden sogenannte Nichtklassizitäts-Quasiverteilungen eingeführt, die eine vollständige Untersuchung der Nichtklassizität eines beliebigen Quantenzustands mit einfachen Mitteln erlauben. Ihre theoretischen Grundlagen werden sorgfältig ausgearbeitet, und die Praktikabilität der Methode wird mit experimentell vermessenen Zuständen unter Beweis gestellt. Am Ende werden einige Zusammenhänge zwischen Nichtklassität und ihrem weit verbreiteten Spezialfall, der Verschränkung, diskutiert, wobei ebenfalls experimentelle Daten geeigneter Zustände verwendet werden.

Contents

Part I.

Dissertation thesis

1. Introduction

What is the difference between classical physics and the quantum world? Is it necessary to apply quantum mechanics to describe the behavior of matter and light? Do we have to discuss fields of light, which are not in a specific state, but in a superposition of many different states? Or is it possible to develop a theory, founded on classical electrodynamics and supplemented with a statistical framework, which also describes all experimental phenomena? These questions have been of great interest from the early rise of quantum theory, since they are related to our deep understanding of physics. For instance, we may hardly imagine Schrödingers cat, which is supposed to be in a superposition of two states, "dead" or "alive", but does it already mean that it is impossible to describe this situation in terms of classical physics?

In quantum optics, these issues are closely related to the notion of nonclassicality. Expressing it in a simple way, a nonclassical state is a state of the optical field of light, whose properties cannot be fully described in terms of classical electrodynamics. More precisely, these properties are correlation functions of the electromagnetic field, which can be measured with specific optical devices. If one is not able to derive these outcomes of the measurement from classical theory, the state must have some typically quantum properties. Hence, quantum optical methods are necessary for its characterization.

The term nonclassicality has been defined decades ago by Titulaer and Glauber [1] as the failure of the so-called Glauber-Sudarshan P function [2, 3] to exhibit the properties of a classical probability density. They have seen that the P function can be formally used as probability density to calculate expectation values of quantum optical observables, but may have negativities, which is impossible for a probability density. Furthermore, they showed that nonclassical states possess certain field correlation functions, which can be measured in experiments, but not explained by classical physics. Therefore, nonclassicality is a signature of quantumness.

Although this definition is known for several decades, its practical application is difficult, since the Glauber-Sudarshan P function is highly singular for many states, which prevents it from experimental reconstruction. To overcome this problem, many different signatures of nonclassicality have been derived, such as squeezing [4] or antibunching [5]. However, they only provide sufficient criteria for a state to be nonclassical. On the contrary, there are also sets of complete criteria of nonclassicality, which are based on determinants of moments [6] or characteristic functions of the state [7]; but these criteria are based on infinite hierarchies of in-

equalities, which cannot be checked all in practice. Therefore, there existed a lack of a complete, but still simple criterion for the nonclassicality of a quantum state.

The main goal of this thesis is to tackle this problem. Our solution is the introduction of so-called nonclassicality probabilities, which overcome the singularities of the P function, but indicate nonclassical effects by negativities. We show that it is sufficient to equip the nonclassicality quasiprobability with a single real width parameter in order to derive a complete criterion for the verification of nonclassicality. In this sense, our criterion is similar to the original definition. Moreover, the nonclassicality quasiprobabilities are designed to be accessible from experimental data, and their application is demonstrated in this work.

For this purpose, we begin with an introduction to phase-space methods in quantum optics. These are necessary for the definition of nonclassicality. After a review of some of the previously known nonclassicality criteria and an examination of their experimental application, we proceed with the reconstruction of the P function of a nonclassical state, which is approximately possible for certain states. Then we introduce the concept of nonclassicality quasiprobabilities, which overcomes problems of the previous approaches, and demonstrate their experimental applicability.

At the end of this thesis, we make a small excursion to the verification of entanglement. This is a special nonclassical phenomenon of particular interest, but has to be treated in a completely different manner. This work provides some additional investigation of the features of nonclassicality and the relation between nonclassicality and entanglement.

2. Phase space methods in quantum mechanics

We start our considerations with a general introduction into the phase-space formalism of quantum mechanics. We begin with a short description of coherent states, which provide the basis for phase-space functions. Then we explain the definition and use of symbols, which are complex-valued functions representing the quantum mechanical operators. The Glauber-Sudarshan P function, being the key for the definition of nonclassicality, is a special symbol of the density operator of a quantum state. Finally, we conclude with some remarks on the experimental reconstruction of phase-space functions of the density operator in order to show that these theoretical concepts have important consequences for practical applications. We note that there is a list of frequently used symbols at the end of this thesis, which shall help the reader to follow the notation.

2.1. Coherent states

The electromagnetic field of a single optical mode is described as a quantum mechanical harmonic oscillator. Its description in phase space is founded on a particular set of states, the prominent coherent states $|\alpha\rangle$, which are parameterized by a complex number α. Formally, they can be introduced as the eigenstates of the annihilation operator,

$$\hat{a}\,|\alpha\rangle = \alpha\,|\alpha\rangle\,. \tag{2.1}$$

These states are of particular relevance, since they are seen as the closest analogues to the classical states of the oscillator: the absolute value of α represents the amplitude of the expectation value of the position or field strength oscillation, while its argument describes the relative phase. The coherent states satisfy a resolution of unity,

$$\frac{1}{\pi}\int d^2\alpha\,|\alpha\rangle\,\langle\alpha| = \hat{I}, \tag{2.2}$$

which allows us to represent all pure states in terms of coherent states. However, even each mixed state, described by a density operator $\hat{\rho}$, can be written as a linear combination of coherent state projectors,

$$\hat{\rho} = \int d^2\alpha P(\alpha)\,|\alpha\rangle\,\langle\alpha|\,. \tag{2.3}$$

The function $P(\alpha)$ is referred to as Glauber-Sudarshan P function and plays the key role in the discussion of nonclassicality. To go more into detail, we need some knowledge about the so-called Weyl quantization.

2.2. Weyl symbols of operators

General quantum mechanical states are represented by a positive semidefinite density operator $\hat{\rho}$, whose trace is normalized to 1. Furthermore, observables are commonly represented by Hermitian operators $\hat{A}$, and their expectation values are given by

$$\langle \hat{A} \rangle = \mathrm{Tr}\left\{ \hat{\rho}\hat{A} \right\}. \tag{2.4}$$

For practical calculations, we may represent these operators in a particular basis, e.g. the basis of photon number states (also referred to as Fock states). In this case, the operators are described as complex infinite dimensional matrices.

In this thesis, it is more convenient to work in the Weyl quantization [8, 9]. We start from the creation and annihilation operators $\hat{a}^\dagger$ and $\hat{a}$, satisfying the commutation relations $[\hat{a}, \hat{a}^\dagger] = \hat{1}$. With these operators, we can define the displacement operator

$$\hat{D}(\beta) = e^{\beta\hat{a}^\dagger - \beta^*\hat{a}}, \tag{2.5}$$

which depends on a complex variable β. Now we assign a function $\Phi_W^{\hat{A}}(\beta)$ to a given operator $\hat{A}$ by the relation

$$\Phi_W^{\hat{A}}(\beta) = \mathrm{Tr}\left\{ \hat{A}\hat{D}(\beta) \right\}. \tag{2.6}$$

This function is referred to as characteristic function of the Wigner function (indicated by the index W), assigned to the operator $\hat{A}$. If we consider the characteristic function of the density operator, we will omit the superscript $\hat{A}$. The inverse relation is given by

$$\hat{A} = \frac{1}{\pi} \int d^2\beta \, \Phi_W^{\hat{A}}(\beta) \, \hat{D}(-\beta). \tag{2.7}$$

In this way, all operators are represented by complex-valued characteristic functions. To be complete, we further need to express expectation values in terms of characteristic functions. Inserting the relation (2.7) for both density operator $\hat{\rho}$ and observable $\hat{A}$ into Eq.(2.4), we obtain

$$\langle \hat{A} \rangle = \frac{1}{\pi^2} \int d^2\beta \, \Phi_W(\beta) \int d^2\gamma \, \Phi_W^{\hat{A}}(\gamma) \mathrm{Tr}\left\{ \hat{D}(-\beta)\hat{D}(-\gamma) \right\}. \tag{2.8}$$

By using the orthogonality relation

$$\mathrm{Tr}\left\{ \hat{D}(\beta)\hat{D}(\gamma) \right\} = \pi\delta(\beta + \gamma) \tag{2.9}$$

and knowing that $\Phi_W(-\beta) = \Phi_W^*(\beta)$, we arrive at

$$\langle \hat{A} \rangle = \frac{1}{\pi} \int d^2\beta \Phi_W^*(\beta) \Phi_W^{\hat{A}}(\beta). \tag{2.10}$$

In this way, we are able to formulate quantum mechanics completely in terms of characteristic functions.

We may also consider the Fourier transform of the characteristic function, defined as

$$W_{\hat{A}}(\alpha) = \frac{1}{\pi^2} \int d^2\beta e^{\alpha\beta^* - \alpha^*\beta} \Phi_W^{\hat{A}}(\beta). \tag{2.11}$$

This function is referred to as Weyl symbol of the operator $\hat{A}$. Furthermore, the symbol of the density operator is referred to as Wigner function of the state. This function is one of the commonly used phase-space representations of a quantum state. It contains complete information as its characteristic function, and can therefore be used to fully characterize a quantum state. It can also be used to calculate expectation values: Due to Parseval's theorem [10], one can show that

$$\langle \hat{A} \rangle = \pi \int d^2\alpha W(\alpha) W_{\hat{A}}(\alpha). \tag{2.12}$$

The Wigner function is a special case of a quasiprobability. It satisfies the normalization $\int d^2\alpha W(\alpha) = 1$ and can be used to determine expectation values like a classical probability distribution, but may attain negative values. This violation of the properties of a classical probability is already an indicator of nonclassicality. However, one may define quasiprobabilities also in different ways. Therefore, it is (up to this point) not clear which quasiprobability shall be used to define nonclassicality.

2.3. Glauber-Sudarshan- and generalized quasiprobabilities

The ambiguity of the definition of a quasiprobability is caused by the fact that the operators $\hat{a}$ and $\hat{a}^\dagger$ do not commute. More precisely, one can use the Baker-Campbell-Hausdorff theorem [11] to show that

$$e^{\beta\hat{a}^\dagger - \beta^*\hat{a}} = e^{\beta\hat{a}^\dagger} e^{-\beta^*\hat{a}} e^{-|\beta|^2/2} = e^{-\beta^*\hat{a}} e^{\beta\hat{a}^\dagger} e^{|\beta|^2/2}. \tag{2.13}$$

Hence, if we use the density operator $\hat{\rho}$ in Eq. (2.6) and the normally ordered form of the kernel , $e^{\beta\hat{a}^\dagger} e^{-\beta^*\hat{a}}$ – where all creation operators $\hat{a}^\dagger$ are written to the left of all annihilation operators $\hat{a}$ – we arrive at a different characteristic function, representing the same state:

$$\Phi(\beta) = \mathrm{Tr}\left\{\hat{\rho} e^{\beta\hat{a}^\dagger} e^{-\beta^*\hat{a}}\right\} = \Phi_W(\beta) e^{|\beta|^2/2}. \tag{2.14}$$

This quantity is the characteristic function of the P function. Since we use this function frequently, we omit a possible index P. The Fourier transform defines the Glauber-Sudarshan P function,

$$P(\alpha) = \frac{1}{\pi^2} \int d^2\beta e^{\alpha\beta^* - \alpha^*\beta} \Phi(\beta). \tag{2.15}$$

One can show that the P function is suitable to write the density operator of the quantum state as a formal mixture of coherent states [2, 3],

$$\hat{\rho} = \int d^2\alpha P(\alpha) \left|\alpha\right\rangle \left\langle\alpha\right| . \tag{2.16}$$

As already mentioned, this relation is the foundation of nonclassicality. However, the P function may not be well-behaved, since it may have singularities of δ-type and even worse. These obstacles prevent it from simple practical application.

One may generalize the notion of quasiprobability distributions by filtering the characteristic function in the form

$$\Phi_\Omega(\beta) = \Phi(\beta)\Omega(\beta). \tag{2.17}$$

The filter function $\Omega(\beta)$ shall be differentiable, satisfy a normalization condition $\Omega(0) = 1$ and have no zeros. Its Fourier transform,

$$P_\Omega(\alpha) = \frac{1}{\pi^2} \int d^2\beta e^{\alpha\beta^* - \alpha^*\beta} \Phi_\Omega(\beta), \tag{2.18}$$

is a quasiprobability distribution in the sense of Agarwal and Wolf [12][1]. They have shown that the filter $\Omega(\beta)$ is related to a specific ordering scheme of the creation and annihilation operators. For instance, if we choose $\Omega(\beta) = e^{-|\beta|^2/2}$, we obtain the characteristic function of the Wigner function, cf. Eq. (2.14), which is the expectation value of the displacement operator $\hat{D}$ in symmetric ordering, cf. Eq. (2.6). Moreover, for $\Omega(\beta) = e^{-|\beta|^2}$, we find the characteristic function of the Husimi-Q-function. In general, for $\Omega(\beta) = e^{(s-1)|\beta|^2/2}$, we obtain the family of s-parameterized quasiprobability distributions of Cahill and Glauber [13].

If we want to calculate expectation values with the help of quasiprobability distributions, we have to modify both the characteristic function of the state and the observable. We rewrite Eq. (2.10) in the following form:

$$\langle\hat{A}\rangle = \frac{1}{\pi} \int d^2\beta \left[\Phi_W(\beta) e^{|\beta|^2/2} \Omega(\beta)\right]^* \times \left[\Phi_W^{\hat{A}}(\beta) e^{-|\beta|^2/2} \Omega^{-1}(\beta)\right] . \tag{2.19}$$

[1] We define the filter $\Omega(\beta)$ slightly different from the one by Agarwal and Wolf, $\Omega_{\mathrm{AW}}(\beta, \beta^*)$. The relation between them reads as $\Omega(\beta) = e^{-|\beta|^2/2} \Omega_{AW}^{-1}(\beta, \beta^*)$. The reason for doing so is that the P function plays the central role for the discussion of nonclassicality, while Agarwal and Wolf take the symmetric ordering as the basis for defining their quasiprobabilities.

The first factor is exactly the filtered characteristic function $\Phi_\Omega(\beta)$, see Eq. (2.14) and Eq. (2.17). The second factor defines a new characteristic function of the operator $\hat{A}$,

$$\Phi^{\hat{A}}_{\tilde{\Omega}}(\beta) = \Phi^{\hat{A}}_W(\beta) e^{-|\beta|^2/2} \Omega^{-1}(\beta), \tag{2.20}$$

which is well-defined since $\Omega(\beta)$ is nonzero for all β. For instance, if we want to calculate expectation values with the characteristic function of the P function of a state, i.e. $\Omega(\beta) \equiv 1$, we need to use the characteristic function of the Q function $\Phi^{\hat{A}}_{\tilde{\Omega}}(\beta) = \Phi^{\hat{A}}_W(\beta) e^{-|\beta|^2/2}$ of the observable $\hat{A}$. Due to Parseval's theorem, this holds not only for the characteristic functions, but for the corresponding quasiprobability distributions as well.

The introduction of general quasiprobabilities may look like a theorist's playground without any further use. In the past, there has already been established a relation between the s-parameter of the Cahill-Glauber quasiprobabilities and the quantum efficiency η in a measurement [11]. In this thesis, the general quasiprobabilities provide the foundation of the so-called nonclassicality quasiprobabilities, which we are going to define in Chap. 4. The P function plays the central role in the discussion of nonclassicality, but its singularities make it impossible for experimental reconstruction for a large class of states. To circumvent this problem, we will filter the characteristic function of the P function in the form (2.17), such that the resulting quasiprobability becomes a regular function, but resembles the properties of the P function we are interested in. Since it will be chosen to be well-behaved, it can be reconstructed from experimental data.

2.4. Experimental reconstruction of quasiprobabilities

One of the main goals of this work is to connect the investigation of nonclassicality to experimental data. Therefore, it is useful to describe a scheme how one can reconstruct the quasiprobabilities from measurements. Optical quantum tomography is based on balanced homodyne detection [14]: the signal is coherently superposed with a local oscillator in a coherent reference state at a symmetric beam splitter, and the two output fields are sent to photodetectors. It can be shown that the difference of the photocurrents is proportional to the quadrature operator $\hat{x}(\varphi)$ of the optical field, where the phase φ equals to the difference of the phases of the local oscillator and the signal. Measuring large sets of quadratures $\{x_j(\varphi_k)\}_{j=1}^N$ at different phases φ_k, one obtains information about the quadrature distributions $p(x;\varphi)$ [15]. The knowledge of the quadrature distributions for all phases in $[0,\pi)$ delivers full information about the quantum state [16]. For a review, see [17].

Hence, the question arises how one can obtain the quasiprobabilities from quadrature distributions. The relations between these quantities are shown in Fig. 2.1. The measured quadrature distributions $p(x;\varphi)$ are located at the upper left corner of the scheme. In the upper line, we have the quasiprobabilities, such as the

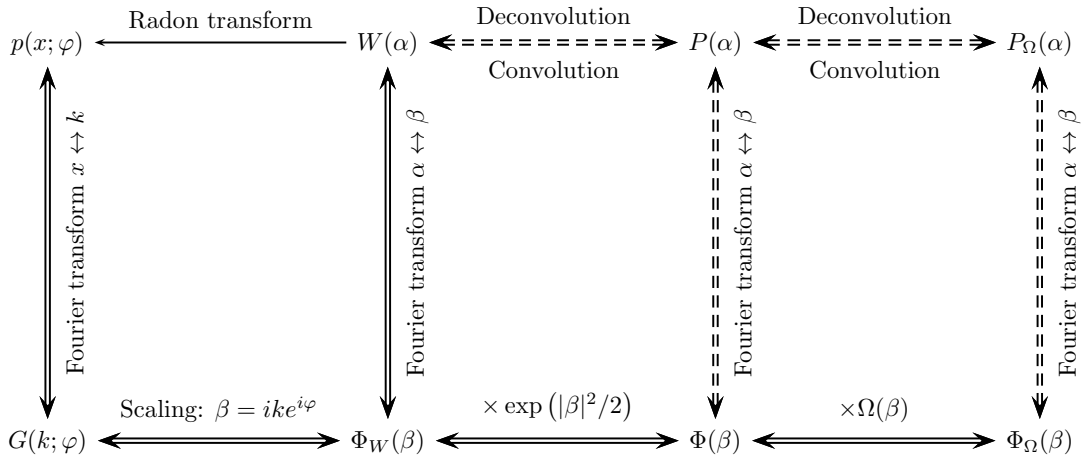

Figure 2.1.: Relations between the quadrature distribution $p(x;\varphi)$, quasiprobability distributions and their characteristic functions. If an arrow is dashed, one of the connected quantities may be irregular.

Wigner function $W(\alpha)$, the Glauber-Sudarshan P function $P(\alpha)$ and the generalized quasiprobabilities $P_\Omega(\alpha)$. The relations between them are given by different integral transforms, which cannot be inverted easily. In particular, the connection between $p(x;\varphi)$ and $W(\alpha)$ is not obvious.

In the lower line, we find the corresponding characteristic functions, given as the Fourier transforms of the upper quantities. The relations between these quantities are quite simple, we only have rescaling of arguments or multiplication with specific factors. Therefore, it is convenient to calculate the characteristic function $G(k;\varphi)$ of the quadrature distribution and follow the scheme to the quasiprobabilities we are interested in. For instance, we obtain the Wigner function by calculating $\Phi_W(\beta)$ by rescaling of $G(k;\varphi)$ and computing the Fourier transform of $\Phi_W(\beta)$. This procedure is commonly referred to as inverse Radon transform, being one standard procedure of quantum tomography [16].

The only problem which we might face is that we cannot perform the Fourier transform from a characteristic function to a quasiprobability, namely if the former function is not integrable and the latter cannot be understood as a well-behaved function. For the Wigner function, this is never the case, but for the P function this will happen for many states. In the present work, we will therefore look at generalized quasiprobabilities, whose filter $\Omega(\beta)$ regularizes the P function, but preserves as much information about nonclassicality as possible.

In practice, it is not necessary to start the reconstruction with the quadrature distributions $p(x;\varphi)$ when one has measured a set of N quadratures points $\{x_j(\varphi)\}_{j=1}^N$.

Let us look at the definition of the characteristic function $G(k;\varphi)$:

$$G(k;\varphi) = \int_{-\infty}^{\infty} p(x) e^{ikx}\, dx. \tag{2.21}$$

This quantity may be interpreted as the expectation value of the function e^{ikx} with respect to x. Therefore, we might estimate it by the empirical mean [18],

$$\overline{G}(k;\varphi) = \frac{1}{N} \sum_{j=1}^{N} e^{ikx_j(\varphi)}. \tag{2.22}$$

The bar indicates that this quantity is an estimate of the expectation value (2.21). This method has the advantage that we do not have to care about systematic errors due to binning the data points $x_j(\varphi)$ in certain classes, when we estimate the quadrature distribution $p(x,\varphi)$. Furthermore, we can also estimate its variance empirically,

$$\sigma^2\{\overline{G}(k;\varphi)\} = \frac{1}{N}\left(1 - |\overline{G}(k;\varphi)|^2\right). \tag{2.23}$$

Since $0 \leq |\overline{G}(k;\varphi)|^2 \leq 1$, we find an upper bound $\sigma^2\{\overline{G}(k;\varphi)\} \leq \frac{1}{N}$. Furthermore, the variance also approaches this bound for large k, since $G(k;\varphi) \to 0$ for $k \to \infty$.

Based on the sampling formula (2.22) and its statistical uncertainty (2.23), we are also able to estimate the uncertainties of the characteristic functions $\Phi_\Omega(\beta)$ and the corresponding quasiprobabilities $P_\Omega(\alpha)$. The former are basically the characteristic function $\overline{G}(k;\varphi)$, with rescaled argument and multiplied with some factor. Therefore, their variance can be obtained by multiplying Eq. (2.23) with $\left|e^{|\beta|^2/2}\Omega(\beta)\right|^2$,

$$\sigma^2\{\overline{\Phi}_\Omega(\beta)\} = \frac{1}{N}\left(|\Omega(\beta)|^2 e^{|\beta|^2} - |\overline{\Phi}_\Omega(\beta)|^2\right). \tag{2.24}$$

Furthermore, the map between a characteristic function and the corresponding quasiprobability is just a linear one, allowing direct error propagation. This might be more involved, but is still feasible with standard methods. For more information about the estimation of characteristic functions and quasiprobabilities, see [19] and [TK1].

Summary

Up to now, we have introduced the phase-space description of the harmonic oscillator, as it is frequently used in quantum optics. We have seen that it is possible to represent the quantum mechanical operators in terms of phase space functions, which, however, may show strongly singular behavior. As we will show in the next chapter, the phase-space representation of quantum mechanics serves as the foundation for the investigation of nonclassical effects, and the Glauber-Sudarshan P function provides the link between classical and quantum optics.

3. Nonclassicality of the harmonic oscillator

Nonclassicality is an interesting topic in quantum mechanics, since it provides some information about the question if one can describe a physical system in terms of classical physical theories, say Newtonian mechanics or Maxwell's electrodynamics. However, we have to say precisely what we mean when we talk about nonclassicality. For this purpose, we first define what a classical state of a quantum optical system should be, and define nonclassical states simply as being not a classical state. Then, we continue with a short discussion of criteria, which allow to distinguish between classical and nonclassical states. We will show that there are criteria which are simple, but not necessarily satisfied by all nonclassical states, and there are criteria which are necessary and sufficient, but practically involved. Some of these criteria and their applicability will be compared with the help of experimental data. At the end, we will examine the role of quasiprobabilities in the discussion of nonclassicality both theoretically and experimentally, again by application to experimental data of a measured quantum state.

3.1. Definition of nonclassicality

In quantum optics, the coherent states $|\alpha\rangle$ are seen as the pure states which resemble the behavior of a classical oscillator best. First, the expectation values of position and momentum operator oscillate precisely like a classical oscillator with amplitude $|\alpha|$ and relative phase $\arg(\alpha)$. Second, the variances of position and momentum, which are introduced by quantum mechanics, are minimal and satisfy the lower bound of Heisenberg's uncertainty relation. Consequently, the relative uncertainty of position and momentum vanishes in the classical limit $|\alpha| \to \infty$. In contrast, the eigenstates of the harmonic oscillator, being the states with fixed photon number, do not show any oscillation in the position expectation values, independently of their energy. The latter situation is unknown in classical physics.

When we have identified the coherent states as classical, the question arises how we can define classical states in general. If we only admit statistical superpositions of coherent states (but not quantum mechanical superpositions), the density

operator is given in the form

$$\hat{\rho}_{\mathrm{cl}} = \int d^2\alpha \, P_{\mathrm{cl}}(\alpha) \, |\alpha\rangle \langle\alpha| \,, \tag{3.1}$$

with $P_{\mathrm{cl}}(\alpha)$ being a classical probability distribution, satisfying $\int d^2\alpha \, P(\alpha) = 1$ and $P(\alpha) \geq 0$. However, due to the overcompleteness of the coherent states, one is able to write the density operator of *any* state in this form,

$$\hat{\rho} = \int d^2\alpha \, P(\alpha) \, |\alpha\rangle \langle\alpha| \,, \tag{3.2}$$

cf. Eq. (2.16), if we relax both the conditions of nonnegativity and regularity of $P(\alpha)$. Therefore, we call any state, whose P function exhibits all properties of a classical probability distribution, as classical. Conversely, all other states are referred to as nonclassical [1].

This definition of nonclassicality is highly self-consistent. First, we may ask which pure states are nonclassical in the sense of this definition. Hillery showed that these are only coherent states, from which we started the discussion of nonclassicality [20]. In this sense, any state which has to be described as a quantum-mechanical superposition of coherent states, is nonclassical. In this way, nonclassicality is a clear indicator of quantum mechanical superpositions of states. Second, the set of classical states is convex: If we consider a statistical superposition of two classical states, the resulting state still remains classical. In other words, classical statistics does not introduce nonclassicality into the state. Third, if one measures correlation functions of the electromagnetic field, one may derive them from a statistical superposition of classical electromagnetic waves with complex amplitudes α, if the underlying quantum state is classical; and the P function plays the role of the corresponding statistical probability density.

From the Eqs. (2.14) and (2.15), the P function of an arbitrary quantum state is uniquely defined.[1] However, the practical application of the definition of nonclassicality is complicated due to the fact that the P function may be highly singular. Therefore, various criteria to check nonclassicality have been developed.

3.2. Nonclassicality criteria

3.2.1. Nonclassicality witnesses

A large class of nonclassicality tests is based on so-called nonclassicality witnesses [6, 22]: Let $\hat{A}$ be an operator, whose expectation value is nonnegative for all classical

[1] In the set of ultradistributions, where the Fourier transform is maybe not bijective anymore, one may still find other P functions for the same state, but they only differ by the addition of highly singular distributions. However, this does not affect any of the statements in this thesis. For more details, see [21].

states $\hat{\rho}_{\mathrm{cl}}$,

$$\langle \hat{A} \rangle_{\mathrm{cl}} = \mathrm{Tr}\left\{ \hat{\rho}_{\mathrm{cl}} \hat{A} \right\} \geq 0. \tag{3.3}$$

If we now calculate or measure the expectation value of $\hat{A}$ for some specific state $\hat{\rho}$ and find a negative result,

$$\langle \hat{A} \rangle = \mathrm{Tr}\left\{ \hat{\rho} \hat{A} \right\} < 0, \tag{3.4}$$

the state $\hat{\rho}$ must be nonclassical. In this sense, the operator $\hat{A}$ witnesses the nonclassicality of the state. More generally, if we consider the set of expectation values $I_{\hat{A},\mathrm{cl}}$ among all classical states,

$$I_{\hat{A},\mathrm{cl}} = \left\{ \mathrm{Tr}\left\{ \hat{\rho}_{\mathrm{cl}} \hat{A} \right\} \ : \ \hat{\rho}_{\mathrm{cl}} \ \text{ is classical} \right\}, \tag{3.5}$$

and observe an expectation value $\mathrm{Tr}\left\{ \hat{\rho} \hat{A} \right\}$ for a state $\hat{\rho}$, which is not in this set of classically allowed values,

$$\mathrm{Tr}\left\{ \hat{\rho} \hat{A} \right\} \notin I_{\hat{A},\mathrm{cl}}, \tag{3.6}$$

then the state $\hat{\rho}$ is nonclassical.

This structure can be found in many nonclassicality criteria. For instance, squeezing of the field quadrature $\hat{x}$ is a typical signature of nonclassicality [4]. For all classical states, the variance of $\hat{x}$ is greater or equal than the variance of the vacuum state:

$$V_x = \langle (\hat{x} - \langle \hat{x} \rangle)^2 \rangle_{\mathrm{cl}} \geq \langle (\hat{x} - \langle \hat{x} \rangle)^2 \rangle_{\mathrm{vac}} \equiv V_{\mathrm{vac}} \tag{3.7}$$

Therefore, if a quadrature is squeezed, i.e. its variance is below the variance of vacuum, the state is nonclassical. This criterion has been applied in experiments numerous times, the first demonstration can be found in [23]. In [24, 25], a generalized notion of squeezing has been proposed, the so-called higher-order squeezing: A state is nonclassical if the number

$$q_{2N} = \frac{\langle (\hat{x} - \langle \hat{x} \rangle)^{2N} \rangle}{(2N-1)!!} - V_{\mathrm{vac}}^N \tag{3.8}$$

is negative.

Further nonclassical effects, which are based on inequalities for expectation values, are the Sub-Poissonian statistics and photon antibunching. The former occurs when the variance of the photon statistics is less than the mean photon number, $\langle (\hat{n} - \langle \hat{n} \rangle)^2 \rangle < \langle \hat{n} \rangle$ [26]. In photon antibunching, one finds that the second-order intensity correlation, which can be measured in a Hanbury Brown-Twiss setup, is below its classically allowed value [5, 27, 28]. This effect can be frequently found in resonance fluorescence measurements and can be regarded as an experimental verification for the existence of a photon being a particle-like object.

The general form of nonclassicality witnesses can be found if we examine the relation between expectation values and the P function, see Eq. (2.19) with $\Omega(\beta) \equiv 1$ and $\Phi_W(\beta)e^{|\beta|^2/2} = \Phi(\beta)$:

$$\langle \hat{A} \rangle = \frac{1}{\pi} \int d^2\beta \Phi(\beta)^* \times \left[\Phi_W^{\hat{A}}(\beta) e^{-|\beta|^2/2} \right]. \tag{3.9}$$

The second factor is the characteristic function of the Q function of the operator $\hat{A}$. Due to Parseval's theorem, we may also write this equation with the P function itself:

$$\langle \hat{A} \rangle = \pi \int d^2\alpha P(\alpha) Q_{\hat{A}}(\alpha). \tag{3.10}$$

Now let us consider a nonnegative function $Q_{\hat{A}}(\alpha)$: If the state is classical, i.e. $P(\alpha)$ is nonnegative, then the expectation value of $\hat{A}$ is also nonnegative. However, if the state is nonclassical, i.e. the Glauber-Sudarshan P function may have some negativities, the expectation value may become negative. Hence, a nonnegative Q function may serve as a representation of a nonclassicality witness $\hat{A}$. It can be shown that the set of all operators, whose Q representation is the square of some polynomial, is already sufficient for testing the nonclassicality of an arbitrary quantum state in this way [22]. Furthermore, this is equivalent to the examination of normally ordered squares of operators: Starting from an operator $\hat{f}(\hat{a}, \hat{a}^\dagger)$, the squared operator $\hat{f}^\dagger(\hat{a}, \hat{a}^\dagger)\hat{f}(\hat{a}, \hat{a}^\dagger)$ is nonnegative. However, if all creation operators are sorted to the left of all annihilitation operators without respecting the commutation rules, we obtain a different, so-called normally ordered operator, denoted by $:\hat{f}^\dagger(\hat{a}, \hat{a}^\dagger)\hat{f}(\hat{a}, \hat{a}^\dagger):$. The expectation value of the latter can easily be calculated from the P function as

$$\langle : \hat{f}^\dagger(\hat{a}, \hat{a}^\dagger)\hat{f}(\hat{a}, \hat{a}^\dagger) : \rangle = \int d^2\alpha P(\alpha) |f(\alpha, \alpha)|^2. \tag{3.11}$$

Therefore, if this expectation value is negative, this is a clear signature of negativities in the P function, indicating nonclassicality [6].

A novel approach to the construction of nonclassicality witnesses is dedicated to the examination of probability distributions instead of expectation values [29, 30]. The idea is to set bounds on probabilities of certain outcomes, which are satisfied for all classical states, but violated by nonclassical ones. Since probabilities are calculated as expectation values of projection operators or positive operator valued measures, the underlying concept is comparable to the above considerations.

3.2.2. Matrices of moments and characteristic functions

A second class of nonclassicality criteria is based on the nonnegativity of a set of matrices. As an example, one of the first has been proposed in [31]: a state is

nonclassical if at least one of the matrices of normally ordered quadrature moments,

$$M^{(l)} = \begin{pmatrix} 1 & \langle: \hat{x} :\rangle & \dots & \langle: \hat{x}^{l-1} :\rangle \\ \langle: \hat{x} :\rangle & \langle: \hat{x}^2 :\rangle & \dots & \langle: \hat{x}^{l} :\rangle \\ \vdots & \vdots & \ddots & \vdots \\ \langle: \hat{x}^{l-1} :\rangle & \langle: \hat{x}^{l} :\rangle & \dots & \langle: \hat{x}^{2l-2} :\rangle \end{pmatrix}, \tag{3.12}$$

is not positive semidefinite. For instance, taking $l = 2$, we find for nonclassicality

$$\langle: \hat{x}^2 :\rangle - \langle: \hat{x} :\rangle^2 < 0, \tag{3.13}$$

which is equivalent to squeezing of the state. A generalization of this approach can be found in [32], where a necessary and sufficient hierarchy of inequalities for determinants of moments is developed. However, such hierarchies are constituted of an infinite number of inequalities, which makes it practically impossible to check completely if a state is classical or nonclassical. One may only conclude nonclassicality if one of these determinants is negative. Furthermore, the experimental application becomes complicated, since the expectation values may be easily measured, but the estimation of the significance of the negativity of a determinant becomes involved when the matrix becomes large.

Similar matrices can also be constructed for photon number distributions [33, 34] and their moments [35, 36]. If states are independent of phase, i.e. completely described by their photon number distribution, these criteria are necessary and sufficient. However, they also consist of an infinite hierarchy of inequalities, which can never be checked completely in practice.

A different approach considers the characteristic function of the P function, $\Phi(\beta)$. Due to a theorem of Bochner [37], a function $P(\alpha)$ exhibits all properties of a probability distribution, if and only if its characteristic function $\Phi(\beta)$ satisfies

1. $\Phi(0) = 1$,

2. $\Phi(-\beta) = \Phi^*(\beta)$, and

3. for all $N \in \mathbb{N}, (\beta_1, \dots \beta_N) \in \mathbb{C}^N$, the matrix

$$D^{(N)} = \begin{pmatrix} \Phi(\beta_1 - \beta_1) & \Phi(\beta_1 - \beta_2) & \dots & \Phi(\beta_1 - \beta_N) \\ \Phi(\beta_2 - \beta_1) & \Phi(\beta_2 - \beta_2) & \dots & \Phi(\beta_2 - \beta_N) \\ \vdots & \vdots & \ddots & \vdots \\ \Phi(\beta_N - \beta_1) & \Phi(\beta_N - \beta_2) & \dots & \Phi(\beta_N - \beta_N) \end{pmatrix} \tag{3.14}$$

is positive semidefinite [7].

The most simple, but nontrivial criterion can be obtained by checking if the determinant of $D^{(2)}$ is negative [38]. For a nonnegative P function, this leads to the following simple inequality

$$|\Phi(\beta)| \leq 1, \tag{3.15}$$

which has to be satisfied for all complex β. Conversely, if one finds one point β such that this inequality is violated, then the P function must have some negativities, and the corresponding quantum state is nonclassical. It turns out that this condition is already sufficient for the demonstration of nonclassicality of many states. For instance, nonclassicality of a statistical superposition of a single photon and a vacuum state has been verified by this condition in [18].

However, the examination of matrices with $N > 2$ turns out to be complicated. For single-photon added thermal states [33], this might be necessary since Eq. (3.15) is satisfied if the mean photon number is sufficiently large. It has been shown theoretically and experimentally that the determinant of $D^{(3)}$ shows negativities which indicates the nonclassicality of the state [39, 40]. However, this task can be cumbersome, since one has to search for violations by varying two complex parameter.

3.2.3. Comparison of different nonclassicality criteria

Now the question arises, which of such criteria may perform better than others in the experimental verification of nonclassicality. Of course, it is hard to give a general answer, and we are not sure if there exists a definite one which is valid at least for many kinds of states. However, for specific classes of states, one may get some more insight.

This has been done in [TK2]. We examined a class of quantum states, which appear in experiments for improving the sensitivity of gravitational wave detection [41, 42]. They are based on so-called squeezed vacuum states, whose Wigner function is simply Gaussian, characterized by some variances V_x and V_p and a phase angle φ, which specifies the orientation of the covariance ellipse in phase space. Since the state is squeezed, we have w.l.o.g. $V_x < V_{\mathrm{vac}}$, which is a clear signature of nonclassicality, see Eq. (3.7). Now we generate a mixture of these states by choosing the phase angle φ randomly, first Gaussian distributed with standard deviation σ, afterwards uniformly distributed in $[0, 2\pi)$. Due to this mixing, the squeezing vanishes if the phase noise is broad enough. This gives rise to the question if the state remains nonclassical, and how we can detect its nonclassicality. We compared the application of the q_{2n}-parameter (3.8), the nonnegativity of Agarwal's matrix (3.12) and the violation of the lowest order criterion on characteristic functions (3.15), and found that the state's nonclassical character can be demonstrated best by the last method. The numbers q_{2n} only indicate nonclassicality if we already observe squeezing, an effect which is due to the particular structure of our states.

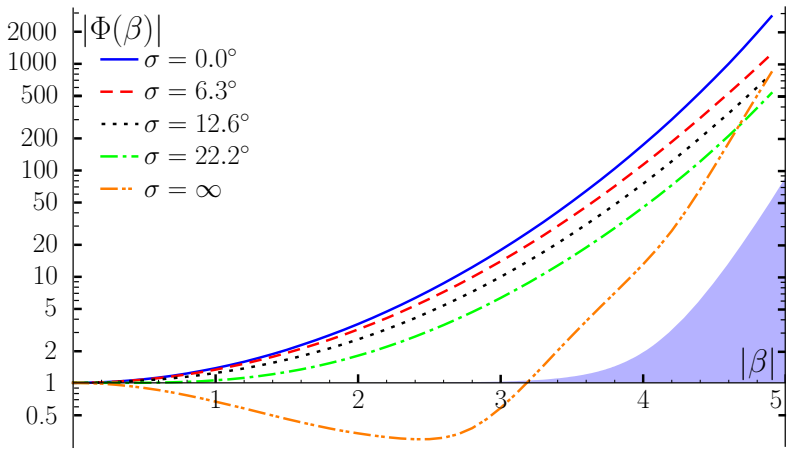

Figure 3.1.: Characteristic functions of different phase-diffused squeezed vacuum states. The parameter σ is the standard deviation of the Gaussian phase noise distribution, $\sigma = \infty$ refers to a uniform phase distribution. The shaded area corresponds to one standard deviation of the characteristic functions, resulting from the statistical uncertainties.

With Agarwal's matrices it is already possible to demonstrate nonclassicality beyond squeezing. However, characteristic functions are suitable for the detection of nonclassicality in all cases with good significance, see Fig. 3.1. Even if the state is completely phase randomized, nonclassical effects can be clearly observed. Furthermore, the violation of condition (3.15) serves as a simple tool to show theoretically that all states of this type are nonclassical.

3.2.4. Negativities of quasiprobabilities

So far, we have only discussed indirect criteria for the verification of nonclassicality. However, is it possible to demonstrate nonclassical effects with a quasiprobability representation of a quantum state, by showing that it cannot be interpreted as a classical probability density? As we have already mentioned, this is not possible with the P representation itself in general: For instance, looking at the characteristic functions of phase-diffused squeezed vacuum states in Fig. 3.1, it is obvious that the Fourier transform of these quantities cannot be a well-behaved function, since the characteristic functions are not integrable. But is there some different quasiprobability which may illustrate the nonclassical effects?

In literature, the s-parameterized quasiprobabilities play an important role [13]. In particular, the Wigner function [43] and the Husimi Q-representation [44] are discussed frequently, since they are always well-behaved functions which can be easily illustrated. However, the latter of both quantities, the Q function, is always nonnegative. Therefore it satisfies all requirements of a classical probability density

and is not of great use in the discussion of nonclassicality. The Wigner function is more interesting. Many nonclassical states have Wigner functions showing negativities, such as all photon number states [11]. It can also be shown that negativities of the Wigner function have their origin in negativities of the P function, therefore being a clear signature of nonclassicality [45]. Therefore, Wigner functions, which cannot be interpreted as classical probabilities, are often discussed in the context of nonclassicality, and have experienced numerous experimental investigations (see, for instance, [46]).

However, the negativity of the Wigner function is only sufficient for nonclassicality, but not necessary. Let us take the prominent squeezed states as an example: Although these states are nonclassical, their Wigner function is a Gaussian and hence nonnegative. Moreover, any of the s-parameterized quasiprobabilities is simply a Gaussian, provided that it is well-behaved. The nonclassical character of the squeezed state is only expressed in singularities of the P function, which can be formally written as

$$P_{\mathrm{sv}}(\alpha) = e^{-\frac{V_x-V_p}{8}\left(\frac{\partial^2}{\partial\alpha^2}+\frac{\partial^2}{\partial\alpha^{*2}}-2\frac{V_x+V_p-2}{V_x-V_p}\frac{\partial}{\partial\alpha}\frac{\partial}{\partial\alpha^*}\right)}\delta(\alpha). \tag{3.16}$$

Hence, the verification of nonclassicality of squeezed states by s-parameterized quasiprobabilities is impossible, since these functions are either Gaussian or highly singular and not accessible from experiment. This does not change if we statistically mix squeezed states, as we have done it in [TK2]. However, as we will show in the next chapter, one may find quasiprobabilities, which are suitable for the verification of nonclassicality of any nonclassical state, even for squeezed states.

Nevertheless, there are some specific nonclassical states whose P function does not show singularities. An important class are states which consist of photons being created on a thermal background with mean photon number $\bar{n}$. The most simple states of this type are single-photon added thermal states (SPATS), whose P function is given by

$$P(\alpha) = \frac{1}{\pi\bar{n}^3}\left[(1+\bar{n})|\alpha|^2-\bar{n}\right]e^{-|\alpha|^2/\bar{n}}. \tag{3.17}$$

They have already been generated frequently and have been subject of many investigations of nonclassicality [33, 40, 47]. Such states give rise to the question if their P function can be reconstructed from experimental data. A feasible method has been prepared in my diploma thesis [19] and published in [TK3]. The starting point is the reconstructed characteristic function $\Phi(\beta)$, which can be seen in Fig. 3.2 for two different states. Curve (a) belongs to a SPATS with $\bar{n} = 1.11$, prepared with a quantum efficiency of $\eta = 0.62$, the state (b) is a mixture of a SPATS with $\bar{n} = 3.71$ and $\eta = 0.62$ and a fraction of 19% thermal background. It can be seen that the characteristic functions of both states tend to zero for growing β. However, it is also obvious that the standard deviation of these quantities grows rapidly for large β.

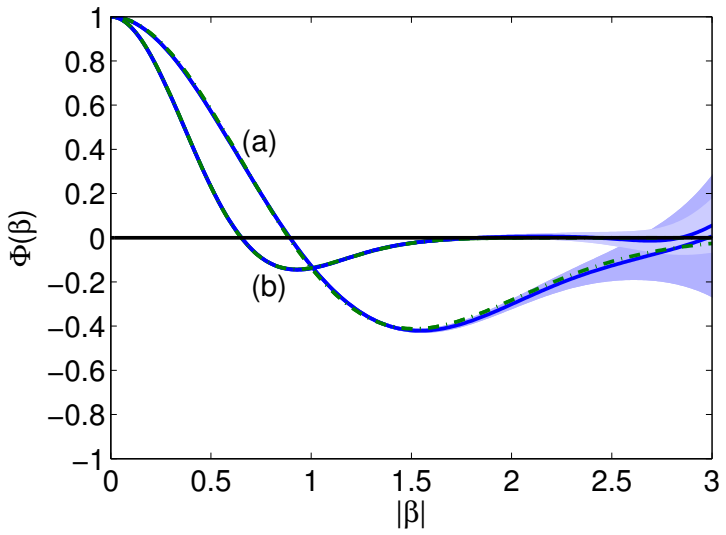

Figure 3.2.: Characteristic functions of two single-photon added thermal states: (a) SPATS with $\bar{n} = 1.11$ and $\eta = 0.62$, (b) mixture of a SPATS and 19% of thermal background, with $\bar{n} = 3.71$ and $\eta = 0.62$. The shaded area corresponds to one standard deviation.

Therefore, some kind of regularization is required to estimate the Fourier transform with finite uncertainty.

The most simple approach is to set the characteristic function to zero for all arguments being larger than some cut-off parameter $|\beta|_c$, $|\beta| > |\beta|_c$. In this sense, the Fourier transform (2.15) is approximated by

$$P_c(\alpha) = \frac{1}{\pi^2} \int_{|\beta|<|\beta|_c} \Phi(\beta) e^{\alpha\beta^* - \alpha^*\beta} d^2\beta. \tag{3.18}$$

This procedure necessarily leads to a systematic error, given by

$$\Delta_P(\alpha) = \frac{1}{\pi^2} \int_{|\beta|\geq|\beta|_c} \Phi(\beta) e^{\alpha\beta^* - \alpha^*\beta} d^2\beta = P(\alpha) - P_c(\alpha), \tag{3.19}$$

which has to be taken into consideration when we examine the negativities of the resulting function $P_c(\alpha)$. This systematic error can only be estimated from some a-priori assumptions. In our case, we used the theoretical characteristic function in Eq. (3.19), with parameters as already given in the text.

In Fig. 3.3, the experimentally obtained P functions of the given states, together with statistical and systematic uncertainties, are shown. We clearly observe a distinct negativity for the state (a), with a significance of five standard deviations. This directly proves that this state is nonclassical by the original definition of nonclassicality. The state (b) shows the limit of the verification of nonclassicality: for

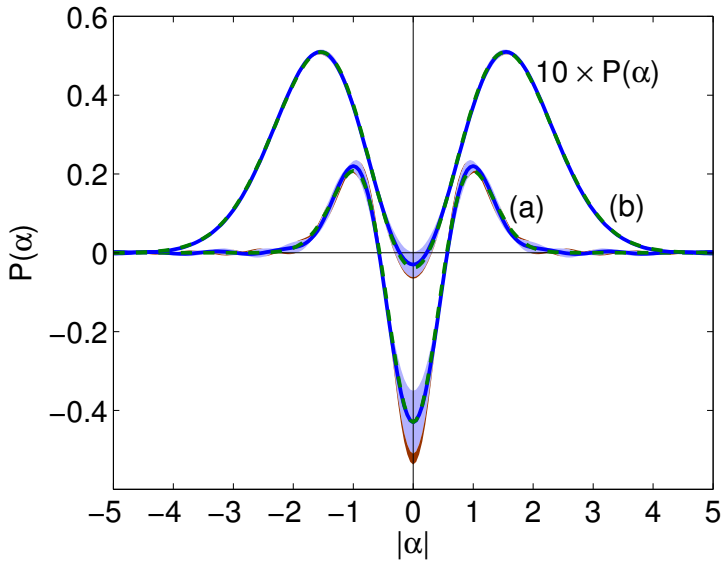

Figure 3.3.: Cross-sections of the P function of the states shown in Fig. 3.2. The blue shaded area corresponds to one standard deviation, resulting from the finite set of data points. The red shaded area is the systematic error, stemming from the cut-off procedure.

a larger mean thermal photon number and additional thermal (i.e. classical) contributions, the negativities dramatically decrease. For the state (b), the significance is reduced to one standard deviation, which does not allow a definite statement about the nonclassicality of this state anymore.

Summary

In this chapter, we have introduced the notion of nonclassicality of quantum optical states, and discussed the obstacles of the verification of nonclassicality by the application of the original definition. We considered some criteria, which are commonly used for nonclassicality tests, and studied their experimental applicability. Altogether, there are two criteria, which seem to be some kind of complementary: First, if the characteristic function $\Phi(\beta)$ of the P function of a state exceeds the value of one, the state is nonclassical. If this condition does not hold, it might be likely that $\Phi(\beta)$ is not only bounded, but also integrable, and its Fourier transform, the P function, is a regular function. If this is indeed the case, the negativities of the latter function are necessary and sufficient for nonclassicality.

Now, the question arises if this complementarity is strict, or if there exist states whose characteristic function is bounded, but not integrable, and its P function

is not well-behaved. If the latter is true, can we find some procedure to identify nonclassicality of states for which the above two criteria cannot be applied? Or is there a simple criterion which even applies to arbitrary quantum states? These questions will be answered positively in the next chapter.

4. Nonclassicality quasiprobabilities

As we have already seen, we can identify nonclassicality in two cases: First, if the characteristic function of the P function is not bounded by 1,

$$|\Phi(\beta)| > 1 \quad \text{for some } \beta \in \mathbb{C}, \tag{4.1}$$

then the state under investigation is nonclassical. Second, if $\Phi(\beta)$ is not only bounded by 1, but integrable, then the P function itself can be obtained. The latter indicates nonclassical effects by some negativities. The remaining question is what we can do if the former criterion does not apply, but the P function is irregular. In this chapter, we present the solution of this problem. As a first step, we argue that there are states, whose nonclassicality cannot be detected by the two criteria presented so far, underlining the importance of our work. Then, we point out that the singularities of the P function are the key problem which prevents us from direct application of the definition of nonclassicality. Therefore, we present a regularization method to remove the singularities, and discuss the requirements which have to be fulfilled by our procedure in order to deliver a meaningful criterion, see [TK4]. Finally, we show that this scheme is universal, i.e. it applies to all quantum states and can also be used in connection with experimental data. Two applications to experiments are presented, see [TK5, TK6].

4.1. Necessity of complete nonclassicality criteria

4.1.1. Nonclassicality criteria for pure states

In principle, we can use a result of Hillery to find out if a pure state is nonclassical or not [20]: Only coherent states are pure classical states. However, it is not easy to find out if an examined pure state is a coherent state, if one only has experimental data at hand. Of course, one can try to calculate the fidelity between the measured state and a coherent state, but this requires some optimization over all coherent states. We do not know if this is practically useful, in particular when one also wants to estimate the significance.

The application of condition (4.1) provides a more direct approach. Moreover, we can show that (4.1) is necessary and sufficient for the nonclassicality of all pure states. For this purpose, we adapt a result of Cahill [48]. He has shown that all states, for which the P function contains at most finite derivatives of the δ-function,

are given by a finite linear combination of Fock states $|n\rangle$, on which a displacement operator $\hat{D}(\alpha)$ may act:

$$|\psi\rangle = \hat{D}(\alpha) \sum_{n=0}^{N} c_n |n\rangle . \tag{4.2}$$

This is equivalent to the fact that the characteristic function of the state is bounded by some polynomial $p(\beta)$,

$$|\Phi(\beta)| \leq |p(\beta)|. \tag{4.3}$$

Clearly, all pure states, which do not satisfy the latter inequality, are nonclassical, since their characteristic function grows faster than a polynomial and therefore satisfies the condition (4.1). Therefore, we are only left to the discussion of states of the form (4.2).

Next, we note that the displacement of states by an amplitude α, $|\psi_\alpha\rangle = \hat{D}(\alpha)|\psi\rangle$, has no influence on the condition (4.1), since the characteristic functions of both states are simply connected by a factor of unit modulus,

$$\Phi_{\hat{D}(\alpha)|\psi\rangle}(\beta) = e^{2i\mathrm{Im}(\alpha^*\beta)} \Phi_{|\psi\rangle}(\beta). \tag{4.4}$$

Therefore, it is sufficient to consider states of the form (4.2) with $\alpha = 0$. Their characteristic function is given by

$$\Phi_{|\psi\rangle} = \sum_{m,n=0}^{N} c_n c_m^* \langle m| e^{\beta \hat{a}^\dagger} e^{-\beta^* \hat{a}} |n\rangle = \sum_{m,n=0}^{N} c_n c_m^* p_{mn}(\beta), \tag{4.5}$$

with $p_{mn}(\beta)$ being a polynomial of degree $m+n$ [8]:

$$p_{mn}(\beta) = \sqrt{m!\, n!} \sum_{k=0}^{\min(m,n)} \frac{\beta^{m-k} (-\beta^*)^{n-k}}{k!(m-k)!(n-k)!}. \tag{4.6}$$

How can these states not satisfy the nonclassicality condition (4.1)? This is only possible if $\Phi(\beta)$ is a polynomial of zeroth degree, which requires $c_n \propto \delta_{0,n}$. Therefore, the only pure states, which do not satisfy (4.1), have the form

$$|\psi\rangle = \hat{D}(\alpha)|0\rangle = |\alpha\rangle , \tag{4.7}$$

being exactly the coherent states. All other pure states satisfy the lowest-order nonclassicality criterion for the characteristic function, Eq. (4.1). As we have already shown, this condition is of practical use, since it can be easily applied to experimental data from balanced homodyne tomography.

4.1.2. Nonclassicality criteria for mixed states

As we have seen, the nonclassicality criterion based on the characteristic function is necessary and sufficient for pure states, and moreover, it is easily accessible to experimental application. For mixed states, this does not hold true anymore. Simple counterexamples can be found in literature, see e.g. [49], among them also the single photon added thermal states, as can be seen from Fig. 3.2 and Fig. 3.3 in the previous chapter. In this case, one might try to check higher order criteria for the characteristic function, which become more involved. Alternatively, it may be possible to approximately estimate the P function and verify nonclassical effects by its negativities. However, are there states, for which both criteria – the one based on $\Phi(\beta)$ and the one based on a regular P function with negativities – do not work?

Such states can be easily constructed. Let us consider a mixture of a SPATS and vacuum, both with equal probability. The P function of this state reads as

$$P(\alpha) = \frac{1}{2} P_{\mathrm{SPATS}}(\alpha) + \frac{1}{2}\delta(\alpha). \tag{4.8}$$

Since the P function of a SPATS is negative for some $\alpha \neq 0$, the P function of the mixed state is negative as well, and consequently the state is nonclassical. Furthermore, the P function is singular, such that it cannot be directly obtained from experimental data. This can also be seen from the characteristic function,

$$\Phi(\beta) = \frac{1}{2}\Phi_{\mathrm{SPATS}}(\beta) + \frac{1}{2}. \tag{4.9}$$

The first term is integrable, but the second is not, therefore the Fourier transform of the sum does not exist as a well-behaved function. Moreover, since $\Phi_{\mathrm{SPATS}}(\beta)$ is bounded by 1, i.e. nonclassicality cannot be observed by condition (4.1), the sum is also bounded by 1,

$$|\Phi(\beta)| \leq \frac{1}{2}|\Phi_{\mathrm{SPATS}}(\beta)| + \frac{1}{2} \leq 1. \tag{4.10}$$

Therefore, this mixture of a SPATS and vacuum is nonclassical, but its nonclassicality cannot be revealed by the most simple condition on the characteristic function, Eq. (4.1), and also not by negativities of a regular P function. For such classes of states, it is necessary to develop different nonclassicality criteria.

4.2. Nonclassicality filters and quasiprobabilities

In order to find a simple criterion, it is helpful to precisely analyze the difficulty of the verification of nonclassicality. Obviously, as nonclassicality is based on a property of the Glauber-Sudarshan P function, it may be convenient to consider

a quantity which is closely related to the P function itself. However, it should be free of the singularities which appear in the P function, since they prevent it from experimental accessibility. Hence, we search for some kind of phase-space distribution being similar to the P function, but well-behaved for all quantum states.

The singularities of the P function can be conveniently characterized by the characteristic function, which is always well-behaved. If $\Phi(\beta)$ is not integrable, then $P(\alpha)$ has some singularities. If $\Phi(\beta)$ is bounded by some polynomial of β, then $P(\alpha)$ is a so-called tempered distribution and contains only finite derivatives of the δ-distribution [48]. If $\Phi(\beta)$ grows exponentially, then $P(\alpha)$ has to be described with infinite derivatives of the δ-function. However, one may show that there exists an upper bound for the characteristic function of any quantum state [8], namely

$$|\Phi(\beta)| \leq e^{|\beta|^2/2}. \tag{4.11}$$

The existence of this bound is important for finding quasiprobabilities which are regular for all quantum states.

As the singularities of the P function are expressed by the non-integrability of the characteristic function $\Phi(\beta)$, we may try to filter the latter in order to make it integrable and the P function regular. This filter procedure has the form

$$\Phi_\Omega(\beta) = \Phi(\beta)\Omega_w(\beta), \tag{4.12}$$

where $\Omega_w(\beta)$ is a filter function. The Fourier transform of $\Phi_\Omega(\beta)$ is referred to as filtered P function and given by the convolution of the state's P function and the Fourier transform $\tilde{\Omega}_w(\alpha)$ of $\Omega_w(\beta)$,

$$P_\Omega(\beta) = \int P(\alpha')\tilde{\Omega}_w(\alpha - \alpha')d^2\alpha'. \tag{4.13}$$

In order to be useful, the filter $\Omega_w(\beta)$ has to satisfy certain requirements:

1. We want to apply this filtering to an arbitrary quantum state, which means that $\Phi_\Omega(\beta)$ shall be integrable for all characteristic functions $\Phi(\beta)$. Since the latter are bounded by $e^{|\beta|^2/2}$, it is sufficient that $\Omega_w(\beta)e^{|\beta|^2/2}$ is integrable. Furthermore, the bound (4.11) is tight, such that the integrability condition is also necessary.

   This condition has a remarkable side effect. In the discussion of the statistical uncertainty on the characteristic function, Eqs. (2.23) and (2.24), we showed that the standard deviation $\sigma\{\Phi_\Omega(\beta)\}$ is bounded by $\frac{1}{\sqrt{N}}|\Omega_w(\beta)|e^{|\beta|^2/2}$. Consequently, regularization of the characteristic function immediately leads to regularization of the standard deviation. Therefore, if $P_\Omega(\beta)$ is regular for all quantum states, it can also be estimated with finite statistical uncertainty. This issue is of great practical importance.

2. We want to use the filtered P function for the verification of nonclassicality. Therefore, $P_\Omega(\beta)$ should reveal negativities of the P function. Conversely, if the state is classical, the filtered P function must not show any negativity. Having Eq. (4.13) in mind, it is clearly sufficient that $\tilde{\Omega}_w(\alpha)$ is a nonnegative function. In this case, any negativity in $P_\Omega(\alpha)$ is due to negativities in $P(\alpha)$ and therefore the nonclassicality of the state. Moreover, this condition is also necessary: Since $P_\Omega(\alpha)$ shall be nonnegative for the vacuum state, which is described by $P_{\text{vac}}(\alpha) = \delta(\alpha)$, we have

$$P_{\Omega,\text{vac}}(\alpha) = \int \delta(\alpha')\tilde{\Omega}_w(\alpha - \alpha')d^2\alpha' = \tilde{\Omega}_w(\alpha) \geq 0. \tag{4.14}$$

   Therefore, we have to require the filter $\Omega_w(\beta)$ to possess a nonnegative Fourier transform.

3. Since we cannot expect that a single filter function $\Omega_w(\beta)$ may be suitable to detect the nonclassicality of any quantum state, we consider a family of filters, parameterized by a real width parameter w. As the name suggests, it shall control how strongly the characteristic function $\Phi(\beta)$ is modified by the filter function $\Omega_w(\beta)$. For instance, one might regard the cutoff value $|\beta|_c$ in the discussion of the approximate reconstruction of the P function of a SPATS as such a variable, see Sec. 3.2.4. The width parameter shall be defined in such a way that in the limit of $w \to \infty$, the filtered characteristic function $\Phi_\Omega(\beta)$ shall pointwise tend to the one of the original state, $\Phi(\beta)$. This obviously requires

$$\forall \beta \in \mathbb{C}: \quad \lim_{w\to\infty} \Omega_w(\beta) = 1. \tag{4.15}$$

   Practically, this can be realized by choosing a filter $\Omega_1(\beta)$ such that $\Omega_1(0) = 1$ and defining

$$\Omega_w(\beta) = \Omega_1(\beta/w). \tag{4.16}$$

   Clearly, for $w \to \infty$ the regularized P function tends to the original one, with all its singularities. However, for finite width the function $P_\Omega(\alpha)$ shall be well-behaved according to our first requirement.

In [TK4], we have shown that for any nonclassical state and any family of filters $\Omega_w(\beta)$ which satisfies our requirements, there exists a finite width parameter w such that the regularized P function shows some negativities. Hence for verification of nonclassicality it is necessary and sufficient to examine the function $P_\Omega(\alpha)$: If the state is nonclassical, then it will show negativities for sufficiently large width w. Conversely, if the state is classical, such a width w does not exist. Therefore, we refer to the filters $\Omega_w(\beta)$ as nonclassicality filters.

Now the question is how suitable filters look like. A simple example is a twodimensional triangular function,

$$\Omega_w(\beta) = \mathrm{tri}(\mathrm{Re}\beta/w)\mathrm{tri}(\mathrm{Im}\beta/w), \quad \text{with } \mathrm{tri}(x) = \begin{cases} 1-|x| & |x| \leq 1 \\ 0 & \text{elsewhere.} \end{cases} \tag{4.17}$$

Since this function has a bounded support on $[-w, w] \times [-w, w]$, it clearly regularizes the characteristic function of an arbitrary quantum state, see requirement (1). Furthermore, we can directly show that the Fourier transform of the triangular function is nonnegative, as needed to satisfy our condition (2). Moreover, the width parameter w is introduced as proposed in (3). Therefore, this filter is a nonclassicality filter.

The only remaining problem is that such a filter with compact support does not preserve all information about the quantum state, since the course of the characteristic function is lost outside the support of $\Omega_w(\beta)$. In other words, Eq. (4.12) is not invertible for such a filter. This can only be changed if $\Omega_w(\beta)$ satisfies one further requirement:

4. The filter function should not be zero for all β, $\Omega_w(\beta) \neq 0$. In this case, the filtering procedure is invertible, and the regularized P function still contains all information about the quantum state.

We refer to such a regularized P function as nonclassicality quasiprobability. This quantity delivers a complete characterization of the quantum state as a regular function, and its negativities directly indicate the nonclassicality of the state. On the other hand, a nonnegative nonclassicality quasiprobability is no proof for classicality. But for an arbitrary nonclassical quantum state, we will find negativities for a sufficiently large width parameter. Compared to other complete nonclassicality criteria, such as presented in Sec. 3.2.2, our new condition is rather simple, since it only requires to look for negativities of a function of a complex argument, with one additional free parameter, the filter width. This makes our approach attractive for both theoretical and experimental application.

4.3. Construction of nonclassicality filters

We already gave a simple example for a nonclassicality filter in Eq. (4.17), which can be applied for the detection of nonclassicality. However, if we want to determine nonclassicality quasiprobabilities, we cannot use filters with compact support. Therefore, the question arises how to construct filters for the latter purpose. This can be done in the following way: First, we take some nonzero function $\omega(\beta)$, which decays faster than any Gaussian function. This condition is slightly stronger than the regularization condition (1), but necessary in order to ensure that our filter will

satisfy (1) for all width parameter. For instance, we may take

$$\omega(\beta) = e^{-|\beta|^4}. \tag{4.18}$$

Then we calculate the autocorrelation function of $\omega(\beta)$,

$$\Omega_1(\beta) = \frac{1}{\mathcal{N}} \int \omega(\beta')\omega(\beta + \beta')d^2\beta, \tag{4.19}$$

with a normalization constant $\mathcal{N} = \int |\omega(\beta')|^2 d^2\beta$. It is well-known that the autocorrelation has a nonnegative Fourier transform, namely the square of the Fourier transform of $\omega(\beta)$. Therefore, $\Omega_1(\beta)$ satisfies the nonnegativity condition (2). Furthermore, we showed that if $\omega(\beta)$ decays faster than any Gaussian function, $\Omega_1(\beta)$ does it as well, see [TK4]. Moreover, if $\omega(\beta)$ is nonzero for all β, the same holds for $\Omega_1(\beta)$. Hence, $\Omega_1(\beta)$ satisfies conditions (1), (2) and (4). The filter width can simply be introduced as suggested in Eq. (4.16).

4.4. Relation to different filtering procedures

Before considering examples of specific states and their nonclassicality quasiprobabilities, let us elaborate the relation of nonclassicality filters and nonclassicality quasiprobabilities to formerly known filtering procedures. First, there is the well-known set of Cahill-Glauber quasiprobability distributions [13], defined by the corresponding characteristic functions

$$\Phi_s(\beta) = \Phi(\beta)e^{(s-1)|\beta|^2/2}. \tag{4.20}$$

For the parameter $s = 1$, we obtain the P representation and its characteristic function $\Phi(\beta)$, for $s = 0$ the Wigner function and for $s = -1$ the Husimi Q function. Comparing this expression with Eq. (4.12), we immediately see that the factor $e^{(s-1)|\beta|^2/2}$ plays the role of the filter. However, although this function has a nonnegative (Gaussian) Fourier transform for all $s < 1$, it is not a nonclassicality filter, since it fails to satisfy the regularization condition (1): For all $s > 0$, the product $e^{(s-1)|\beta|^2/2}e^{|\beta|^2/2}$ is not integrable, and consequently the corresponding quasiprobabilities can show singularities. Squeezed states are a prominent example. Their Cahill-Glauber quasiprobabilities are either Gaussian – and therefore nonnegative – or highly singular – and therefore not accessible from experimental data.

The more general concept of quasiprobabilities has been given by Agarwal and Wolf [12], which we already discussed in Sec. 2.3. All quasiprobabilities presented so far can be seen as special cases of their representations. The authors examined the relation of quasiprobabilities to operator representations with different ordering of annihilation and creation operators $\hat{a}, \hat{a}^\dagger$. Therefore, their considerations are not focussed on the examination of nonclassicality. Our nonclassicality quasiprobabilities are specifically designed to meet the requirements of the latter topic.

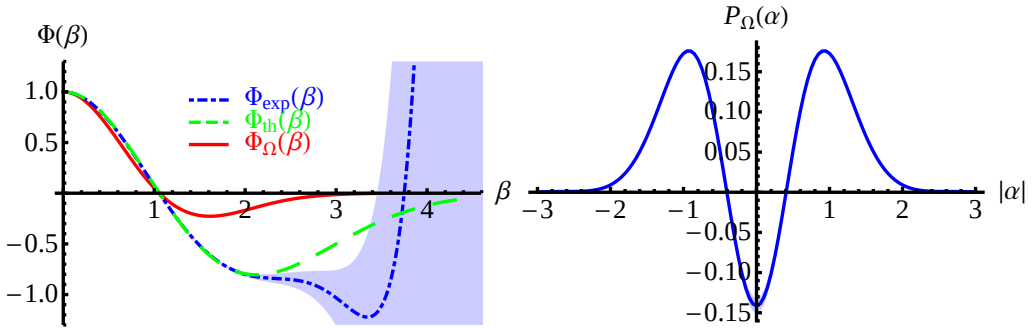

Figure 4.1.: Characteristic function and nonclassicality quasiprobability of a SPATS with $\bar{n} = 0.49$. Left: Experimentally reconstructed characteristic function $\Phi_{\text{exp}}(\beta)$, its theoretical expectation $\Phi_{\text{th}}(\beta)$ and the filtered characteristic function $\Phi_\Omega(\beta)$ with a filter width $w = 1.4$. The shaded area corresponds to one standard deviation. Right: The corresponding nonclassicality quasiprobability shows clear negativities, indicating nonclassicality of the state.

There is another filter, which has been proposed in literature and already applied to experimental reconstruction of quasiprobabilities. In [50], Klauder showed that any quantum state can be approximated by an infinitely differentiable P function with arbitrary precision. For this purpose, he applied Eq. (4.12) with an infinitely differentiable filter with compact support. However, this filter is also not a nonclassicality filter, since one can show that its Fourier transform has negativities. The author simply did not design his filter for purposes of nonclassicality verification. This filter has already been applied experimentally to data of a squeezed state [51], but cannot be used for the examination of nonclassicality.

4.5. Application to a single-photon added thermal state

First results of an experimental reconstruction of a nonclassicality quasiprobability have been presented in [TK5]. Therein, we again consider single-photon added thermal states, but with a mean photon number $\bar{n} = 0.49$, being lower than in Sec. 3.2.4. This leads to a characteristic function which slower tends to zero, as can be seen in the left graph in Fig. 4.1. Now, we can hardly justify only from experimental data that it approaches zero, and cannot apply the cut-off procedure proposed in Sec. 3.2.4. However, the filtered characteristic function $\Phi_\Omega(\beta)$ with $w = 1.4$ is integrable, and also its standard deviation, which is below the line width of the curve in Fig. 4.1, is finite. Therefore, its Fourier transform can be estimated and is shown on the right side. It is clearly negative at $\alpha = 0$. From the

construction of nonclassicality quasiprobabilities, these negativities are not due to the filter, but solely to the nonclassicality of the state. The significance of the effect approximately equals to 15 standard deviations. Furthermore, the consideration of systematic errors is obsolete.

4.6. Direct sampling of nonclassicality quasiprobabilities

So far, we have shown that the experimental reconstruction of nonclassicality quasiprobabilities is possible and can be used to verify nonclassicality. In this section, we present a method to directly obtain a nonclassicality quasiprobability from quadrature measurements, i.e. without evaluation of the characteristic function of the P function. Our approach is based on suitable pattern functions, which enable us to sample the quantity of interest [52, 53]. More specifically, we construct a function $f_\Omega(x, \varphi; \alpha, w)$, whose average over the quadrature distributions $p(x; \varphi)$ with respect to quadrature x and phase φ delivers the nonclassicality quasiprobability $P_\Omega(\alpha)$ with a width w at a point α:

$$P_\Omega(\alpha) = \langle f_\Omega(x, \varphi; \alpha, w)\rangle_{x,\varphi} = \frac{1}{\pi}\int_0^\pi \int_{-\infty}^\infty p(x; \varphi) f_\Omega(x, \varphi; \alpha, w) dx d\varphi. \tag{4.21}$$

On this foundation, one can reconstruct the quasiprobability as follows: One chooses a phase φ_i randomly from a uniform distribution in $[0, \pi)$, and measures the quadrature x_i at this phase from balanced homodyne detection, which is distributed according to the quadrature distribution $p(x; \varphi_i)$ at the phase φ. In this way, one obtains a set of quadrature points $\{(x_i, \varphi_i)\}_{i=1}^N$, whose joint probability density is given by $\frac{1}{\pi}p(x; \varphi)$. Then, one may estimate the expectation value (4.21) empirically as

$$P_\Omega(\alpha) = \frac{1}{N}\sum_{i=1}^N f_\Omega(x_i, \varphi_i; \alpha, w). \tag{4.22}$$

Therefore, $P_\Omega(\alpha)$ is the empirical mean of the sampling points $f_i = f_\Omega(x_i, \varphi_i; \alpha, w)$. Consequently, its variance can be estimated from the empirical variance of the numbers f_i. Moreover, since the latter are independently and identically distributed with a finite variance, the estimated value $P_\Omega(\alpha)$ is Gaussian distributed due to the central limit theorem.

An appropriate pattern function has been constructed in [TK6]. For a filter $\Omega_w(\beta)$, which only depends on the modulus of β, but not on the complex phase, it is given by

$$f_\Omega(x, \varphi; \alpha, w) = \int_{-\infty}^\infty \frac{|b|}{\pi} e^{ibx} e^{2i|\alpha|b\sin(\arg(\alpha)-\varphi-\frac{\pi}{2})} e^{b^2/2}\Omega_w(b) db. \tag{4.23}$$

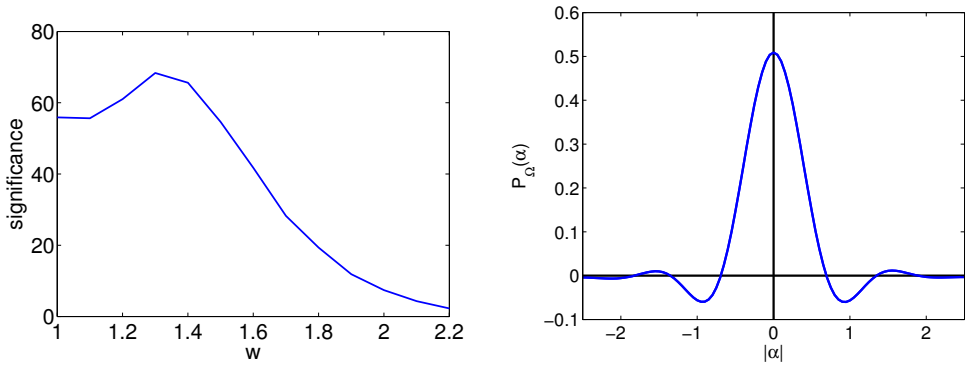

Figure 4.2.: Nonclassicality quasiprobability of a squeezed vacuum state. Left: Significance of the negativity is optimum for $w = 1.3$. Right: Cross section of the quasiprobability, showing clear negativities. The statistical uncertainty is hidden by the line width.

Unfortunately, we do not know a suitable filter $\Omega_w(\beta)$ for which this integral can be determined analytically. However, one may efficiently calculate it with Fourier techniques.

This method has been applied to measurements of a squeezed vacuum state with variances $V_x = 0.36$ and $V_p = 5.28$. As we already mentioned, squeezed states are of particular interest, since they are nonclassical, but most of the widely used quasiprobabilities – such as the ones of Cahill and Glauber – are either nonnegative or highly singular and therefore not interesting for the verification of nonclassical effects. The data contains 10^5 quadrature measurements at each of 21 phases, recorded in the group of R. Schnabel. The filter is constructed as suggested in Sec. 4.3. The width is chosen such that the significance of the negativities, i.e. the ratio of $P_\Omega(\alpha)$ and its standard deviation, reaches its optimum of about 70 standard deviation, see left side of Fig. 4.2. In this case, we clearly observe negativities in the nonclassicality quasiprobability, which is shown on the right side. This demonstrates the nonclassicality of the squeezed state by means of negativities of quasiprobabilities for the first time.

Finally, we show the two-dimensional graph of the nonclassicality quasiprobability in Fig. 4.3, here for a larger width parameter $w = 1.8$. We observe that the negativities are more pronounced than for the optimal width $w = 1.3$. However, the variance of this functions is larger due to the increased width. This is the reason why the statistical significance of the negativities only equals to 18 standard deviations, being much less than in the case of $w = 1.3$.

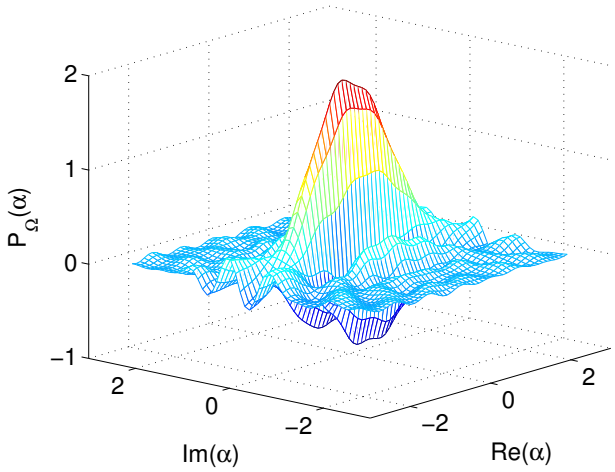

Figure 4.3.: Nonclassicality quasiprobability of a squeezed vacuum state for a width $w = 1.8$. Here, the negativities are better visible, but their statistical significance is not optimal.

Summary

We have seen that the negativities of nonclassicality quasiprobabilities provide a complete criterion for the detection of nonclassicality. For any state, we may examine a family of nonclassicality quasiprobabilities, which is parameterized by a single real number, the width w. If a single function of this family shows negativities, the state is unambiguously nonclassical in the sense of the definition based on the P function. Only if the nonclassicality quasiprobability is nonnegative for all width parameter w, the state is classical. To our best knowledge, this is the most simple, but still complete criterion for nonclassicality. It also proved to be experimentally useful in our examples.

5. Experimental bipartite entanglement verification

A special class of nonclassical phenomena in quantum optics is related to entanglement. The notion of entanglement describes nonclassical correlations between different degrees of freedom of a quantum system, e.g. different physical quantities of a single particle or physical properties of different particles. This led to the development of completely new fields of research, such as quantum computation, quantum cryptography and quantum information, and is therefore of great interest [54].

Here, we shortly discuss the definition of entanglement and its relation to nonclassicality. In particular, it is possible to describe entanglement in terms of suitable quasiprobabilities. However, they have been developed quite recently and cannot be applied easily yet. Therefore, we propose a different scheme to detect entanglement, and apply it to a special class of states, which is closely related to the phase-diffused squeezed states, whose nonclassicality has been demonstrated in Sec. 3.2.3. We show experimentally that mixing such a state with vacuum at a beam splitter creates an entangled state. Finally, we also discuss the possibility of extracting maximally entangled states from the examined one.

5.1. Entanglement and its relation to nonclassicality

5.1.1. Definition of bipartite entanglement

Entanglement can be defined in a similar way as nonclassicality. Let us look at a bipartite system, composed of a system A and a system B. First, we ask which type of pure states are the classically correlated ones? Clearly, if a quantum state shows no correlations between its subsystems, the latter can also be explained classically. In this case, if the system A is in the state $|\phi\rangle_A$ and the system B is in the state $|\chi\rangle_B$, the composed system AB is in the product state $|\psi\rangle_{AB} = |\phi\rangle_A \otimes |\chi\rangle_B \equiv |\phi, \psi\rangle$. Any operation and measurement on the state in system A does not affect the state in system B and vice versa. Conversely, if the composed system is not in such a product state, but a superposition of several product states, measurements on one system can affect the state of the other system. This may even happen if the systems are spatially separated, giving rise to various interesting quantum effects,

such as the EPR paradoxon [55], violation of Bell's inequalities [56, 57], quantum teleportation [58] and more. A pure state of the joint system, which cannot be written as a product state, is referred to as entangled.

Mixed states, described by a density operator $\hat{\rho}$, are classically correlated if they can be written as a classical statistical mixture of classically correlated pure states,

$$\hat{\rho} = \sum_k p_k \left|\phi_k, \chi_k\right\rangle \left\langle\phi_k, \chi_k\right| , \tag{5.1}$$

where the p_k are nonnegative probabilities. Conversely, all other states are referred to as entangled. However, it has been shown that an arbitrary state can be written in such a way, if one allows negative weights p_k [59, 60]. Therefore, the p_k in general form a quasiprobability, playing the same role for entanglement as the Glauber-Sudarshan P function in the discussion of nonclassicality.

It is easy to see that any classical bipartite state, defined by

$$\hat{\rho} = \int d^2\alpha_1 \int d^2\alpha_2 \, P(\alpha_1, \alpha_2) \left|\alpha_1, \alpha_2\right\rangle \left\langle\alpha_1, \alpha_2\right| , \tag{5.2}$$

with $P(\alpha_1, \alpha_2) \geq 0$ being a classical probability, is also a separable state: Here, the quasiprobability p_k is given by the Glauber-Sudarshan P function, and the classically correlated states are the two-mode coherent states. Therefore, every classical state is separable, and all entangled states must be nonclassical ones.

5.1.2. On quasiprobabilities for the detection of entanglement

Although the definitions of nonclassical and entangled states look fairly similar, there are important differences. First, it has been shown that for any entangled state, whose density operator has infinite rank, one can find a finite-rank projection onto a certain subspace, in which the projected density operator is entangled [61]. In other words, even for continuous-variable quantum states, it is sufficient to verify entanglement in truncated density matrices with finite rank. Therefore, it is sufficient to assume discrete quasiprobabilities p_k instead of probability densities on the set of product states. In contrast to that, there is no equivalent theorem for nonclassicality. One may even show that if the density matrix of a state is truncated in Fock space, then the state is nonclassical for sure.

Since the consideration may be restricted to discrete quasiprobabilities, one is free of the problem of singularities, which give rise to the difficulties in the verification of nonclassicality. From this point of view, the verification of entanglement seems to become simpler than the detection of nonclassicality. However, in the case of entanglement we have to handle a different problem: In Eq. (5.1), we write $\hat{\rho}$ as a linear combination of projection operators of factorizable states. However,

the projectors in this set are not linearly independent in general[1]. Therefore, one may express a particular projector $|\phi,\chi\rangle\langle\phi,\chi|$ as a linear combination of different projectors on factorizable states,

$$|\phi,\chi\rangle\langle\phi,\chi| = \sum_k p'_k |\phi'_k,\chi'_k\rangle\langle\phi'_k,\chi'_k| . \tag{5.3}$$

Inserting the latter equation into Eq. (5.1), one immediately obtains a new quasiprobability representation of $\hat{\rho}$, involving both the p_k and p'_k. Therefore we realize that the representation of $\hat{\rho}$ in terms of factorizable states is not unique. This is different from the P function, which is uniquely defined.

These ambiguities in the quasiprobabilities requires a completely new scheme to verify entanglement. If one finds a nonnegative quasiprobability p_k, one may infer that the state is separable. To verify entanglement, however, one has to show that such a nonnegative quasiprobability does not exist. Methods for the determination of suitable quasiprobabilities of entanglement have been developed in [62, 60]. Theoretically, they have a nice mathematical structure, but for universal practical application there is still work to be done. Therefore, we will not use this concept in our experimental examinations.

5.1.3. Entanglement criteria

As already seen, one can use appropriately chosen quasiprobabilities to check whether a given state is entangled or not, but their calculation is more difficult than the one of nonclassicality quasiprobabilities and not ready to direct application. Therefore, different entanglement criteria have to be used in practice. There are numerous proposals, which cannot be listed completely in this thesis. Notably, some of them have a similar structure to nonclassicality criteria: For instance, there exist entanglement witnesses [63] and matrices of moments [64]. For a more detailed overview, see [65]. Furthermore, there is a partial transpose criterion of Peres, which is just sufficient, but can be used for a large class of entangled states [66]. Consider the density matrix elements of the density operator $\hat{\rho}$ in some basis, $\langle k,l|\hat{\rho}|m,n\rangle$, then the partially transposed density matrix is defined by

$$\langle k,l|\hat{\rho}^{PT}|m,n\rangle = \langle k,n|\hat{\rho}|m,l\rangle . \tag{5.4}$$

The ordinary transposition of the density matrix of a single-party state always delivers a density matrix, which can be interpreted as the state with inverse phase. Therefore, the partial transposition of a separable state simply maps the states in

[1] To see this, consider a two-qubit system. The dimension of the Hilbert space of states equals to four, and there are infinitely many factorizable states. The dimension of the set of projectors equals to $4 \times 4 = 16$. Therefore, the projectors on more than 16 different factorizable states cannot be linearly dependent.

one subsystem onto new states, but the composed state is still a separable one. However, for entangled states it may happen that the partially transposed density matrix violates the nonnegativity constraint of a density operator, by having a negative eigenvalue. Therefore, a negative eigenvalue of the partially transposed density matrix clearly indicates entanglement of the original state. In the following, we denote states with a negative partial transpose as PT-entangled.

There are different generalizations of the Peres criterion, see for instance [67] and [68], which can become involved. For small bipartite systems, namely two-qubit systems or a qubit-qutrit system, the Peres criterion is also necessary. In our work [TK7], we will apply this fact, together with suitable projections into finite dimensional subspaces, to the detection of entanglement in an infinite-dimensional system.

5.2. Nonclassicality and entanglement at a beam splitter

To get more insight into the relation between nonclassicality and entanglement, let us consider the action of a beam splitter on a nonclassical state. Let us assume that the two states at the beam splitter input ports are uncorrelated, i.e. factorizable. It is known that if one wants to create an entangled output state, one requires at least one of the two input states to be nonclassical [69]. Therefore, nonclassicality is a precondition for entanglement at the output of the beam splitter.

As an input state, we take a completely phase-diffused squeezed vacuum state, whose nonclassicality has already been examined in Sec. 3.2.3. We know that this state does not show squeezing, and its nonclassical character cannot be verified with second moments of the quadratures only. The other input port of the beam splitter shall be in the vacuum state. Then the question arises if the joint state of the two output modes is entangled, and how we can verify this entanglement. We addressed this issue in [TK7].

First, we showed theoretically that entanglement in the output state can only be detected by means of second moments of the quadratures, if already the input state shows nonclassicality in its second moments of quadratures. More precisely, we demonstrated that the Simon criterion [70], which is necessary and sufficient for entanglement of bipartite Gaussian states, can only be satisfied if the input state is squeezed. In this sense, Gaussian nonclassicality – i.e. squeezing – is necessary and sufficient for Gaussian entanglement (which can be detected by second moments). Due to the similar structure of criteria of matrices of moments for nonclassical and PT-entangled states, we conjecture that this also holds for arbitrary orders of moments. However, a more careful examination of this statement seems to be involved such that we did not spend enough time for strictly proving it.

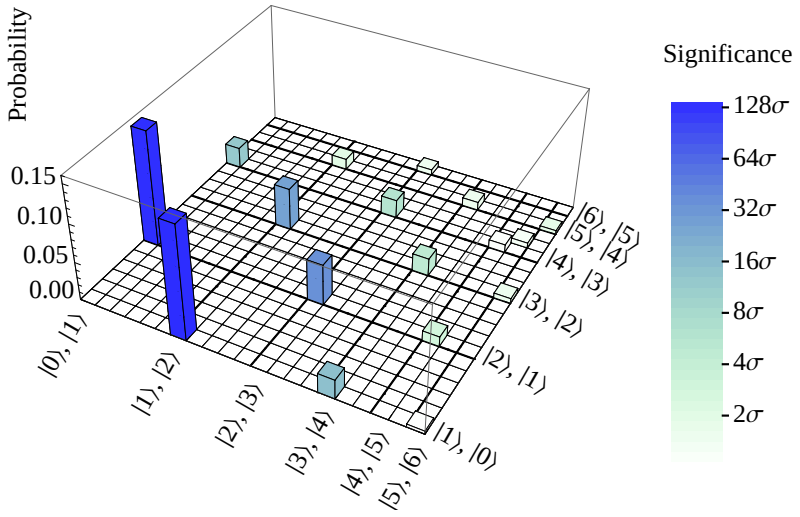

Figure 5.1.: Probability for the occurrence of entangled two-qubit subspaces in the density matrix of the examined state. The color indicates the significance of the negativity of the smallest eigenvalue of the partially transposed density matrix.

Second, as we now know that the entanglement cannot be detected with quadrature covariances directly, we search for a different simple criterion. We have seen in Sec. 3.2.3 that characteristic functions are a good tool for detecting nonclassical effects. However, this does not hold true for entanglement. In principle, one can write down a criterion for PT-entanglement which is similar to the matrices of characteristic functions. However, one can show that one has to look at least at three-by-three matrices. As the characteristic function now also depends on two complex variables (each for one degree of freedom), one has to examine a determinant depending on four complex variables, leading to a heavily involved inequality which has to be satisfied for entanglement. In our minds, this is too complicated for a practical entanglement test.

Therefore, we choose a more simple way. We first reconstruct the density matrix of the state in Fock basis, up to matrix elements for 6 photons. The matrix elements for higher-number Fock states vanish within the statistical uncertainty. Then, we take two-qubit subsystems of the joint state. In each of these subsystems, we can completely examine entanglement by the Peres-criterion. A two-qubit subsystem is represented by a four-by-four matrix, whose partially transposed density matrix can have one (but not more) negative eigenvalues [59]. The existence of such a negative eigenvalue proves entanglement of the two qubits. If this approach would fail, it could also be extended to higher dimensional subspaces. We now examined the entanglement of all possible two-qubit subsystems of the reconstructed density matrix and obtained Fig. 5.1. On both horizontal axes, the qubit subspaces in each

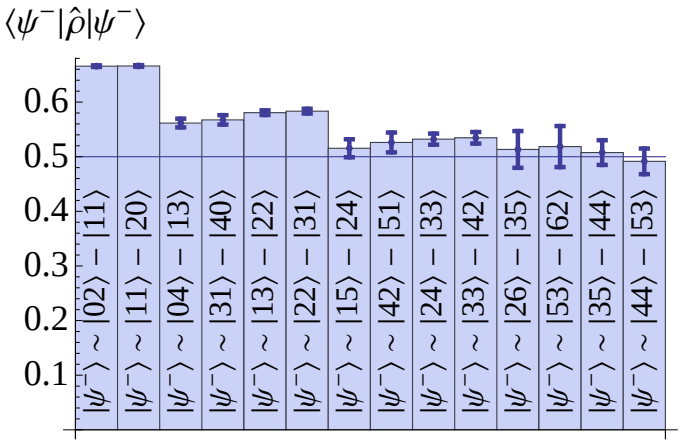

Figure 5.2.: Probability of the occurrence of a singlet state $|\psi^-\rangle$ in the entangled two-qubit subsystems. The errorbars correspond to one standard deviation.

of the modes are labelled by their basis vectors, starting from $|0\rangle, |1\rangle$ to $|0\rangle, |6\rangle$, continuing from $|1\rangle, |2\rangle$ to $|1\rangle, |6\rangle$ and so on. If in a particular subsystem entanglement is detected by a negative eigenvalue of the partially transposed matrix, the probability of projecting the full state onto this subsystem is shown by the height of the bar. Furthermore, the color indicates the significance of the negativity of the eigenvalue in units of one standard deviation. In some subspaces, we detect entanglement with a significance up to 128 standard deviations. We also find that projecting both modes onto the same subsystem, for instance the ones with the basis $|0\rangle, |1\rangle$, only delivers separable states. This fact is quite remarkable, since the joint state is invariant under the exchange of both modes, hence highly symmetric.

Obviously, our method does not only detect if the state is entangled, but also provides information about where the entanglement is located in the density matrix. In this sense, we uncover details about the structure of entanglement in the given quantum state. This may be useful for diverse applications of entangled states. For instance, it is commonly believed that maximally entangled states, such as the singlet state

$$|\psi^-\rangle = \frac{1}{\sqrt{2}} \left(|i_A\rangle |j_B\rangle - |j_A\rangle |i_B\rangle \right) \tag{5.5}$$

in the subsystem composed of the basis vectors $|i_A\rangle, |j_A\rangle$ in mode A and $|i_B\rangle, |j_B\rangle$ in mode B, are optimal for applications in quantum information processing. The quantum state in our investigation is not in such a singlet state, but is it possible to extract such a singlet state by local operations? This question is closely connected to the field of entanglement distillation, which examines protocols which solve exactly this task. It has been shown that entangled qubit systems are distillable [71]. Furthermore, if the probability of projecting a given two-qubit subsystem onto a

singlet state is greater than $\frac{1}{2}$, then the protocol in [72] can be directly applied to perform the distillation. Figure 5.2 shows that these probabilities are greater than this bound for many of the entangled subsystems. Therefore, our entanglement test shows that one is in principle able to extract a maximally entangled state from the subsystems of the joint entangled state, which can be used for different quantum information tasks.

Summary

In this chapter, we have considered entanglement as a special nonclassical effect, which has a lot of applications in quantum optics and quantum information processing. We pointed out that entanglement can be described by negativities of certain quasiprobabilities, which, however, are not directly connected to the Glauber-Sudarshan P function or nonclassicality quasiprobabilities. Therefore, we have to apply a novel entanglement test, based on the two facts: First, entanglement in any state can be found in finite dimensional subsystems, and second, the Peres criterion is necessary and sufficient for two-qubit systems. This test has been applied to an entangled state, which is obtained from to the phase-diffused squeezed vacuum state studied in Sec. 3.2.3. We verify entanglement with high statistical significance and show that maximally entangled states can be distilled from the composed state. However, how one can experimentally implement a distillation protocol, which is appropriate for the entangled subsystems we have discovered, is still an unsolved question and may be subject to further research.

6. Outlook

In this work and the corresponding publications, we shed some new light on the examination of the experimental verification of nonclassicality. We discussed the formerly known nonclassicality criteria with its advantages and disadvantages. Then we developed the so-called nonclassicality quasiprobabilities, whose negativities unambiguously verify the nonclassicality of a given quantum state. They are designed in such a way that they can be reconstructed from experimental data, and therefore provide a practical method for the examination of nonclassical effects. Finally, we also discussed the experimental verification of entanglement, which is an important subclass of nonclassical effects.

There are different aspects which require further research.

1. While the generalization of nonclassicality quasiprobabilities to the discussion of multimode states is straightforward, the examination of time-dependent nonclassical effects is nontrivial. Remembering that nonclassicality is defined as the impossibility of a classical explanation of optical field correlations, we can generalize this definition by considering time-dependent correlations [73]. As the corresponding P functional may also be highly singular, the question of a suitable regularization arises. However, one needs a proper time-dependent phase-space description, also taking care of the time ordering in the calculation of expectation values. The work of Agarwal and Wolf [74] may serve as a good basis for this work.

2. To our best knowledge, there is no satisfactory generalization of nonclassicality to anharmonic systems. For instance, one may try to use the algebraic approach to coherent states, based on the action of the displacement operator on a fiducial state [8]. However, this approach has a major drawback: For all anharmonic systems, the free time evolution immediately converts a coherent state into a non-coherent one. Therefore, if the coherent states shall be denoted as classical, the free time evolution introduces nonclassicality, which is completely counterintuitive. Another approach may start with the so-called Gazeau-Klauder coherent states, which are temporarily stable [75]. However, it is not clear to us if they resemble the classical behavior, and if there exists an appropriate P representation of a quantum state.

3. The application of quasiprobabilities for the description of entanglement has to be explored more and made accessible for practical experimental use. We

are in doubt that phase-space methods may be a good tool for this purpose, since there are fundamental differences between nonclassicality and entanglement. The theory of entanglement quasiprobabilities has already been developed and offers a beautiful mathematical framework, but suitable methods for experimental applications still require further research.

We believe that these questions are of fundamental importance as well as of practical interest, and therefore the investigation of quasiprobabilities should be continued.

List of frequently used symbols

State vectors and operators

$\|\alpha\rangle$	Coherent state with complex amplitude α.
$\|n\rangle$	n-photon Fock state.
$\hat{\rho}$	Density operator of a quantum state.
$\hat{D}(\beta)$	Displacement operator.
$\langle\hat{A}\rangle$	Expectation value of an operator $\hat{A}$.
$\mathrm{Tr}(\hat{A})$	Trace of an operator $\hat{A}$.

Phase space quantities

$\Phi_W^{\hat{A}}(\beta)$	Characteristic function of the Wigner function of the operator $\hat{A}$. If $\hat{A}$ is omitted, it is the characteristic function of a quantum state. If W is omitted, it is the characteristic function of the P function of $\hat{A}$.
$W_{\hat{A}}(\alpha)$	Weyl symbol or Wigner function of a Hermitian operator $\hat{A}$. If $\hat{A}$ is omitted, it is the Wigner function of a quantum state.
$P(\alpha)$	Glauber-Sudarshan P function of a quantum state.
$\Omega_w(\beta)$	(Nonclassicality) filter with width parameter w.
$\Phi_\Omega(\beta)$	Filtered characteristic function.
$P_\Omega(\beta)$	Regularized P function or nonclassicality quasiprobability.

Quadrature distributions and statistical quantities

$p(x;\varphi)$	Probability density of the quadrature x at a fixed phase φ.
$G(k;\varphi)$	Characteristic function of the quadrature distribution at a fixed phase φ.
$\sigma^2\{X\}$	Variance of some quantity X.

Abbreviations

SPATS Single-photon added thermal state.

List of Figures

Bibliography

[1] U. M. Titulaer and R. J. Glauber, *Correlation Functions for Coherent Fields*, Phys. Rev. **140**, B676 (1965).

[2] E. C. G. Sudarshan, *Equivalence of Semiclassical and Quantum Mechanical Descriptions of Statistical Light Beams*, Phys. Rev. Lett. **10**, 277 (1963).

[3] R. J. Glauber, *Coherent and Incoherent States of the Radiation Field*, Phys. Rev. **131**, 2766 (1963).

[4] D. F. Walls, *Squeezed states of light*, Nature **306**, 141 (1983).

[5] H. J. Kimble, M. Dagenais, and L. Mandel, *Photon Antibunching in Resonance Fluorescence*, Phys. Rev. Lett. **39**, 691 (1977).

[6] E. Shchukin, T. Richter, and W. Vogel, *Nonclassicality criteria in terms of moments*, Phys. Rev. A **71**, 011802 (2005).

[7] T. Richter and W. Vogel, *Nonclassicality of Quantum States: A Hierarchy of Observable Conditions*, Phys. Rev. Lett. **89**, 283601 (2002).

[8] A. Perelomov, *Generalized coherent states and their applications*, Texts and monographs in physics, Springer Berlin (1986).

[9] L. Mandel and E. Wolf, *Optical coherence and quantum optics*, Cambridge University Press (1995).

[10] G. B. Arfken and H. J. Weber, *Mathematical Methods for Physicists*, Harcourt (2001).

[11] W. Vogel and D.-G. Welsch, *Quantum optics*, Wiley-VCH, third, revised and extended edition (2006).

[12] G. S. Agarwal and E. Wolf, *Calculus for Functions of Noncommuting Operators and General Phase-Space Methods in Quantum Mechanics. I. Mapping Theorems and Ordering of Functions of Noncommuting Operators*, Phys. Rev. D **2**, 2161 (1970).

[13] K. E. Cahill and R. J. Glauber, *Ordered Expansions in Boson Amplitude Operators*, Phys. Rev. **177**, 1857 (1969).

[14] H. Yuen and V. W. S. Chan, *Noise in homodyne and heterodyne detection*, Opt. Lett. **8**, 177 (1983).

[15] W. Vogel and J. Grabow, *Statistics of difference events in homodyne detection*, Phys. Rev. A **47**, 4227 (1993).

[16] K. Vogel and H. Risken, *Determination of quasiprobability distributions in terms of probability distributions for the rotated quadrature phase*, Phys. Rev. A **40**, 2847 (1989).

[17] A. I. Lvovsky and M. G. Raymer, *Continuous-variable optical quantum-state tomography*, Rev. Mod. Phys. **81**, 299 (2009).

[18] A. I. Lvovsky and J. Shapiro, *Nonclassical character of statistical mixtures of the single-photon and vacuum optical states*, Phys. Rev. A **65**, 033830 (2002).

[19] T. Kiesel, *Nonclassicality in terms of the Glauber-Sudarshan representation*, Diplomarbeit, University of Rostock (2008).

[20] M. Hillery, *Classical pure states are coherent states*, Phys. Lett. A **111**, 409 (1986).

[21] R. F. Bishop and A. Vourdas, *Coherent mixed states and a generalised P representation*, J. Phys. A: Math. Gen. **20**, 3743 (1987).

[22] J. K. Korbicz, J. I. Cirac, J. Wehr, and M. Lewenstein, *Hilbert's 17th Problem and the Quantumness of States*, Phys. Rev. Lett. **94**, 153601 (2005).

[23] R. E. Slusher, L. W. Hollberg, B. Yurke, J. C. Mertz, and J. F. Valley, *Observation of Squeezed States Generated by Four-Wave Mixing in an Optical Cavity*, Phys. Rev. Lett. **55**, 2409 (1985).

[24] C. K. Hong and L. Mandel, *Higher-Order Squeezing of a Quantum Field*, Phys. Rev. Lett. **54**, 323 (1985).

[25] C. K. Hong and L. Mandel, *Generation of higher-order squeezing of quantum electromagnetic fields*, Phys. Rev. A **32**, 974 (1985).

[26] R. Short and L. Mandel, *Observation of Sub-Poissonian Photon Statistics*, Phys. Rev. Lett. **51**, 384 (1983).

[27] H. J. Carmichael and D. F. Walls, *Proposal for the measurement of the resonant Stark effect by photon correlation techniques*, J. Phys. B-At. Mol. Opt. Phys. **9**, L43 (1976).

[28] H. J. Kimble and L. Mandel, *Theory of resonance fluorescence*, Phys. Rev. A **13**, 2123 (1976).

[29] Á. Rivas and A. Luis, *Nonclassicality of states and measurements by breaking classical bounds on statistics*, Phys. Rev. A **79**, 042105 (2009).

[30] A. Luis, *Nonclassicality tests by classical bounds on the statistics of multiple outcomes*, Phys. Rev. A **82**, 024101 (2010).

[31] G. S. Agarwal, *Nonclassical characteristics of the marginals for the radiation field*, Opt. Commun. **95**, 109 (1993).

[32] E. Shchukin and W. Vogel, *Nonclassical moments and their measurement*, Phys. Rev. A **72**, 043808 (2005).

[33] G. S. Agarwal and K. Tara, *Nonclassical character of states exhibiting no squeezing or sub-Poissonian statistics*, Phys. Rev. A **46**, 485 (1992).

[34] R. Simon, M. Selvadoray, Arvind, and N. Mukunda, *Necessary and Sufficient Classicality Conditions on Photon Number Distributions*, arXiV:quantph/9709030 (1997).

[35] D.N. Klyshko, *Observable signs of nonclassical light*, Phys. Lett. A **213**, 7 (1996).

[36] D.N. Klyshko, *The nonclassical light*, Physics-Uspekhi **39**, 573 (1996).

[37] S. Bochner, *Monotone Funktionen, Stieltjessche Integrale und harmonische Analyse*, Math. Ann. **108**, 378 (1933).

[38] W. Vogel, *Nonclassical States: An Observable Criterion*, Phys. Rev. Lett. **84**, 1849 (2000).

[39] E. Shchukin, T. Richter, and W. Vogel, *Nonclassical quadrature distributions*, J. Opt. B **6**, S597 (2004).

[40] A. Zavatta, V. Parigi, and M. Bellini, *Experimental nonclassicality of single-photon-added thermal light states*, Phys. Rev. A **75**, 052106 (2007).

[41] A. Franzen, B. Hage, J. DiGuglielmo, J. Fiurásek, and R. Schnabel, *Experimental Demonstration of Continuous Variable Purification of Squeezed States*, Phys. Rev. Lett. **97**, 150505 (2006).

[42] H. Vahlbruch, A. Khalaidovski, N. Lastzka, C. Gräf, K. Danzmann, and R. Schnabel, *The GEO 600 squeezed light source*, Class. Quantum Gravity **27**, 084027 (2010).

[43] E. Wigner, *On the Quantum Correction For Thermodynamic Equilibrium*, Phys. Rev. **40**, 749 (1932).

[44] K. Husimi, *Some Formal Properties of the Density Matrix*, Proc. Phys. Math. Soc. Jpn **22**, 264 (1940).

[45] A. Kenfack and K. Życzkowsky, *Negativity of the Wigner function as an indicator of non-classicality*, J. Opt. B **6**, 396 (2004).

[46] U. Leibfried, D. M. Meekhof, B. E. King, C. Monroe, W. M. Itano, and D. J. Wineland, *Experimental Determination of the Motional Quantum State of a Trapped Atom*, Phys. Rev. Lett. **77**, 4281 (1996).

[47] V. Parigi, A. Zavatta, M. Kim, and M. Bellini, *Probing quantum commutation rules by addition and subtraction of single photons to/from a light field*, Science **317**, 1890 (2007).

[48] K. E. Cahill, *Pure states and P representation*, Phys. Rev. **180**, 1239 (1969).

[49] L. Diosi, *Comment on "Nonclassical States: An Observable Criterion*, Phys. Rev. Lett. **85**, 2841 (2000).

[50] J. R. Klauder, *Improved Version of Optical Equivalence Theorem*, Phys. Rev. Lett. **16**, 534 (1966).

[51] M. Lobino, D. Korystov, C. Kupchak, E. Figueroa, B. C. Sanders, and A. I. Lvovsky, *Complete Characterization of Quantum-Optical Processes*, Science **322**, 563 (2008).

[52] G. M. D'Ariano, C. Macchiavello, and M. G. A. Paris, *Detection of the density matrix through optical homodyne tomography without filtered back projection*, Phys. Rev. A **50**, 4298 (1994).

[53] G. M. D'Ariano, *Tomographic measurement of the density matrix of the radiation field*, Quantum Semiclass. Opt. **7**, 693 (1995).

[54] R. Horodecki, P. Horodecki, M. Horodecki, and K Horodecki, *Quantum entanglement*, Rev. Mod. Phys. **81**, 865 (2009).

[55] A. Einstein, B. Podolsky, and N. Rosen, *Can Quantum-Mechanical Description of Physical Reality Be Considered Complete?*, Phys. Rev. **47**, 777 (1935).

[56] J. S. Bell, *On the Problem of Hidden Variables in Quantum Mechanics*, Rev. Mod. Phys. **38**, 447 (1966).

[57] A. Aspect, P. Grangier, and G. Roger, *Experimental Tests of Realistic Local Theories via Bell's Theorem*, Phys. Rev. Lett. **47**, 460 (1981).

[58] C. H. Bennett, G. Brassard, C. Crépeau, R. Jozsa, A. Peres, and W. K. Wootters, *Teleporting an unknown quantum state via dual classical and Einstein-Podolsky-Rosen channels*, Phys. Rev. Lett. **70**, 1895 (1993).

[59] A. Sanpera, R. Tarrach, and G. Vidal, *Local description of quantum inseparability*, Phys. Rev. A **58**, 826 (1998).

[60] J. Sperling and W. Vogel, *Representation of entanglement by negative quasi-probabilities*, Phys. Rev. A **79**, 042337 (2009).

[61] J. Sperling and W. Vogel, *Verifying continuous-variable entanglement in finite spaces*, Phys. Rev. A **79**, 052313 (2009).

[62] J. Sperling and W. Vogel, *Necessary and sufficient conditions for bipartite entanglement*, Phys. Rev. A **79**, 022318 (2009).

[63] M. Horodecki, P. Horodecki, and R. Horodecki, *Separability of mixed states: necessary and sufficient conditions*, Phys. Lett. A **223**, 1 (1996).

[64] E. Shchukin and W. Vogel, *Inseparability Criteria for Continuous Bipartite Quantum States*, Phys. Rev. Lett. **95**, 230502 (2005).

[65] A. Miranowicz, M. Bartkowiak, X. Wang, Y. Liu, and F. Nori, *Testing nonclassicality in multimode fields: A unified derivation of classical inequalities*, Phys. Rev. A **82**, 013824 (2010).

[66] A. Peres, *Separability criterion for density matrices*, Phys. Rev. Lett. **77**, 1413 (1996).

[67] A. C. Doherty, P. A. Parrilo, and F. M. Spedalieri, *Distinguishing Separable and Entangled States*, Phys. Rev. Lett. **88**, 187904 (2002).

[68] O. V. Man'ko, V. I. Man'ko, G. Marmo, A. Shaji, E. C. G. Sudarshan, and F. Zaccaria, *Partial positive scaling transform: a separability criterion*, Phys. Lett. A **339**, 194 (2005).

[69] X. B. Wang, *Theorem for the beam-splitter entangler*, Phys. Rev. A **66**, 024303 (2002).

[70] R. Simon, *Peres-Horodecki Separability Criterion for Continuous Variable Systems*, Phys. Rev. Lett. **84**, 2726 (2000).

[71] M. Horodecki, P. Horodecki, and R. Horodecki, *Inseparable Two Spin- 1/2 Density Matrices Can Be Distilled to a Singlet Form*, Phys. Rev. Lett. **78**, 574 (1997).

[72] C. H. Bennett, G. Brassard, S. Popescu, B. Schumacher, J. A. Smolin, and W. K. Wootters, *Purification of Noisy Entanglement and Faithful Teleportation via Noisy Channelsh*, Phys. Rev. Lett. **76**, 722 (1996).

[73] W. Vogel, *Nonclassical correlation properties of radiation fields*, Phys. Rev. Lett. **100**, 013605 (2008).

[74] G. S. Agarwal and E. Wolf, *Calculus for Functions of Noncommuting Operators and General Phase-Space Methods in Quantum Mechanics. III. A Generalized Wick Theorem and Multitime Mapping*, Phys. Rev. D **2**, 2206 (1970).

[75] J. P. Gazeau and J. R. Klauder, *Coherent states for systems with discrete and continuous spectrum*, J. Phys. A: Math. Gen. **32**, 123 (1999).

Own Publications

[TK1] W. Vogel, T. Kiesel, and J. Sperling, *Characterizing nonclassicality and entanglement*, Opt. Spectrosc. **108**, 197 (2010).

[TK2] T. Kiesel, W. Vogel, B. Hage, J. DiGuglielmo, A. Samblowski, and R. Schnabel, *Experimental test of nonclassicality criteria for phase-diffused squeezed states*, Phys. Rev. A **79**, 022122 (2009).

[TK3] T. Kiesel, W. Vogel, V. Parigi, A. Zavatta, and M. Bellini, *Experimental determination of a nonclassical Glauber-Sudarshan P function*, Phys. Rev. A **78**, 021804 (2008).

[TK4] T. Kiesel and W. Vogel, *Nonclassicality filters and quasiprobabilities*, Phys. Rev. A **82**, 032107 (2010).

[TK5] T. Kiesel, W. Vogel, M. Bellini, and A. Zavatta, *Nonclassicality quasiprobability of single-photon-added thermal states*, Phys. Rev. A **83**, 032119 (2011).

[TK6] T. Kiesel, W. Vogel, B. Hage, and R. Schnabel, *Direct Sampling of Nonclassicality Quasiprobabilities*, arXiv:1103.2032 [quant-ph] (2011).

[TK7] T. Kiesel, W. Vogel, B. Hage, and R. Schnabel, *Entangled Qubits in a non-Gaussian Quantum State*, Phys. Rev. A **83**, 062319 (2011).

[TK8] E. Shchukin, T. Kiesel, and W. Vogel, *Generalized minimum-uncertainty squeezed states*, Phys. Rev. A **79**, 043831 (2009).

Acknowledgments

First of all, I want to thank Werner Vogel for giving me the opportunity to work in the quantum optics group in Rostock. The results we found during the last years have been presented in both my diploma thesis and this dissertation thesis, as well as in several publications. It was an interesting time and challenging work, which I enjoyed very much.

Furthermore, the thesis is based on experimental data, which has been recorded in the laboratories of Marco Bellini in Firenze as well as of Boris Hage and Roman Schnabel in Hannover. I want to thank them for their kind collaboration and interesting remarks, which were helpful for testing my ideas with real data and contributed to some of the articles.

Let me also acknowledge the support of all members of the quantum optics group in Rostock. In particular, I want to thank Jan Sperling for numerous discussions about nonclassicality and entanglement, quantum optics, physics and the world in general. Moreover, I enjoyed our excellent collaboration for preparing and holding the seminars for undergraduate students. As far as I can assess it, we did a good job, from which both, the students and us, learned a lot. Furthermore, I want to thank Peter Grünwald, Falk Töppel, Christian di Fidio, Dmytro Vasylyev, Andrew Semenov, Evgeny Shchukin, Shailendra Kumar Singh, Frank E. S. Steinhoff and Saleh Rahimi-Keshari for being nice and helpful colleagues, as well as Christine Schoof for all administrative support. Eventually, I have to thank Torsten Leddig, Daniela and Mathias Arbeiter, Lissi and Gunnar Schulz as well as Stefan Polei for their friendship and company in the mensa.

Last but not least, I gratefully acknowledge my family for their support during the years. There are my parents, which accompanied me from the beginning. There is my wife, who loves me for over seven years now, and I love her as well. And finally, there is our little Jonas, who also supported my work in the last three months by letting me sleep during the nights, letting me work after lunch, and letting me relax and play with him the time in between.

Part II.

Publications

Contributions to the publications

The following manuscripts have been published in refereed journals or are currently under review. They present the main results of this dissertation thesis. Some of the results are based on experimental data, which have been provided by the quantum optics groups of Prof. Marco Bellini in Florence and Prof. Roman Schnabel in Hannover. The data files consisted of large sets of measured quadrature points.

The key idea for the detection of nonclassicality, namely the corresponding quasiprobabilities and filters, has been found and developed by myself. Moreover, I performed the evaluation of the experimental data, including the reconstruction of the P function and nonclassicality quasiprobability of the single photon added thermal states, the characteristic function, moments and quasiprobabilities of the phase-diffused squeezed vacuum states as well as the reconstruction of the density matrix of the entangled state and the search for entangled qubits.

I contributed to two further papers. The one is a proceedings article for the "International Conference on Quantum Optics and Quantum Computation" in Vilnius (2008), where I reviewed the reconstruction of the P function [TK1]. The second is an investigation of generalized squeezed states, where I contributed a section on the realisation of the discussed states in an ion trap [TK8].

PHYSICAL REVIEW A **78**, 021804(R) (2008)

Experimental determination of a nonclassical Glauber-Sudarshan *P* function

T. Kiesel and W. Vogel
Arbeitsgruppe Quantenoptik, Institut für Physik, Universität Rostock, D-18051 Rostock, Germany

V. Parigi
Department of Physics, University of Florence, I-50019 Sesto Fiorentino, Florence, Italy
and LENS, Via Nello Carrara 1, 50019 Sesto Fiorentino, Florence, Italy

A. Zavatta and M. Bellini
LENS, Via Nello Carrara 1, 50019 Sesto Fiorentino, Florence, Italy
and Istituto Nazionale di Ottica Applicata, CNR, L. go E. Fermi, 6, I-50125, Florence, Italy
(Received 7 April 2008; published 25 August 2008)

A quantum state is nonclassical if its Glauber-Sudarshan *P* function fails to be interpreted as a probability density. This quantity is often highly singular, so that its reconstruction is a demanding task. Here we present the experimental determination of a well-behaved *P* function showing negativities for a single-photon-added thermal state. This is a direct visualization of the original definition of nonclassicality. The method can be useful under conditions for which many other signatures of nonclassicality would not persist.

DOI: 10.1103/PhysRevA.78.021804 PACS number(s): 42.50.Dv, 42.50.Xa, 03.65.Ta, 03.65.Wj

Einstein's hypothetical introduction of light quanta, the photons, was the first step toward the consideration of nonclassical properties of radiation [1]. But what does nonclassicality mean in a general sense? A radiation field is called nonclassical when its properties cannot be understood within the framework of the classical stochastic theory of electromagnetism. For other systems, nonclassicality can be defined accordingly. Here we will focus our attention on harmonic quantum systems, such as radiation fields or quantum-mechanical oscillators, for example, trapped atoms.

In this context the coherent states, first considered by Schrödinger in the form of wave packets [2], play an important role. They represent those quantum states that are most closely related to the classical behavior of an oscillator or an electromagnetic wave. For a single radiation mode, the coherent states $|\alpha\rangle$ are defined as the right-hand eigenstates of the non-Hermitian photon annihilation operator $\hat{a}$, $\hat{a}|\alpha\rangle = \alpha|\alpha\rangle$; cf., e.g., [3]. A general mixed quantum state $\hat{\rho}$,

$$\hat{\rho} = \int d^2\alpha\, P(\alpha)|\alpha\rangle\langle\alpha|, \tag{1}$$

can be characterized by the Glauber-Sudarshan *P* function [3,4]. In this form the quantum statistical averages of normally ordered operator functions can be written as

$$\langle :\hat{f}(\hat{a},\hat{a}^\dagger):\rangle = \int d^2\alpha\, P(\alpha) f(\alpha,\alpha^*), \tag{2}$$

where the normal ordering prescription $:\hat{f}(\hat{a},\hat{a}^\dagger):$ means that all creation operators $\hat{a}^\dagger$ are to be ordered to the left of all annihilation operators $\hat{a}$.

Formally, the resulting expressions (2) for expectation values are equivalent to classical statistical mean values. However, in general, the *P* function does not exhibit all the properties of a classical probability density. It can become negative or even highly singular. Within the chosen representation of the theory, the failure of the Glauber-Sudarshan *P* function to show the properties of a probability density is taken as the key signature of quantumness [5,6].

In this Rapid Communication we demonstrate the experimental determination of a nonclassical *P* function. Within the experimental precision it clearly attains negative values. This is a direct demonstration of nonclassicality: the negativity of the *P* function prevents its interpretation as a classical probability density.

Why is it so difficult to demonstrate the nonclassicality directly on the basis of this original definition? Let us go back to a single photon as postulated by Einstein. Its *P* function is

$$P(\alpha) = \left(1 + \frac{\partial}{\partial\alpha}\frac{\partial}{\partial\alpha^*}\right)\delta(\alpha); \tag{3}$$

cf., e.g., [7]. Already in this case we get a highly singular distribution in terms of derivatives of the δ distribution, which cannot be interpreted as a classical probability. Due to these properties, it is difficult to experimentally determine nonclassical *P* functions in general.

How can one realize nonclassical states whose properties can be demonstrated directly in terms of the original definition, that the *P* function fails to be a probability density? This question is not trivial: for instance, losses introduced by imperfect experimental efficiencies lead only to rescaling of the quadrature variable; cf., e.g., [8]. The *P* function obtained by perfect detection is related to $P_\eta(\alpha)$, obtained with the quantum efficiency η via

$$P(\alpha) = \eta P_\eta(\sqrt{\eta}\alpha). \tag{4}$$

Consequently, singularities in the *P* function are then preserved. Most of the nonclassical states experimentally generated so far have highly singular *P* functions, whose reconstruction is impossible. However, one may start with a thermal state $\hat{\rho}_{\mathrm{th}}$ with mean photon number $\bar{n}$. By photon creation one gets a single-photon-added thermal state

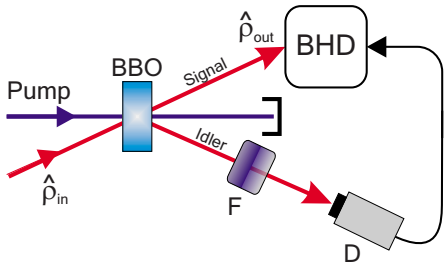

FIG. 1. (Color online) Scheme for the conditional excitation of a thermal light state (denoted by $\hat{\rho}_{in}$) by a single photon. A click in the on-off detector D prepares the photon-added thermal state $\hat{\rho}_{out}$ and triggers its balanced homodyne detection (BHD).

(SPATS), $\hat{\rho}=\mathcal{N}\hat{a}^{\dagger}\hat{\rho}_{th}\hat{a}$, where $\mathcal{N}$ denotes the normalization. Its P function is now well behaved, but violates the properties of a classical probability density [9],

$$P(\alpha)=\frac{1}{\pi\bar{n}^3}[(1+\bar{n})|\alpha|^2-\bar{n}]e^{-|\alpha|^2/\bar{n}}, \tag{5}$$

giving rise to the question of whether its experimental determination could be possible [10]. In the zero-temperature limit, the SPATS includes the special case of the one-photon Fock state with the highly singular P function given in Eq. (3). In this sense the SPATS represents a single photon whose P function is regularized by a controlled thermal background.

Recently, SPATSs could be realized experimentally and some of their nonclassical signatures have been verified [11]. Nevertheless, the reconstruction of a nonclassical P function remains a challenging problem which goes beyond the standard procedures of quantum state reconstruction; for the latter, see, e.g., [7]. A successful determination of the P function of a SPATS would visualize the basic definition of nonclassicality for a quantum state that lies at the heart of Einstein's hypothesis: a regularized version of a single photon.

The core of the experimental apparatus used to produce SPATSs is an optical parametric amplifier based on a type-I β–barium borate (BBO) crystal pumped by radiation at 393 nm (see Fig. 1). The pump is obtained by second harmonic generation in a lithium triborate (LBO) crystal of a mode-locked Ti:sapphire laser emitting 1.5 ps pulses with a repetition rate of 82 MHz. When the parametric amplifier is not injected, spontaneous parametric down-conversion takes place, generating pairs of photons at the same wavelength as the laser source along two directions commonly called the signal and idler channels. We perform a conditional preparation of the quantum states by placing an on-off photodetector (D) after narrow spectral-spatial filters (F) along the idler channel [11,12].

A click of the idler detector prepares the signal state, whose quadratures are measured on a pulse-to-pulse basis using an ultrafast balanced homodyne detection scheme [13]. After verifying the phase independence of the quadrature distributions, the state is then analyzed by acquiring quadrature values with random local oscillator phases. When no fields are present at the inputs of the parametric amplifier, conditioned single-photon Fock states are spontaneously generated in the signal channel [12,14]. On the other hand, we have recently shown that the injection of pure or mixed states results in the conditional production of their single-photon-added versions, always converting the initial states into nonclassical ones [11,15,16].

Here we use a pseudothermal source, obtained by inserting a rotating ground glass disk in a portion of the laser beam, for injecting the parametric amplifier and producing SPATSs. The scattered light forms a random spatial distribution of speckles whose average size is larger than the core diameter of a single-mode fiber used to collect it. When the ground glass disk rotates, light exits the fiber in a clean collimated spatial mode with random amplitude and phase fluctuations, yielding the photon distribution typical of a thermal source [17]. The product between the SPATS preparation rate and the coherence time of the injected thermal state (a few microseconds, and depending on the rotation speed of the disk) is kept much smaller than 1. This condition assures that each state is prepared by adding a single photon to a coherent state having an amplitude and phase which are completely uncorrelated with respect to those of the previous one. This experimental realization of a thermal state directly recalls its P function definition, i.e., a statistical mixture of coherent states weighted by a Gaussian distribution: $P(\alpha)=\exp(-|\alpha|^2/\bar{n})/(\bar{n}\pi)$.

By performing measurements on single-photon Fock states and on unconditioned thermal ones, we have estimated an overall experimental efficiency of 0.62 ± 0.04. Both the limited efficiency in the state preparation ($\approx$0.92) and in homodyne detection ($\approx$0.67) degrade the expected final state by introducing unwanted losses. This does not contaminate the obtained P function; cf. Eq. (4).

Let us now proceed with the reconstruction of the P function. Its characteristic function $\Phi(\beta)$ is related to that of the quadrature $\hat{x}(\varphi)$ [7],

$$\Phi(\beta)=\langle:\hat{D}(\beta):\rangle=\langle e^{i|\beta|\hat{x}[\pi/2-\arg(\beta)]}\rangle e^{|\beta|^2/2}, \tag{6}$$

where $\hat{D}(\beta)$ is the displacement operator. Since the measured state is independent of phase, we may neglect the arguments of β and $\hat{x}$. The expectation value on the right-hand side represents the characteristic function of the observable quadrature. It can be estimated from the sample of N measured quadrature values $\{x_j\}_{j=1}^N$ via (cf. [18])

$$\langle e^{i|\beta|\hat{x}}\rangle\approx\frac{1}{N}\sum_{j=1}^{N}e^{i|\beta|x_j}. \tag{7}$$

Inserting Eq. (7) into (6), we get an estimation $\bar{\Phi}(\beta)$ of $\Phi(\beta)$. The variance of this quantity can be estimated as

$$\sigma^2\{\bar{\Phi}(\beta)\}=\frac{1}{N}[e^{|\beta|^2}-|\bar{\Phi}(\beta)|^2]. \tag{8}$$

The inverse Fourier transform of $\Phi(\beta)$ yields the P function, which for many nonclassical states does not exist as a well-behaved function. However, the sampled characteristic function converges stochastically toward the theoretical one. In our case its Fourier transform is an analytical function.

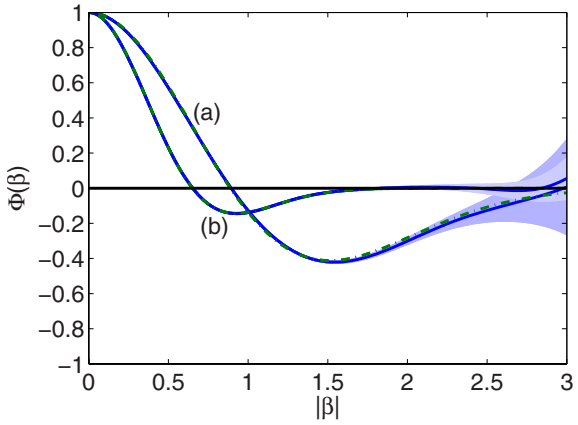

FIG. 2. (Color online) Experimental characteristic functions (solid lines) and best fit to theoretical curves (dashed lines): (a) SPATS, with $\bar{n}=1.11$ and $\eta=0.60$, (b) mixture of SPATS with 19% of the thermal background, with $\bar{n}=3.71$ and $\eta=0.62$. The shaded areas show the standard deviations.

For radial symmetry of the state the two-dimensional Fourier transform reduces to the Hankel transform [19],

$$P(\alpha)=\frac{2}{\pi}\int_0^\infty bJ_0(2b|\alpha|)\Phi(b)db. \tag{9}$$

In our treatment we set the experimental curve to zero for arguments greater than a cutoff value $|\beta|_c$, where the graph becomes small. This limits the disturbing sampling noise on the reconstructed function

$$\bar{P}(\alpha)=\frac{2}{\pi}\int_0^{|\beta|_c} bJ_0(2b|\alpha|)\bar{\Phi}(b)db \tag{10}$$

to a reasonable level. The corresponding variance has been calculated as

$$\sigma^2\{\bar{P}(\alpha)\}=\frac{1}{N}\left(\frac{4}{\pi^2}\int\int_0^{|\beta|_c} bb'J_0(2b|\alpha|)J_0(2b'|\alpha|)\bar{\Phi}(b-b')\times e^{bb'}db\,db'-\bar{P}(\alpha)^2\right). \tag{11}$$

The systematic error

$$\Delta_P(\alpha)=\frac{2}{\pi}\int_{|\beta|_c}^\infty bJ_0(2b|\alpha|)\Phi(b)db \tag{12}$$

is estimated with the help of the fitted theoretical function.

In Fig. 2 we show experimental curves for characteristic functions. Curve (a) is in good agreement with the expected characteristic function $\Phi(\beta)$ for a SPATS,

$$\Phi(\beta)=[1-(1+\bar{n})|\beta|^2]e^{-\bar{n}|\beta|^2}, \tag{13}$$

for the mean thermal photon number $\bar{n}=1.11$ and the global quantum efficiency $\eta=0.60$. Curve (b) shows the characteristic function for a mixture of a SPATS and its thermal background with weights of 0.81 and 0.19, respectively, for $\bar{n}=3.71$ and $\eta=0.62$. For sampling these functions, we have acquired 10^5 and 5×10^5 data points for the curves (a) and (b), respectively. We note that both curves are suited to reconstruct the corresponding P functions by properly choosing cutoff values $|\beta|_c$ of their arguments.

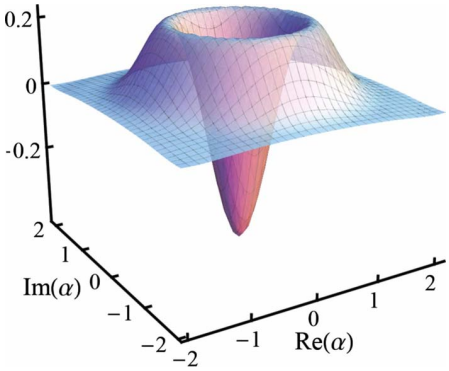

FIG. 3. (Color online) Experimentally reconstructed P function of a SPATS, as obtained from Fig. 2(a).

The reconstructed P function, shown in Fig. 3, is derived from the experimental characteristic function given in Fig. 2(a). Since the measured states are independent of the phase, the reconstructed P representation is phase independent as well. It is clearly seen that the P function attains negative values, so that it fails to have the properties of a classical probability density. This is direct proof of the nonclassicality of the experimentally realized SPATS, based on the original definition of nonclassicality [5,6].

For a more careful discussion, we also examine a cross section along a radial line, as shown in Fig. 4(a). The experimentally determined curve is drawn with the solid line. Obviously, it is in good agreement with the theoretical expectation (dashed curve). The distance between the minimum value and the $|\alpha|$ axis is approximately equal to five standard deviations, which is not diminished by the systematic error of $|\Delta_P(\alpha)|<0.07|P(0)|$, obtained by the cutoff $|\beta|_c=2.8$. The statistically significant negativity of the P function prevents

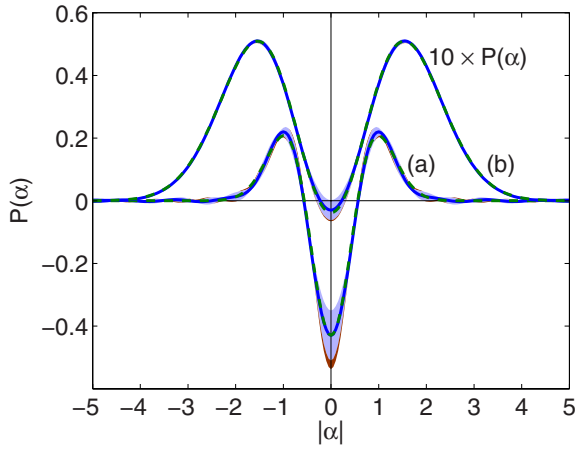

FIG. 4. (Color online) P functions (solid lines) in parts (a) and (b) are obtained from the experimental characteristic functions in Figs. 2(a) and 2(b), respectively. They are compared with the corresponding theoretical fits (dashed curves). The standard deviations (light shaded areas) and the systematic errors (dark shaded areas) are also given.

it from being interpreted as a classical probability density. This provides clear evidence of nonclassicality per definition.

Special nonclassical signatures of SPATSs, which are consequences of the negativities of the P function, have been experimentally demonstrated recently [11]. It is important to note that the reconstruction of the P function is just possible for sufficiently large thermal photon number $\bar{n}$. On the contrary, other criteria for nonclassicality, such as negativities of the Wigner function, the Klyshko criterion, and the entanglement potential, start to fail for increasing values of $\bar{n}$. To show the power of the reconstruction of the P function under such conditions, we have demonstrated its use at the limits: for a SPATS with $\bar{n}=3.71$, which is additionally contaminated with a 19% admixture of the corresponding thermal background. By using a cutoff $|\beta|_c=1.9$, we still obtain a P function being negative within one standard deviation, cf. Fig. 4(b). Other nonclassical effects, as discussed above, do not survive for this state.

Criteria for the characteristic functions are known, which are equivalent to the negativity of the P function [20]. For many states the characteristic function displays their nonclassicality by violating the condition $|\Phi(\beta)|\leqslant 1$; cf. [21]. If the condition is satisfied, $\Phi(\beta)$ may be integrable and then the P function can be obtained to directly verify nonclassicality. SPATSs belong to this category: for sufficiently high $\bar{n}$ most criteria for nonclassicality (including the lowest-order one based on the characteristic function) fail [11], but it is still possible to retrieve a negative P function.

Let us consider how sensitively the negativities of the P function depend on the overall efficiency η. Balanced homodyne detection measures the "true" state quadratures when the efficiency is unity. For imperfect detection ($\eta<1$) one records a convolution of the quadrature distribution with Gaussian noise, whose variance increases with decreasing η; cf. [22]. In the Wigner function, this increasing noise smooths out its structures and may destroy their negativities. As can be seen from Eq. (4), the shape and the relative noise level of the reconstructed P function do not depend on the efficiency. Hence the negativities of $P(\alpha)$ are in principle preserved even for a small efficiency, whereas for other phase-space distributions, such as the Wigner function, they are quickly lost.

In conclusion, we have reconstructed the Glauber-Sudarshan P function of an experimentally prepared single-photon-added thermal state. We obtain a well-behaved function with statistically significant negativities, so that it fails to show the properties of a classical probability density. This is a direct demonstration of nonclassicality according to its original definition. The approach works well, just when many other methods of demonstrating nonclassicality fail.

This work was partially supported by Ente Cassa di Risparmio di Firenze and CNR, under the RSTL initiative.

[1] A. Einstein, Ann. Phys. **17**, 132 (1905).
[2] E. Schrödinger, Naturwiss. **14**, 664 (1926).
[3] R. J. Glauber, Phys. Rev. **131**, 2766 (1963).
[4] E. C. G. Sudarshan, Phys. Rev. Lett. **10**, 277 (1963).
[5] U. M. Titulaer and R. J. Glauber, Phys. Rev. **140**, B676 (1965).
[6] L. Mandel, Phys. Scr., T **T12**, 34 (1986).
[7] W. Vogel and D.-G. Welsch, *Quantum Optics*, 3rd ed. (Wiley-VCH, Weinheim, 2006).
[8] A. A. Semenov, D. Yu. Vasylyev, and B. I. Lev, J. Opt. B: Quantum Semiclassical Opt. **39**, 905 (2006).
[9] G. S. Agarwal and K. Tara, Phys. Rev. A **46**, 485 (1992).
[10] T. Richter, J. Mod. Opt. **48**, 1881 (2001).
[11] A. Zavatta, V. Parigi, and M. Bellini, Phys. Rev. A **75**, 052106 (2007).
[12] A. Zavatta, S. Viciani, and M. Bellini, Phys. Rev. A **70**, 053821 (2004).
[13] A. Zavatta, M. Bellini, P. L. Ramazza, F. Marin, and F. T. Arecchi, J. Opt. Soc. Am. B **19**, 1189 (2002).
[14] A. I. Lvovsky, H. Hansen, T. Aichele, O. Benson, J. Mlynek, and S. Schiller, Phys. Rev. Lett. **87**, 050402 (2001).
[15] A. Zavatta, S. Viciani, and M. Bellini, Science **306**, 660 (2004).
[16] V. Parigi, A. Zavatta, M. S. Kim, and M. Bellini, Science **317**, 1890 (2007).
[17] F. T. Arecchi, Phys. Rev. Lett. **15**, 912 (1965).
[18] A. I. Lvovsky and J. H. Shapiro, Phys. Rev. A **65**, 033830 (2002).
[19] A. J. Jerri, *Integral and Discrete Transforms with Applications and Error Analysis* (Marcel Dekker, New York, 1992).
[20] T. Richter and W. Vogel, Phys. Rev. Lett. **89**, 283601 (2002).
[21] W. Vogel, Phys. Rev. Lett. **84**, 1849 (2000).
[22] W. Vogel and J. Grabow, Phys. Rev. A **47**, 4227 (1993).

Experimental test of nonclassicality criteria for phase-diffused squeezed states

T. Kiesel and W. Vogel
Arbeitsgruppe Quantenoptik, Institut für Physik, Universität Rostock, D-18051 Rostock, Germany

B. Hage, J. DiGuglielmo, A. Samblowski, and R. Schnabel
Institut für Gravitationsphysik, Leibniz Universität Hannover, 30167 Hannover, Germany
and Max-Planck-Institut für Gravitationsphysik (Albert-Einstein-Institut), Callinstrasse 38, 30167 Hannover, Germany
(Received 16 December 2008; published 27 February 2009)

We experimentally examine the nonclassical character of a class of non-Gaussian states known as phase-diffused squeezed states. These states may show no squeezing effect at all and therefore provide an interesting example to test nonclassicality criteria. The characteristic function of the Glauber-Sudarshan representation (P function) proves to be a powerful tool to detect nonclassicality. Using this criterion we find that phase-diffused squeezed states are always nonclassical, even if the squeezing effect vanishes. Testing other criteria of nonclassicality based on higher-order squeezing and the positive semidefiniteness of special matrices of normally ordered moments, it is found that these criteria fail to reveal the nonclassicality for some of the prepared phase-diffused squeezed states.

DOI: 10.1103/PhysRevA.79.022122 PACS number(s): 03.65.Wj, 42.50.Dv, 42.50.Xa

I. INTRODUCTION

The definition of nonclassicality of a quantum state of the harmonic oscillator is closely connected to the coherent states. These are the eigenstates of the annihilation operator, $\hat{a}|\alpha\rangle=\alpha|\alpha\rangle$, where the complex number α defines the amplitude and phase of the field [1]. Sudarshan [2] and Glauber [3] showed that the density operator of an arbitrary optical quantum state can be formally written as a statistical mixture of coherent states,

$$\hat{\rho}=\int d^2\alpha P(\alpha)|\alpha\rangle\langle\alpha|, \tag{1}$$

where the Glauber-Sudarshan representation $P(\alpha)$ plays the role of the probability distribution of coherent states. However, in quantum optics $P(\alpha)$ often violates the properties of a probability density. Hence, a state is referred to as nonclassical if its P function does not exhibit the properties of a classical probability density [4].

Only recently, nonclassicality of experimentally generated states has been demonstrated by means of this definition [5]. In many cases, however, the P functions of nonclassical states are highly singular, such that they cannot be reconstructed from the measured experimental data. This is the case for squeezed states, having a quadrature variance of less than the quadrature variance of the vacuum state. For instance, the P function of a squeezed vacuum state with quadrature variances V_x and V_p (we assume that $V_x<1$, where unity represents the normalized vacuum noise) may be formally written as

$$P_{\mathrm{sv}}(\alpha)=\exp\left[-\frac{V_x-V_p}{8}\left(\frac{\partial^2}{\partial\alpha^2}+\frac{\partial^2}{\partial\alpha^{*2}}-2\frac{V_x+V_p-2}{V_x-V_p}\frac{\partial}{\partial\alpha}\frac{\partial}{\partial\alpha^*}\right)\right]\delta(\alpha). \tag{2}$$

This quantity cannot be understood as a well-behaved function. In such cases some other nonclassicality criteria, reflecting the negativities of the P function, have to be applied [6].

Phase-diffused squeezed states define an interesting class of states with a, in general, not accessible P function. In very recent experiments these states were used to demonstrate *purification* and *distillation* for continuous variable quantum information protocols [7,8]. Phase-diffused squeezed states are a mixture of squeezed (vacuum) states with a stochastically distributed phase. They are related to a realistic decoherence process and may be produced from pure squeezed states in a phase noisy transmission channel. They reveal a non-Gaussian noise distribution, have a positive Wigner function, and, for strong phase noise, may show no squeezing effect at the level of second moments of the quadrature operators.

In this paper, we use phase-diffused squeezed states in order to experimentally test nonclassicality criteria for the case where the P function cannot directly be reconstructed from the homodyne detector quadrature data. First, we concentrate on the *characteristic function* of the P function, which is always well behaved, and investigate the criterion proposed in [9]. Second, we examine *moments* of the quadrature operator and search for higher-order squeezing [10]. Third, we check a hierarchy of criteria based on *normally ordered moments*, as suggested in [11]. We find that the characteristic function of the P function outperforms the other criteria of nonclassicality.

Let us consider a statistical mixture of squeezed states, each described by a Wigner function [12],

$$W_{\mathrm{sv}}(x,p;\varphi)=\frac{1}{2\pi\sqrt{V_xV_p}}\exp\left\{-\frac{x_\varphi^2}{2V_x}-\frac{p_\varphi^2}{2V_p}\right\}, \tag{3}$$

where $x_\varphi=x\cos(\varphi)+p\sin(\varphi)$ and $p_\varphi=-x\sin(\varphi)+p\cos(\varphi)$ are the quadrature variables, rotated around an angle φ, and V_x,V_p are the variances of both quadratures x_φ,p_φ, satisfying the Heisenberg uncertainty relation $V_xV_p\geq 1$. Let $p(\varphi)$ de-

TABLE I. Parameter of the examined states.

	V_x=0.36, V_p=5.28				
σ/°	0.0	6.3	12.6	22.2	∞
V_{eff}	0.36	0.42	0.59	1.00	2.82

note the statistical distribution of the phase fluctuations, then the Wigner function of the mixed state reads

$$W(x,p) = \int p(\varphi) W_{\text{sv}}(x,p;\varphi) d\varphi. \tag{4}$$

In our examination of nonclassicality, the characteristic function $\Phi(\beta)$ of the P function plays a decisive role. It is connected to the Wigner function via Fourier transform,

$$\Phi(\beta) = e^{|\beta|^2/2} \int W(x,p) e^{i(x \text{ Im } \beta - p \text{ Re } \beta)} dx\, dp. \tag{5}$$

For a squeezed state, as defined by Eq. (3), we find

$$\Phi_{\text{sv}}(\beta;\varphi) = \exp\left(\frac{|\beta|^2}{2} \{1 - V_x \cos^2[\arg(\beta) - \varphi] - V_p \sin^2[\arg(\beta) - \varphi]\} \right). \tag{6}$$

The characteristic function for the mixed state is given in close analogy to Eq. (4),

$$\Phi(\beta) = \int p(\varphi) \Phi_{\text{sv}}(\beta;\varphi) d\varphi. \tag{7}$$

In our experiment we generated phase-diffused squeezed vacuum states with varying strengths of the phase noise. The phase noise was chosen to be distributed according to a zero mean Gaussian and could therefore be completely characterized by the standard deviation. A summary of states generated is given in Table I. The undisturbed squeezed vacuum states had quadrature variances V_x=0.36 and V_p=5.28. For the strongest phase noise we used a flat distribution with a width of 720°, which is labeled with σ=∞ in Table I. We also listed the minimum quadrature variance of each state,

$$V_{\text{eff}} = \frac{V_x + V_p}{2} - \frac{V_p - V_x}{2} e^{-2\sigma^2}, \tag{8}$$

to show that the states with σ=6.3° and σ=12.6° are still squeezed, but the squeezing vanishes at σ=22.2°. Hence, one cannot decide about the nonclassicality of the last two states by examination of the quadrature variance.

II. EXPERIMENTAL SETUP

The squeezed states were generated by a degenerate optical parametric amplifier (OPA). The OPA consisted of a type-I noncritically phase-matched second-order nonlinear crystal (7% Mg:$LiNbO_3$) inside a standing-wave optical resonator with a linewidth of 25 MHz. The OPA process was continuously pumped by 50 mW of second-harmonic light

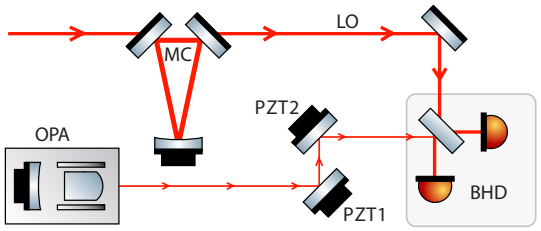

FIG. 1. (Color online) Simplified sketch of the experimental setup. MC: spatial mode cleaner, LO: local oscillator, OPA: squeezed light source, BHD: balanced homodyne detector, and PZT: piezoelectrically actuated mirror. PZT1 was used to control the average phase and PZT2 applied the phase noise.

yielding a classical power amplification factor of 6. Both the length (resonance frequency) of the resonator as well as the orientation of the squeezing ellipse were stably controlled by electronic servo loops. With this setup we directly measured a minimal squeezed variance of −4.5 dB and an antisqueezed variance of +7.2 dB with respect to the unity vacuum variance. From these measurements we inferred an overall efficiency of 75% and an initial squeezing factor of −8.2 dB.

The squeezed field propagated in free space from the OPA passing high-reflection mirrors, two of which were moved by piezoelectric transducers (PZTs). One (PZT1, Fig. 1) was used to control the average phase of the squeezed field. The other (PZT2, Fig. 1) was driven by a quasirandom voltage to apply the phase diffusion. This voltage was generated by a high quality personal computer (PC) sound card connected to an appropriate amplifier. The sound card played back a previously generated sound file which was carefully designed to meet the desired shape of its frequency spectrum and its histogram. The former covered the *flat* part of the frequency response of the PZT except the frequency band of any control loop; the latter was chosen to be Gaussian for the partial phase diffusion and had to be absolutely flat in the totally randomized case.

Balanced homodyne detection (BHD) was used to measure the quadrature amplitude of the phase-diffused squeezed field. The visibility of the squeezed beam and the spatially filtered [mode cleaner (MC), Fig. 1] local oscillator was 98.9% and was limited by OPA crystal inhomogeneities. The average quadrature phase of the BHD was servo loop controlled except for the total phase randomization where no mean phase exists. The signals of the two individual BHD photodetectors were electronically mixed down at 7 MHz and low pass filtered with a bandwidth of 400 kHz to address a modulation mode showing good squeezing and a high dark noise clearance of the order of 20 dB. The resulting signals were fed into a PC based data-acquisition system and sampled with 1×10^6 samples/s and 14-bit resolution. For a more detailed description of the main parts of the setup we refer to [7] and [8].

III. NONCLASSICALITY IN TERMS OF THE CHARACTERISTIC FUNCTION

A. Experimental demonstration

First, let us consider a sufficient criterion proposed in [9]: a state is nonclassical if the characteristic function $\Phi(\beta)$ of

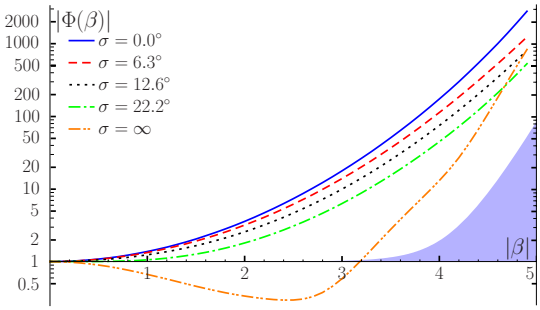

FIG. 2. (Color online) Characteristic functions of different phase-diffused squeezed vacuum states. The shaded area corresponds to one standard deviation; it is added to the nonclassical boundary $\Phi_{\mathrm{vac}} \equiv 1$. Take note of the logarithmic scale.

the P function exceeds the characteristic function of the vacuum at some point β,

$$\exists \beta: \quad |\Phi(\beta)| > |\Phi_{\mathrm{vac}}| \equiv 1. \tag{9}$$

Note that this condition represents the lowest order of a hierarchy of conditions which completely characterize the nonclassicality [13]. The function $\Phi(\beta)$ can be obtained by [14]

$$\Phi(\beta) = \langle :\hat{D}(\beta): \rangle = \langle e^{i|\beta|\hat{x}[\pi/2-\arg(\beta)]} \rangle e^{|\beta|^2/2}, \tag{10}$$

where $\hat{D}(\beta)$ is the displacement operator. Since we only consider a single quadrature, we may neglect the arguments of β and $\hat{x}$. The expectation value on the right-hand side of Eq. (10) represents the characteristic function of the quadrature. It can be estimated from the sample of N measured quadrature values $\{x_j\}_{j=1}^N$ via (cf. [15])

$$\langle e^{i|\beta|\hat{x}} \rangle \approx \frac{1}{N} \sum_{j=1}^{N} e^{i|\beta|x_j}. \tag{11}$$

Inserting Eq. (11) into Eq. (10), we obtain an estimation $\bar{\Phi}(\beta)$ of $\Phi(\beta)$. The variance of this quantity can be estimated as

$$\sigma^2\{\bar{\Phi}(\beta)\} = \frac{1}{N}[e^{|\beta|^2} - |\bar{\Phi}(\beta)|^2]. \tag{12}$$

For each state we have recorded $N = 10^7$ data points. The resulting characteristic functions are shown in Fig. 2. We only concentrate on the quadrature where the variance of the state is minimum. The shaded area corresponds to the magnitude of one standard deviation; it is added to the nonclassicality border $|\Phi_{\mathrm{vac}}(\beta)| \equiv 1$. In order to demonstrate that a state satisfies the nonclassicality criterion [Eq. (9)], with a significance of s standard deviations, we have to check if the characteristic function satisfies the inequality

$$|\bar{\Phi}(\beta)| > 1 + s\sigma\{\bar{\Phi}(\beta)\}, \tag{13}$$

at least at one point β. It is clearly seen that all recorded states satisfy this lowest-order condition for nonclassicality with a high significance of $s \geq 10$. Hence, we directly observe signatures of nonclassicality in the characteristic functions.

We note that Fig. 2 reveals that the P functions of these states are highly singular. This is due to the fact that condition (9) is satisfied for all β with large modulus, indicating that $\Phi(\beta)$ is not integrable. Therefore, we cannot expect $P(\alpha)$ to be a well-behaved function. However, if $\Phi(\beta)$ does not satisfy Eq. (9), one may be able to compute its Fourier transform and check nonclassicality of the state based on the failure of the P function to be non-negative; see [5].

B. Theoretical generalization of the results

Whereas in the experiment only states with Gaussian phase noise are investigated, we now prove that phase-diffused squeezed vacuum states always fulfill condition (9), indifferent of the phase distribution $p(\varphi)$. Although this criterion is not necessarily fulfilled by an arbitrary nonclassical state, it turns out to be sufficient for any state with a characteristic function of form (7).

First, we note that $\Phi_{\mathrm{sv}}(\beta;\varphi)$ is π periodic in the angle φ. Without any loss of generality, we can assume that the function $p(\varphi)$ in Eq. (7) can be regarded as a probability density over the interval $[0,\pi]$, i.e., $p(\varphi) \geq 0$ and $\int_0^\pi p(\varphi)d\varphi = 1$. For technical reasons, we may further assume that $p(\varphi)$ is π periodic as the characteristic function of squeezed vacuum, such that the domain of integration in Eq. (7) may be any interval of length π.

We assume that the x quadrature is the squeezed one, so $V_x < 1 < V_p$. Hence, we can find positive real numbers $\delta\varphi$ and ϵ, such that

$$\forall \varphi \in (-\delta\varphi, \delta\varphi): \quad 1 - V_x \cos^2(\varphi) - V_p \sin^2(\varphi) \geq \epsilon > 0. \tag{14}$$

In this interval, the characteristic function increases exponentially with $|\beta|$,

$$\forall \varphi \in (\varphi_0 - \delta\varphi, \varphi_0 + \delta\varphi): \quad |\Phi_{\mathrm{sv}}(|\beta|e^{i\varphi_0};\varphi)| \geq e^{\epsilon|\beta|^2/2}. \tag{15}$$

Of course, we can also find an interval of the same length, centered around some φ_0, with

$$\int_{\varphi_0-\delta\varphi}^{\varphi_0+\delta\varphi} p(\varphi)d\varphi = C > 0. \tag{16}$$

Taking into consideration that the domain of integration in Eq. (7) may be an arbitrary interval of length π, we can rewrite the characteristic function $\Phi(\beta)$ at the point $|\beta|e^{i\varphi_0}$ as

$$\Phi(|\beta|e^{i\varphi_0}) = \int_{\varphi_0-\pi/2}^{\varphi_0+\pi/2} p(\varphi)\Phi_{\mathrm{sv}}(|\beta|e^{i\varphi_0};\varphi)d\varphi. \tag{17}$$

Since the integrand is non-negative, a diminution of the domain of integration decreases the value of the integral,

$$\Phi(|\beta|e^{i\varphi_0}) \geq \int_{\varphi_0-\delta}^{\varphi_0+\delta} p(\varphi)\Phi_{\mathrm{sv}}(|\beta|e^{i\varphi_0};\varphi)d\varphi. \tag{18}$$

Due to Eqs. (15) and (16), we finally find

TABLE II. Degree of squeezing q_{2n} for different orders $2n$ and standard deviations of phase noise σ.

$\sigma/^\circ$	q_2	q_4	q_6	q_8	q_{10}
0.0	−0.6362±0.3%	−0.8667±0.16%	−0.9506±0.12%	−0.9813±0.09%	−0.9927±0.07%
6.3	−0.5717±0.04%	−0.8090±0.03%	−0.9102±0.03%	−0.9549±0.04%	−0.9754±0.06%
12.6	−0.4060±0.08%	−0.5509±0.15%	−0.5459±0.60%	−0.3852±4.2%	0.0798±95%
22.2	0.0196±3.2%	0.6864±0.53%	2.982±0.84%	10.61±1.7%	37.27±3.3%
∞	1.908±0.09%	10.68±0.16%	51.72±0.32%	249.6±0.65%	1222±1.23%

$$|\Phi(|\beta|e^{i\varphi_0})| \geq e^{\epsilon|\beta|^2/2}\int_{-\delta\varphi}^{\delta\varphi} p(\varphi+\varphi_0)d\varphi = Ce^{\epsilon|\beta|^2/2}. \quad (19)$$

Obviously, the characteristic function $\Phi(\beta)$ is not bounded, independently of the phase noise distribution $p(\varphi)$. Consequently, we are always able to prove nonclassicality by means of Eq. (9), which is the most simple criterion among a necessary and sufficient hierarchy [13].

IV. NONCLASSICALITY IN TERMS OF MOMENTS

Besides the signatures of nonclassicality in terms of the characteristic function, different criteria for demonstrating nonclassicality are known. Since we measured time series of individual quadrature values we can calculate all higher-order moments of the quadrature operator $\hat{x}$.

A. Hong-Mandel squeezing

We begin by examining higher-order squeezing as proposed by Hong and Mandel [10]. To this end, we calculate the degree of $2n$th order squeezing,

$$q_{2n} = \frac{\langle(\Delta\hat{x})^{2n}\rangle}{(2n-1)!!} - 1, \quad n \in \mathbb{N}, \quad (20)$$

where $\Delta\hat{x}=\hat{x}-\langle\hat{x}\rangle$. The moments can be estimated from the sample of quadrature data quite naturally by replacing expectation values by their arithmetic means. It is sufficient to verify nonclassicality if at least one of the q_{2n} is negative.

Table II shows the degree of squeezing for different orders and different phase noise strengths. Obviously, only if the lowest-order parameter q_2 is negative, then the parameter q_{2n} of higher order can also be negative. Hence, we may only observe higher-order squeezing if the state already shows standard squeezing. The investigation of the degree of higher-order squeezing does not extend the range of detection of nonclassicality of phase-diffused squeezed states. This is not surprising since it can be shown that for Gaussian states [Eq. (3)] the degree of squeezing is given by

$$q_{2n}(\varphi) = [V_x\cos(\varphi) + V_p\sin(\varphi)]^n - 1. \quad (21)$$

For these states, squeezing always implies higher-order squeezing and vice versa [10]. Phase diffusion can only smooth out the phase dependence of the moments and diminish the nonclassical effect.

B. Matrices of normally ordered moments

Normally ordered moments of the quadrature operator $\hat{x}$ can be estimated from measured data points $\{x_j\}_{j=1}^N$ via appropriate sampling relations (see Appendix),

$$\langle:\hat{x}^k:\rangle \approx \frac{1}{2^{k/2}N}\sum_{j=1}^{N} H_k\left(\frac{x_j}{\sqrt{2}}\right), \quad (22)$$

where $H_k(x)$ are the Hermite polynomials. With these moments at hand, we can examine the nonclassicality criterion of Agarwal [11]. It has been shown that a state is nonclassical if at least one of the matrices

$$M^{(l)} = \begin{pmatrix} 1 & \langle:\hat{x}:\rangle & \cdots & \langle:\hat{x}^{l-1}:\rangle \\ \langle:\hat{x}:\rangle & \langle:\hat{x}^2:\rangle & \cdots & \langle:\hat{x}^{l}:\rangle \\ \vdots & \vdots & \ddots & \vdots \\ \langle:\hat{x}^{l-1}:\rangle & \langle:\hat{x}^{l}:\rangle & \cdots & \langle:\hat{x}^{2l-2}:\rangle \end{pmatrix} \quad (23)$$

is not positive semidefinite. This can be verified by showing that at least one of the principal minors of such a matrix is negative [16]. However, to this end we had to check up to 2^l-1 principal minors for each matrix $M^{(l)}$, which is a computationally expensive task.

Here we use the fact that the existence of a negative eigenvalue of $M^{(l)}$ demonstrates the violation of positive semidefiniteness. Therefore, we determine

$$\lambda_{\min}^{(l)} = \min_{\vec{x}\neq\vec{0}} \frac{\vec{x}^T M^{(l)}\vec{x}}{\vec{x}^T\vec{x}} \quad (24)$$

via a conjugate gradient algorithm; see, e.g., [17]. It can be shown that $\lambda_{\min}^{(l)}$ equals the minimum eigenvalue of $M^{(l)}$. In this way, we only need to calculate one quantity per matrix to examine its definiteness. Its standard deviation is determined by using a bootstrap method: we generate new quadrature data, distributed as the experimentally measured quadratures, 100 times to obtain a statistical sample of eigenvalues, which gives the standard deviation; cf. [18].

The experimental results are shown in Table III. We only consider matrices of even dimension since we noted that the minimum eigenvalues of $M^{(2n)}$ and $M^{(2n+1)}$ are equal. This may be due to the fact that odd moments of squeezed vacuum states vanish, giving the matrices a special structure. We observe that all matrices, which belong to the states showing squeezing, have significantly negative eigenvalues.

TABLE III. Table of minimum eigenvalues of the matrices $M^{(l)}$ for different l and phase noise σ. The existence of significantly negative values indicates the nonclassicality.

$\sigma/°$	2×2 matrix	4×4 matrix	6×6 matrix	8×8 matrix	10×10 matrix
0.0	$-0.6362\pm0.25\%$	$-4.294\pm0.86\%$	$-104.0\pm2.5\%$	$-6201\pm6.1\%$	$-722\times10^3\pm12\%$
6.3	$-0.5717\pm0.03\%$	$-3.337\pm0.11\%$	$-69.93\pm0.35\%$	$-3593\pm0.98\%$	$-335\times10^3\pm2.5\%$
12.6	$-0.4060\pm0.08\%$	$-2.040\pm1.1\%$	$-6.728\pm53\%$	$-107.4\pm110\%$	$-1259\times10^3\pm49\%$
22.2	$0.0197\pm3.0\%$	$-0.2323\pm1.1\%$	$-0.5358\pm4.1\%$	$-2.299\pm71\%$	$-459\times10^3\pm40\%$
∞	$1.0000\pm0\%$	$0.7856\pm1.2\%$	$0.5493\pm12\%$	$10.85\pm13\%$	$1113\pm94\%$

Hence, their nonclassical character can be directly observed in the sign of the smallest eigenvalue. Furthermore, for the states with $\sigma\geq22.2°$ the matrix $M^{(2)}$ is positive semidefinite since this directly corresponds to the absence of quadrature squeezing. However, for the state with $\sigma=22.2°$ the matrices $M^{(l)}$ with $l\geq4$ possess a negative eigenvalue. Therefore, Agarwal's criterion [11] extends the range of detection of nonclassicality. Only for the completely phase-diffused state, are we not able to prove nonclassicality by this method. For this state, the effect might appear in higher-dimensional matrices, but the statistical uncertainty might hide the effect.

V. CONCLUSION

We have used experimental data sets of quadrature measurements on phase-diffused squeezed states for a test of different nonclassicality criteria. Even for a *completely* phase-diffused squeezed state, i.e., where the measured statistics were identical for all homodyne detection phase angles, we found a pronounced nonclassical character. This could be illustrated with the help of the characteristic function of the P function: it directly shows nonclassical features in the lowest-order criterion in [13] and the nonclassicality was detected with a rather high signal-to-noise ratio. Other nonclassicality criteria, such as higher-order squeezing or the violation of positive semidefiniteness of Agarwal's matrices [11], fail to reveal nonclassicality beyond squeezing or only show nonclassical behavior in matrices of higher dimension. Therefore, we demonstrated for the radiation under study that the characteristic function of the P function, which contains information about all moments of the state, can be a more powerful tool for the examination of nonclassicality than a finite set of moments.

Eventually, we note that the evaluation of the statistical significance of nonclassical effects is much easier in terms of characteristic functions since Eq. (12) provides a simple relation between the variance and the value of $\Phi(\beta)$. Testing the definiteness of matrices of moments requires complex nonlinear procedures, for instance, the calculation of the smallest eigenvalue or the principal minors. This leads to complications in the estimation of the statistical significance, which increase the computational effort. For matrices of high orders the resulting errors are large and they may hide the sought nonclassical effects.

ACKNOWLEDGMENT

We thank J. Fiurášek for many helpful discussions.

APPENDIX: SAMPLING FORMULA FOR NORMALLY ORDERED MOMENTS

The characteristic function $\Phi(\beta)$ can be given in terms of normally ordered moments of the creation and annihilation operator [14],

$$\Phi(\beta)=\sum_{k=0}^{\infty}\frac{1}{k!}\langle:(\beta\hat{a}^{\dagger}-\beta^{*}\hat{a})^{k}:\rangle. \tag{A1}$$

Introducing the phase-dependent quadrature operator $\hat{x}(\varphi)=\hat{a}^{\dagger}e^{-i\varphi}+\hat{a}e^{i\varphi}$, we have

$$\Phi(\beta)=\sum_{k=0}^{\infty}\frac{(i|\beta|)^{k}}{k!}\left\langle:\hat{x}\left[\frac{\pi}{2}-\arg(\beta)\right]^{k}:\right\rangle. \tag{A2}$$

Consequently, the normally ordered moments $\langle:\hat{x}(\varphi)^{k}:\rangle$ can be calculated from the characteristic function of the P function as

$$\langle:\hat{x}(\varphi)^{k}:\rangle=\frac{\partial^{k}}{\partial(ib)^{k}}\Phi(ibe^{-i\varphi})|_{b=0}. \tag{A3}$$

To obtain a formula which can be applied in practice, we insert Eq. (10) into Eq. (A3) and use the definition of the Hermite polynomials in the form $(-1)^{k}H_{k}(\xi)e^{-\xi^{2}}=\frac{\partial^{k}}{\partial\xi^{k}}e^{-\xi^{2}}$ with $\xi=ib/\sqrt{2}$. Neglecting the phase argument, we find

$$\begin{aligned}\langle:\hat{x}^{k}:\rangle&=\frac{\partial^{k}}{\partial(ib)^{k}}\langle e^{ib\hat{x}}\rangle e^{b^{2}/2}|_{b=0}\\&=\left\langle\frac{\partial^{k}}{\partial(\sqrt{2}\xi)^{k}}e^{-[\xi-\hat{x}/\sqrt{2}]^{2}}e^{\hat{x}^{2}/2}\right\rangle\Bigg|_{\xi=0}\\&=\left\langle\frac{(-1)^{k}}{2^{k/2}}H_{k}\left(\xi-\frac{\hat{x}}{\sqrt{2}}\right)\exp\left(-\left[\xi-\frac{\hat{x}}{\sqrt{2}}\right]^{2}\right)\exp\left(\frac{\hat{x}^{2}}{2}\right)\right\rangle\Bigg|_{\xi=0}\\&=\frac{1}{2^{k/2}}\left\langle H_{k}\left(\frac{\hat{x}}{\sqrt{2}}\right)\right\rangle.\end{aligned} \tag{A4}$$

Hence, we obtain normally ordered moments from measured quadratures via

$$\langle:\hat{x}^{k}:\rangle\approx\frac{1}{2^{k/2}N}\sum_{j=1}^{N}H_{k}\left(\frac{x_{j}}{\sqrt{2}}\right). \tag{A5}$$

The approximation sign indicates that the right-hand side is a statistical estimator.

[1] E. Schrödinger, Naturwiss. **14**, 664 (1926).
[2] E. C. G. Sudarshan, Phys. Rev. Lett. **10**, 277 (1963).
[3] R. J. Glauber, Phys. Rev. **131**, 2766 (1963).
[4] U. M. Titulaer and R. J. Glauber, Phys. Rev. **140**, B676 (1965).
[5] T. Kiesel, W. Vogel, V. Parigi, A. Zavatta, and M. Bellini, Phys. Rev. A **78**, 021804(R) (2008).
[6] A. Zavatta, V. Parigi, and M. Bellini, Phys. Rev. A **75**, 052106 (2007).
[7] A. Franzen, B. Hage, J. DiGuglielmo, J. Fiurášek, and R. Schnabel, Phys. Rev. Lett. **97**, 150505 (2006).
[8] B. Hage, A. Franzen, J. DiGuglielmo, P. Marek, J. Fiurášek, and R. Schnabel, New J. Phys. **9**, 227 (2007).
[9] W. Vogel, Phys. Rev. Lett. **84**, 1849 (2000).
[10] C. K. Hong and L. Mandel, Phys. Rev. Lett. **54**, 323 (1985).
[11] G. S. Agarwal, Opt. Commun. **95**, 109 (1993).
[12] J. Fiurášek, P. Marek, R. Filip, and R. Schnabel, Phys. Rev. A **75**, 050302(R) (2007).
[13] T. Richter and W. Vogel, Phys. Rev. Lett. **89**, 283601 (2002).
[14] W. Vogel and D.-G. Welsch, *Quantum Optics* (Wiley-VCH, Weinheim, 2006).
[15] A. I. Lvovsky and J. H. Shapiro, Phys. Rev. A **65**, 033830 (2002).
[16] E. V. Shchukin and W. Vogel, Phys. Rev. A **72**, 043808 (2005).
[17] X. Yang, T. K. Sarkar, and E. Arvas, IEEE Trans. Acoust., Speech, Signal Process. **37**, 1550 (1989).
[18] J. Shao and D. Tu, *The Jackknife and Bootstrap* (Springer, New York, 1995).

PHYSICAL REVIEW A **82**, 032107 (2010)

Nonclassicality filters and quasiprobabilities

T. Kiesel and W. Vogel
Arbeitsgruppe Quantenoptik, Institut für Physik, Universität Rostock, D-18051 Rostock, Germany
(Received 1 April 2010; published 13 September 2010)

Necessary and sufficient conditions for the nonclassicality of bosonic quantum states are formulated by introducing nonclassicality filters and nonclassicality quasiprobability distributions. Regular quasiprobabilities are constructed from characteristic functions which can be directly sampled by balanced homodyne detection. Their negativities uncover the nonclassical effects of general quantum states. The method is illustrated by visualizing the nonclassical nature of a squeezed state.

DOI: 10.1103/PhysRevA.82.032107 PACS number(s): 03.65.Ta, 03.65.Wj, 42.50.Dv

I. INTRODUCTION

The foundations of quantum theory have been known for several decades, but the relation to classical physics is still a topic of current research. In quantum optics, the notion of nonclassicality caused long-lasting discussions. The quantum state of a radiation field is often examined by means of photodetectors which measure normally ordered field-correlation functions. The latter are properly described by the quasiprobability distribution or P function of Sudarshan [1] and Glauber [2]. Following Titulaer and Glauber [3], "states with positive P functions . . . are . . . possessing classical analogs." The other way around, a quantum state is nonclassical if the P function does not exhibit the properties of a classical probability distribution (cf., e.g., [4]).

Any quantum state of a harmonic oscillator can be given as a quasimixture of coherent states $|\alpha\rangle$:

$$\hat{\rho} = \int d^2\alpha\, P(\alpha)|\alpha\rangle\langle\alpha|, \tag{1}$$

where $P(\alpha)$ is the P function mentioned earlier (cf. [1,2]). The coherent state is known to be that quantum state which is most closely related to the classical behavior of an oscillator. Its P function is formally equivalent to the deterministic classical phase-space distribution, representing a single point in phase space. If the P function has the properties of a classical probability density, $P(\alpha) \equiv P_{\rm cl}(\alpha)$, the state is a true classical mixture of coherent states. Hillery has shown that the coherent states are the only pure quantum states having a non-negative P function [5]. Hence, for any classical mixture of coherent states, the P function exactly reflects the classical behavior of the oscillator in phase space—including its free evolution. The failure of the interpretation of $P(\alpha)$ as a probability density, $P(\alpha) \neq P_{\rm cl}(\alpha)$, is intimately related to the quantum superposition principle; thus it most naturally displays the quantumness of any quantum state.

However, in general, the P function can only be understood as a generalized function which is often not accessible. For this reason, different representations of a quantum state are considered. An often used one is the Wigner function [6], which also covers the full information on the quantum state. A generalization yields the set of s-parametrized quasiprobability distributions [7]. By fixing the parameter s, different quasiprobabilities are obtained. If one of these functions violates the requirements of a classical probability distribution, the given state is nonclassical. Unfortunately, this set of functions does not reveal all nonclassical effects in terms of regular functions: For a squeezed state, they are either non-negative or highly singular. In order to develop quasiprobabilities to uncover nonclassicality in general, the generalized quasiprobabilities of Agarwal and Wolf will be a powerful foundation [8].

Another general representation of a quantum state is its characteristic function, defined as the Fourier transform of a given quasiprobability. Its advantage lies in the fact that it is always a regular function, even the characteristic function of an irregular nonclassical P function. Useful nonclassicality conditions have been derived [9,10] and applied in experiments [11–13]. However, for a full characterization of nonclassicality, one needs to check an infinite hierarchy of conditions, which may be a cumbersome procedure. We will use them as the starting point for our examination.

In this article, we introduce regular quasiprobabilities with the aim to uncover all types of nonclassical effects by their negativities. A distribution of this type, to be called nonclassicality quasiprobability, belongs to the set of the Agarwal-Wolf quasiprobabilities. For our purposes, the filter functions occurring in the latter must obey specific constraints. We study the properties which are needed to make the filters useful for experimental applications, and we show how to construct them.

The article is structured as follows. In Sec. II, we introduce the requirements for general nonclassicality filters and discuss the relation to previously known filter procedures. Section III is devoted to nonclassicality quasiprobabilities, which, in addition, contain full information about the quantum state. The method is illustrated for the example of a squeezed vacuum state. In Sec. IV, we briefly summarize our results.

II. NONCLASSICALITY FILTERS

A. Characteristic functions and Bochner's theorem

Let us now consider the possibility of getting general insight into the properties of the P function in an experiment. The characteristic function $\Phi(\beta)$, defined as the Fourier transform of $P(\alpha)$, can be sampled by balanced homodyne detection (cf. [13,14]). From a set of quadrature data $\{x_j(\varphi)\}_{j=1}^N$ at some fixed phases φ, it can be estimated by

$$\Phi(\beta) = \frac{1}{N}\sum_{j=1}^{N} e^{i|\beta|x_j[\pi/2-\arg(\beta)]} e^{|\beta|^2/2}. \tag{2}$$

Thus we have direct experimental access to the characteristic function Φ. It may be a rising function of $|\beta|$ whose Fourier transform only exists as a highly singular distribution [13]. The standard deviation of Φ is, for a given sample of data, bounded by [14]

$$\sigma\{\Phi(\beta)\} \leqslant \frac{e^{|\beta|^2/2}}{\sqrt{N}}. \tag{3}$$

Interestingly, also, the characteristic function $\Phi(\beta)$ of any quantum state is bounded by $e^{|\beta|^2/2}$ [15].

If $\Phi(\beta)$ is not square integrable, its Fourier transform is highly singular. In such cases, the nonclassicality of the quantum state can be identified via Bochner's theorem [16]. The function $\Phi(\beta)$ is in general continuous, with $\Phi(0) = 1$, $\Phi(-\beta) = \Phi^*(\beta)$. The P function has the properties of a probability density if and only if, for all positive integers N and complex $\beta_1, \ldots, \beta_N$, the matrix $(\Phi(\beta_i - \beta_j))_{i,j=1,\ldots,N}$ is positive semidefinite. This leads to an infinite hierarchy of nonclassicality conditions [10] which in practice cannot be examined completely. However, for $N = 2$, we obtain a simple inequality which is valid for all β and necessary for classicality [9]:

$$|\Phi(\beta)| \leqslant 1. \tag{4}$$

The violation of this inequality can be used to experimentally demonstrate the nonclassicality of a quantum state [11–13].

In cases when the inequality (4) is fulfilled, one cannot directly infer classicality, but there is a chance that the characteristic function is square integrable. A prominent example are the photon-added thermal states [17]. Then one can perform the Fourier transform to obtain the P function and check nonclassicality by its original definition [14]. Severe problems occur to identify nonclassicality if the characteristic function satisfies (4) but is not square integrable.

B. Filtered P functions

Let us now develop a simple and general method for identifying the nonclassicality of a quantum state under realistic experimental conditions. It is based on filtering of the characteristic function:

$$\Phi_\Omega(\beta; w) = \Phi(\beta)\Omega_w(\beta), \tag{5}$$

with a filter function $\Omega_w(\beta)$, which we will allow to depend on a real parameter w. The filter shall satisfy the following specific properties:

(a) *Universality.* For any quantum state, the filtered characteristic function $\Phi_\Omega(\beta; w)$ is square integrable such that its Fourier transform, $P_\Omega(\beta; w)$, is a well-behaved function. Since $\Phi(\beta)$ and its standard deviation [cf. Eq. (3)] are bounded by $e^{|\beta|^2/2}$, we need that $\Omega_w(\beta)e^{|\beta|^2/2}$ is square integrable for all w. This ensures that the method is universal: It applies to any quantum state and to realistic experimental data.

(b) *Non-negativity.* To detect nonclassicality of unknown quantum states by negativities in the regularized function $P_\Omega(\beta; w)$, the latter shall be non-negative for all classical states. Equivalently, the filter $\Omega_w(\beta)$ shall not cause additional negativities in the regularized function P_Ω. This requires that $\Omega_w(\beta)$ itself has a non-negative Fourier transform.

(c) *Completeness with respect to the nonclassicality of the P function.* The parameter w represents the width of the filter. It may be introduced by a scaling transform:

$$\Omega_w(\beta) = \Omega_1(\beta/w). \tag{6}$$

For an infinitely wide filter, the P_Ω function approaches the original P function. This requires, for all β, that

$$\lim_{w\to\infty} \Phi_\Omega(\beta; w) = \Phi(\beta), \tag{7}$$

or equivalently, $\Omega_w(0) = 1$ and $\lim_{w\to\infty} \Omega_w(\beta) = 1$.

The most simple example of such a filter is a two-dimensional triangular filter, $\Omega_w(\beta_r + i\beta_i) = \mathrm{tri}(\beta_r/w)\mathrm{tri}(\beta_i/w)$, where $\mathrm{tri}(x) = 1 - |x|$ for $|x| < 1$ and $\mathrm{tri}(x) = 0$ elsewhere. Since this function has compact support for all $w > 0$, it satisfies the condition (a). Furthermore, it obeys the constraints (b) and (c) since the Fourier transform of the triangular function is non-negative and $\lim_{w\to\infty} \Omega_w(\beta) = 1$, respectively.

This example clearly shows that there exist filters which satisfy all our requirements. Most interestingly, they can be used to detect nonclassicality of any nonclassical state. The other way around, the negativities are uniquely caused by the nonclassicality of the state, not by the filter. For all nonclassical states, we can find a regularized function P_Ω which displays negativities. We refer to such filters $\Omega_w(\beta)$ as nonclassicality filters. For the proof of their general properties, we refer the readers to Theorem 1 in Appendix A.

C. Relation to known filtering procedures

Filtering procedures of the P function having the structure of Eq. (5) are already known. However, there is no procedure known that fulfills all the requirements (a)–(c). Let us briefly consider such filtering approaches together with their shortcomings for nonclassicality detection. Note that the following approaches had not been designed for that purpose.

By choosing $\Omega_s(\beta) = \exp[(s-1)|\beta|^2/2]$ as a family of filters, we consider the s-parametrized quasiprobabilities [7]. For $s = 0$, we get the Wigner function; for $s = 1$, the P function; and for $s = -1$, the Q function. It is obvious that such filters do not fulfill the universality condition (a) for $s \geqslant 0$. Therefore they are not capable of regularizing the P function of an arbitrary state for $s > 0$. There exist nonclassical states which do not possess a regular s-parametrized quasiprobability showing negativities. Squeezed states are a prominent example. If their nonclassical effects would already be displayed for $s = 0$, they could be observed as negativities in the Wigner function. However, the Wigner function of a squeezed state is always non-negative.

Another filter was considered by Klauder [18]. He showed that appropriate filtering of the P function may lead to an infinitely differentiable regular function. This filtering was recently applied to regularize the P function of a squeezed state [19]. However, since Klauder's filtering does not obey the non-negativity condition (b), the corresponding negativities of the regularized functions are not uniquely related to the nonclassicality of the considered quantum state.

Last but not least, a very general approach to define quasiprobabilities and operator ordering was introduced by

Agarwal and Wolf [8]. This may be considered as a general background of our considerations. Since the authors' aim was to provide general methods, they did not consider constraints of the type needed for the nonclassicality filtering.

III. NONCLASSICALITY QUASIPROBABILITIES

A. Filters for quasiprobabilities

Filters with compact support can be easily applied to experimental data. However, one loses information about the quantum state such that the latter cannot be recovered completely from a filtered P function. To overcome this problem, one has to use invertible nonclassicality filters. They have to meet the criteria of Agarwal and Wolf [8], in particular, having no zeros anywhere, in order to preserve all information about the state.

To our knowledge, no simple examples for such filters are known, but they can be constructed in the following way: Let us assume that some positive continuous function $\omega(\beta)$ satisfies $\omega(-\beta)=\omega(\beta)$ and decays sufficiently fast; that is, $\omega(\beta)e^{u|\beta|^2}$ is square integrable for any $u>0$. For example, one may choose

$$\omega(\beta)=\exp(-|\beta|^4). \tag{8}$$

It is easy to see that its autocorrelation function,

$$\Omega(\beta)=\frac{1}{\mathcal{N}}\int \omega(\beta')\omega(\beta+\beta')d^2\beta', \tag{9}$$

with $\mathcal{N}=\int|\omega(\beta)|^2d^2\beta$, is positive and satisfies $\Omega(-\beta)=\Omega(\beta)$. Moreover, we find that $\Omega(0)=1$ and the Fourier transform of an autocorrelation function is always non-negative. Finally, it decays sufficiently fast so that $\Omega(\beta)e^{u|\beta|^2}$ is square integrable for any $u>0$ (cf. Lemma 1 in Appendix B).

Now we define a set of functions by

$$\Omega_w(\beta)=\Omega(\beta/w),\quad w>0. \tag{10}$$

Since $\Omega_w(\beta)$ is continuous, the sequence of functions converges for all β pointwise to 1 when $w\to\infty$:

$$\lim_{w\to\infty}\Omega_w(\beta)=\lim_{w\to\infty}\Omega(\beta/w)=\Omega(0)=1. \tag{11}$$

Hence these functions satisfy all criteria for being a nonclassicality filter. Since $\Omega_w(\beta)$ has no zeros, the regularized function P_Ω contains all the information about the quantum state, and consequently, it represents a generalized phase-space function in the sense of Agarwal and Wolf [8]. Therefore, for any nonclassical state, one can find a regular quasiprobability distribution which displays the nonclassical character by its negativities. We refer to such distributions as nonclassicality quasiprobabilities.

The experimental implementation of the procedure to identify nonclassicality of a general and unknown quantum state is straightforward:

(A) *Sampling.* Direct sampling of the function $\Phi(\beta)$ from experimental data [Eq. (2)] and estimation of its standard deviation [cf. Eq. (3)].

(B) *Filtering.* Choose the set of nonclassicality filters $\Omega_w(\beta)$, for example, the autocorrelation filters in Eqs. (8)–(10). Multiply the sampled $\Phi(\beta)$ with the filter of width w: $\Phi_\Omega(\beta;w)=\Phi(\beta)\Omega_w(\beta)$. The single parameter w is used to optimize the statistical significance of the nonclassical effects to be visualized.

(C) *Fourier transform.* Calculate the Fourier transform P_Ω of Φ_Ω and its statistical error. If it displays statistically significant negativities, the state is clearly nonclassical. The wider the filter, the more nonclassical effects are visible in the regularized function P_Ω, which is only limited by the increasing sampling noise.

B. Example: Squeezed vacuum state

For illustration, let us consider a squeezed vacuum state, described by a characteristic function

$$\Phi(\beta)=\exp[-(\beta+\beta^*)^2V_x/8+(\beta-\beta^*)^2V_p/8+|\beta|^2/2], \tag{12}$$

where V_x and V_p are the variances of two orthogonal quadratures and $V_x<1<V_p$. The P function is highly singular: It is composed of derivatives up to infinite orders of the Dirac δ distribution. Hence it is extremely difficult to verify the nonclassicality of a squeezed vacuum state in this general sense.

All s-parametrized quasiprobability distributions are either Gaussian or highly singular, and therefore none of them has negativities which can be directly reconstructed. Let us now consider a squeezed state with $V_x=0.2$ and $V_p=5.0$, which can be experimentally realized. We construct the filters by Eqs. (8)–(10), with a single control parameter w. Figure 1 shows cross sections of the filtered characteristic functions for two filter widths, $w=1.2$ and $w=1.5$. The broad and narrow curves correspond to the squeezed and antisqueezed axes, respectively. Without regularization, Φ grows exponentially in the direction of the squeezed axis, whereas the filtered function Φ_Ω is square integrable.

Cross sections of the resulting nonclassicality quasiprobabilities P_Ω are given in Fig. 2. For both filter widths, they clearly display negativities which have their origin solely in the nonclassicality of the squeezed state. The larger the width of the filter, the more pronounced the negativities become. In practice, the filter width is only limited by the experimental

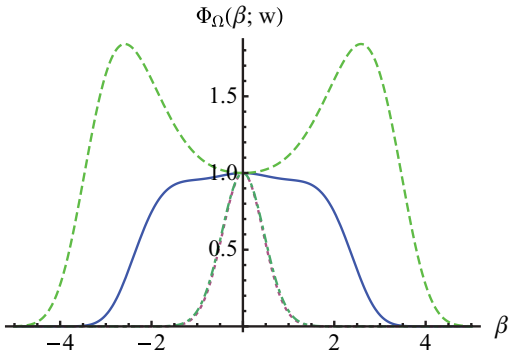

FIG. 1. (Color online) Cross sections of filtered characteristic functions Φ_Ω of a squeezed state with $V_x=0.2$, $V_p=5.0$. The solid line shows Φ_Ω along the squeezed axis with a filter width $w=1.2$, the dashed line with $w=1.5$. The narrow curves belong to the unsqueezed axis.

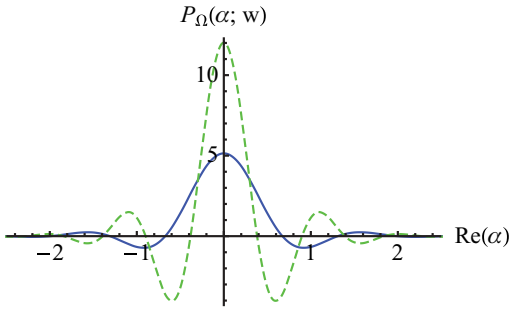

FIG. 2. (Color online) Nonclassicality quasiprobabilities P_Ω of a squeezed state with $V_x = 0.2$, $V_p = 5.0$ along the squeezed axis. The solid curve is obtained with a filter width $w = 1.2$, the dashed one with $w = 1.5$. The negativities unambiguously visualize the nonclassicality of the squeezed state.

uncertainties: It should be sufficiently small to keep the statistical error at a reasonable level.

We stress that the decisive point in our procedure is that the filter has a non-negative Fourier transform. As a consequence, in our approach, the negativities of the filtered function P_Ω can only be due to the nonclassicality of the quantum state under study. In this respect, our method differs from previous regularizations of the P function, for example, the one by Klauder [18], where the used filter has negativities in its Fourier transform. Consequently, negativities of the regularized function P_Ω do not definitely display the nonclassicality of the state. For example, the filtered P function of a coherent state is the displaced Fourier transform of the filter itself. It always shows negativities, even for the only classical pure state. Recently, the P function of a squeezed state has been regularized by such a filter [19]. The obtained negativities, however, cannot be interpreted as the nonclassicality of the state itself.

In another experiment, the (in this case regular) P function of a single-photon added thermal state has been reconstructed by using a rectangular filter [14]. This requires prior knowledge about the state to estimate the systematic error caused by the regularization, in order to ensure the significance of the nonclassical effects. With the methods introduced here, the negativities visualize the nonclassicality without any prior knowledge about the state.

The extension of our methods to several radiation modes is straightforward. The nonclassicality displayed by the nonclassicality quasiprobabilities also includes entanglement. To directly display entanglement, negativities of entanglement quasiprobabilities can be used [20]. Together with the present method, this yields powerful tools for characterizing quantum systems which are useful for various applications.

IV. SUMMARY

We have introduced necessary and sufficient conditions for the nonclassicality of a quantum state which can be directly applied in experiments. Universal nonclassicality filters and regular nonclassicality quasiprobabilities have been introduced which display the nonclassicality of any quantum state without prior knowledge of its properties. We have constructed experimentally useful filter functions which only depend on a single width parameter. The nonclassical properties of a squeezed state have been visualized by negativities of regular functions, which is impossible with s-parametrized quasiprobabilities.

ACKNOWLEDGMENTS

This work was supported by the Deutsche Forschungsgemeinschaft through SFB 652. We are grateful to J. Sperling for valuable comments.

APPENDIX A: GENERAL PROPERTIES OF NONCLASSICALITY FILTERS

The approach we are developing shall be applicable to any quantum state, also on the basis of experimental data. This was already demonstrated in the main text. In addition, negativities of regular functions should prove nonclassicality in a one-to-one manner.

Theorem 1. The P function describes a nonclassical state if and only if the regularized function $P_\Omega(\beta; w)$ shows negativities for a sufficiently large but finite filter width w.

Proof. Let us assume that a state given by its characteristic function $\Phi(\beta)$ is nonclassical. Owing to Bochner's theorem, this implies that [10]

$$\exists N \in \mathbb{N}, \beta_1, \ldots, \beta_N \in \mathbb{C}: \quad D_N = \det\{(\Phi(\beta_i - \beta_j))_{i,j=1,\ldots,N}\} < 0. \tag{A1}$$

Let us take a sequence of filters $\Omega_w(\beta)$ which satisfies all the properties (a)–(c). Then we have for N and $\beta_1, \ldots, \beta_N$ as chosen in Eq. (A1),

$$\lim_{w\to\infty} \det\{(\Phi(\beta_i - \beta_j)\Omega_w(\beta_i - \beta_j))_{i,j=1,\ldots,N}\} = D_N < 0. \tag{A2}$$

Since the determinant is a continuous function, there must exist a finite $w_0 > 0$ such that

$$\det\{(\Phi(\beta_i - \beta_j)\Omega_{w_0}(\beta_i - \beta_j))_{i,j=1,\ldots,N}\} < 0. \tag{A3}$$

Hence we have found a filter $\Omega_{w_0}(\beta)$ such that the filtered state $\Phi_\Omega(\beta; w_0)$ is nonclassical. Since its Fourier transform $P_\Omega(\beta; w_0)$ is a regular function but not a probability density, it must show negativities to display nonclassicality.

The other way around, if $\Phi(\beta)$ represents a classical quantum state, its characteristic function satisfies the conditions of Bochner's criterion. Furthermore, each filter $\Omega_w(\beta)$ shall have a non-negative Fourier transform, and hence it also satisfies the conditions of Bochner. Under these assumptions, it is immediately clear that $\Phi_\Omega(\beta; w)$ also satisfies $\Phi_w(-\beta) = \Phi_w^*(\beta)$ and $\Phi_w(0) = 1$. Moreover, the matrix $(\Phi_\Omega(\beta_i - \beta_j; w))_{i,j=1,\ldots,N}$ is the Hadamard product of the matrices $(\Phi(\beta_i - \beta_j))_{i,j=1,\ldots,N}$ and $(\Omega_w(\beta_i - \beta_j))_{i,j=1,\ldots,N}$. If the latter two matrices are positive semidefinite, their Hadamard product is also positive semidefinite. Consequently, $\Phi_\Omega(\beta; w)$ satisfies the conditions of Bochner's theorem. Hence, for any classical state with a positive semidefinite P function, the regularized function $P_\Omega(\beta; w)$ is a classical probability distribution showing no negativities. ∎

APPENDIX B: DECAY PROPERTIES OF AUTOCORRELATION FILTERS

Here we prove the following lemma, which has been used for introducing nonclassicality quasiprobabilities.

Lemma 1. Let u be a real positive number and $\omega(\beta)$ a real function which satisfies $C = \|\omega(\beta)e^{u|\beta|^2}\|_2 < \infty$, where $\|\cdot\|_2$ is the L^2 norm. Then the autocorrelation function of $\omega(\beta)$,

$$\Omega(\alpha) = \int \omega(\beta)\omega(\alpha+\beta)d^2\beta, \tag{B1}$$

satisfies $\|\Omega(\alpha)e^{v|\alpha|^2}\|_2 < \infty$ for any real $v < u/2$.

Proof. The autocorrelation function can be rewritten in the following way:

$$\Omega(\alpha) = \int \omega(\beta)e^{u|\beta|^2}\omega(\alpha+\beta)e^{u|\alpha+\beta|^2} \times e^{-u|2\beta+\alpha|^2/2}d^2\beta e^{-u|\alpha|^2/2}. \tag{B2}$$

It is bounded from above by

$$|\Omega(\alpha)| \leqslant \|\omega(\beta)e^{u|\beta|^2}\omega(\alpha+\beta)e^{u|\alpha+\beta|^2}e^{-u|2\beta+\alpha|^2/2}\|_1 e^{-u|\alpha|^2/2}, \tag{B3}$$

with $\|\cdot\|_1$ being the L^1 norm. Applying Hölder's inequality [21] in the form $\|fgh\|_1 \leqslant \|f\|_2\|g\|_2\|h\|_\infty$ with $f(\beta) = \omega(\beta)e^{u|\beta|^2}$, $g(\beta) = \omega(\alpha+\beta)e^{u|\alpha+\beta|^2}$, and $\|e^{-u|2\beta+\alpha|^2/2}\|_\infty = 1$, gives

$$|\Omega(\alpha)| \leqslant C^2 e^{-u|\alpha|^2/2}. \tag{B4}$$

Since C is finite, we have

$$\|\Omega(\alpha)e^{v|\alpha|^2}\|_2 \leqslant C^2\|e^{(v-u/2)|\alpha|^2}\|_2, \tag{B5}$$

where the right-hand side is finite if $v < u/2$. ∎

Remark. If $\omega(\beta)$ satisfies the requirements of Lemma 1 for all $u > 0$, the same holds also for $\Omega(\beta)$.

[1] E. C. G. Sudarshan, Phys. Rev. Lett. **10**, 277 (1963).
[2] R. J. Glauber, Phys. Rev. **131**, 2766 (1963).
[3] U. M. Titulaer and R. J. Glauber, Phys. Rev. **140**, B676 (1965).
[4] L. Mandel, Phys. Scr. T **12**, 34 (1986).
[5] M. Hillery, Phys. Lett. A **111**, 409 (1985).
[6] E. Wigner, Phys. Rev. **40**, 749 (1932).
[7] K. E. Cahill and R. J. Glauber, Phys. Rev. **177**, 1882 (1969).
[8] G. S. Agarwal and E. Wolf, Phys. Rev. D **2**, 2161 (1970).
[9] W. Vogel, Phys. Rev. Lett. **84**, 1849 (2000).
[10] T. Richter and W. Vogel, Phys. Rev. Lett. **89**, 283601 (2002).
[11] A. I. Lvovsky and J. H. Shapiro, Phys. Rev. A **65**, 033830 (2002).
[12] A. Zavatta, V. Parigi, and M. Bellini, Phys. Rev. A **75**, 052106 (2007).
[13] T. Kiesel, W. Vogel, B. Hage, J. DiGuglielmo, A. Samblowski, and R. Schnabel, Phys. Rev. A **79**, 022122 (2009).
[14] T. Kiesel, W. Vogel, V. Parigi, A. Zavatta, and M. Bellini, Phys. Rev. A **78**, 021804(R) (2008).
[15] A. M. Perelomov, *Generalized Coherent States and Their Applications* (Springer-Verlag, Berlin, New York, 1986).
[16] S. Bochner, Math. Ann. **108**, 378 (1933).
[17] G. S. Agarwal and K. Tara, Phys. Rev. A **46**, 485 (1992).
[18] J. R. Klauder, Phys. Rev. Lett. **16**, 534 (1966).
[19] M. Lobino, D. Korystov, C. Kupchak, E. Figueroa, B. C. Sanders, and A. I. Lvovsky, Science **322**, 563 (2008).
[20] J. Sperling and W. Vogel, Phys. Rev. A **79**, 042337 (2009).
[21] K. Yosida, *Functional Analysis* (Springer, Berlin, New York, 1995).

PHYSICAL REVIEW A **83**, 032116 (2011)

Nonclassicality quasiprobability of single-photon-added thermal states

T. Kiesel and W. Vogel
Arbeitsgruppe Quantenoptik, Institut für Physik, Universität Rostock, D-18051 Rostock, Germany

M. Bellini and A. Zavatta
Istituto Nazionale di Ottica, INO-CNR, L.go E. Fermi, 6, I-50125, Florence, Italy and
LENS, Via Nello Carrara 1, I-50019 Sesto Fiorentino, Florence, Italy
(Received 10 January 2011; published 18 March 2011)

We report the experimental reconstruction of a nonclassicality quasiprobability for a single-photon-added thermal state. This quantity has significant negativities, which is necessary and sufficient for the nonclassicality of the quantum state. Our method exhibits several advantages compared to the reconstruction of the P function, since the nonclassicality filters used in this case can regularize the quasiprobabilities as well as their statistical uncertainties. *A priori* assumptions about the quantum state are therefore not necessary. We also demonstrate that, in principle, our method is not limited by small quantum efficiencies.

DOI: 10.1103/PhysRevA.83.032116 PACS number(s): 03.65.Wj, 42.50.Dv, 03.65.Ta, 42.50.Xa

I. INTRODUCTION

The relation between classical optics and quantum optics is a fundamental topic in modern physics. The notion of nonclassicality has been introduced by Titulaer and Glauber as the impossibility of describing optical field correlations of a specific state of light in terms of classical electrodynamics [1]. Therefore, nonclassical states are the prerequisite of quantum effects, which are of great interest in quantum optics and quantum information.

The definition of nonclassicality is based on the Glauber-Sudarshan phase-space representation of a quantum state $\hat{\rho}$,

$$\hat{\rho} = \int d^2\alpha\, P(\alpha)|\alpha\rangle\langle\alpha|, \tag{1}$$

where $|\alpha\rangle$ denote the well-known coherent states [2,3]. In general, $P(\alpha)$ is a quasiprobability. If it has the properties of a classical probability distribution, the state $\hat{\rho}$ is a statistical mixture of coherent states, which are closely related to the classical behavior of the oscillator. Conversely, a state is referred to as nonclassical if the P function shows some negativities. However, for many states, already for the single-photon state, this quantity is highly singular. Only in a few cases, when $P(\alpha)$ does not show singularities, it may be accessible from experimental data. Single-photon-added thermal states (SPATS) belong to such a class of states [4], so that their P function could be reconstructed for some parameters [5].

Due to the singularities of the P function, several different nonclassicality criteria have been developed. Simple inequalities often set bounds for classical states, which are violated for certain nonclassical states; we only mention bounds on moments, such as (higher-order) squeezing [6], and probability distributions [7]. However, violation of these criteria is only sufficient, but not necessary for verifying nonclassicality. On the other hand, there are complete hierarchies of criteria, often based on matrices of moments [8] or characteristic functions [9,10]. However, nobody is able to check such hierarchies completely, and practical application becomes involved for large matrices.

In [11], a novel approach for nonclassicality detection was developed, which was based on phase-space methods. It has been shown that for any nonclassical state, there exists a so-called nonclassicality quasiprobability which illustrates the nonclassical property by negativities. Moreover, it was shown that a family of nonclassicality distributions, parameterized by a real filter width w, enables one to decide whether a state is nonclassical or not. If a state is nonclassical, one can always find some finite filter width w, such that the nonclassicality is observable as a negativity of the corresponding nonclassicality quasiprobability. Our method is suitable for experimental application, since it incorporates correct handling of statistical uncertainties. Moreover, it does not require precognition about the state.

In the present paper we demonstrate, by experimental application, the capability of the method. We examine single-photon-added thermal states, whose P function could be reconstructed for a sufficiently large mean thermal photon number [5]. Here we overcome the problems occurring for arbitrary mean photon numbers, and therefore demonstrate the universality of the method of nonclassicality quasiprobabilities.

The paper is structured as follows: In Sec. II, we briefly review the approximate reconstruction of the P function of a SPATS and its limitations for relatively small mean photon numbers. In Sec. III, we discuss the concept of nonclassicality quasiprobabilities and apply it to experimental data. Eventually in Sec. IV, we consider the role of the quantum efficiency on the detection of nonclassicality. A summary and some conclusions are given in Sec. V.

II. APPROXIMATE RECONSTRUCTION OF *P* FUNCTIONS

Let us briefly recall the reconstruction of a Glauber-Sudarshan representation as presented in [5]. The starting point of the discussion was the characteristic function $\Phi(\beta)$ of a SPATS,

$$\Phi(\beta) = [1 - (1 + \bar{n})|\beta|^2]e^{-\bar{n}|\beta|^2}. \tag{2}$$

By Fourier transform the resulting P function is derived as

$$P(\alpha) = \frac{1}{\pi \bar{n}^3}[(1+\bar{n})|\alpha|^2 - \bar{n}]e^{-|\alpha|^2/\bar{n}}, \tag{3}$$

which is a regular function.

Experimental data were used for a mean photon number of $\bar{n} = 1.11$ and a quantum efficiency of $\eta = 0.60$. The function $\Phi(\beta)$ was readily obtained from measured quadratures $\{x_j\}_{j=1}^N$ via

$$\Phi(\beta) = \frac{e^{|\beta|^2/2}}{N}\sum_{j=1}^{N} e^{i|\beta|x_j}. \tag{4}$$

It was directly sampled from 10^5 data points. We observe that the experimentally obtained curve tends to zero within a fraction of its standard deviation,

$$\sigma^2\{\Phi(\beta)\} = \frac{1}{N}[e^{|\beta|^2} - |\Phi(\beta)|^2]. \tag{5}$$

However, the latter grows exponentially with $|\beta|^2$. In order to calculate the Glauber-Sudarshan P function via Fourier transform,

$$P(\alpha) = \frac{1}{\pi^2}\int d^2\beta e^{\alpha\beta^* - \alpha^*\beta}\Phi(\beta), \tag{6}$$

one has to regularize $\Phi(\beta)$. In our previous work, we simply cut off $\Phi(\beta)$ for $|\beta| > |\beta_c|$. This is equivalent to the multiplication of $\Phi(\beta)$ with a rectangular filter, $\Omega_{\text{rect}}(\beta)$, with $\Omega_{\text{rect}}(\beta) = 1$ for $|\beta| < |\beta_c|$ and $\Omega_{\text{rect}}(\beta) = 0$ elsewhere. However, this method can only be applied in special cases. First, the state must be described by a well-behaved P function, and its characteristic function has to decay sufficiently fast in order to justify the cutoff regularization. If this is not the case, one cannot perform the Fourier transform to obtain a P function. Second, the systematic error has to be estimated by some assumptions on the behavior of the characteristic function for large β. We used the theoretical expectation of the characteristic function with properly chosen parameters. For a completely unknown state, such a procedure becomes meaningless. In the case of the SPATS, we obtained the P function for mean thermal photon numbers of $\bar{n} \geqslant 1$ (for details see [5]).

For smaller mean thermal photon numbers the reconstruction of the P function faces severe limitations. The smaller $\bar{n}$, the broader the characteristic function becomes, and the larger is the statistical uncertainty at a reasonable cutoff parameter. Therefore, one cannot find a useful trade-off between the systematic and the statistical error. The former increase with lower $|\beta_c|$, and the statistical uncertainty is growing with larger $|\beta_c|$. For an example we refer the reader to the end of the next section. Under such circumstances, other nonclassicality criteria can be applied [10], which are sufficient but not necessary.

III. NONCLASSICALITY QUASIPROBABILITIES

From a more general perspective to be used in the following, we may multiply the characteristic function by a filter function $\Omega(\beta)$,

$$\Phi_\Omega(\beta) = \Phi(\beta)\Omega(\beta). \tag{7}$$

For a general study of such a scenario cf. [12]. The special case discussed so far is contained in this approach for a rectangular filter. To obtain a quasiprobability—including the full information on the quantum state under study—by Fourier transform of $\Phi_\Omega(\beta)$, the filter must not have zeros anywhere in the complex plane.

In view of the radial symmetry of our quantum states, the Fourier transform of $\Phi_\Omega(\beta)$ is given by

$$P_\Omega(\alpha) = \frac{2}{\pi}\int_0^\infty bJ_0(2b|\alpha|)\Phi_\Omega(b)db. \tag{8}$$

This function, together with its variance,

$$\sigma^2\{P_\Omega(\alpha)\} = \frac{1}{N}\left(\frac{4}{\pi^2}\int\int_0^\infty bb' J_0(2b|\alpha|)J_0(2b'|\alpha|)\Phi(b-b') \times e^{bb'}\Omega(b)\Omega(b')\,db'\,db - P_\Omega(\alpha)^2\right), \tag{9}$$

can be readily calculated from the set of data. This expression for the variance of the quasiprobability is readily derived from the statistical sampling of the characteristic function according to Eq. (4).

A. Concept of nonclassicality quasiprobability

Now we make use of the recently introduced concept of nonclassicality quasiprobabilities [11]. We introduce a so-called nonclassicality filter, $\Omega(\beta) \equiv \Omega_w(\beta)$, with the following properties:

(1) $\Omega_w(\beta)$ decays faster than $\exp(-|\beta|^2/2)$ for any filter width $w > 0$ in order to regularize the P function and its statistical uncertainty for any quantum state.

(2) The Fourier transform of $\Omega_w(\beta)$ is non-negative, such that negativities in the nonclassicality quasiprobability are unambiguously caused by the negativity of the state's P function.

(3) The parameter w scales the filter $\Omega_w(\beta)$ such that for $w \to \infty$ the filter approaches one. Practically, we implement this by $\Omega_1(0) = 1$, $\Omega_w(\beta) = \Omega_1(\beta/w)$.

(4) The support of $\Omega_w(\beta)$ is the complex plane, such that Eq. (7) is invertible for every β.

The first requirement ensures that the integrals in Eqs. (8) and (9) are finite, when the filter $\Omega(\beta)$ is identified with the nonclassicality filter $\Omega_w(\beta)$. The second condition makes sure that the negativity of $P_\Omega(\alpha)$ unambiguously represents the nonclassicality of the state. In contrast to this, a rectangular filter $\Omega_{\text{rect}}(\beta)$ does not have a non-negative Fourier transform. Hence, for such a filter negativities of $P_\Omega(\alpha)$ must not be interpreted as nonclassical effects without assumptions about the influence of the filter on the regularized P function. In [5], this made the estimation of systematic errors necessary. The third condition can be used for maximizing the significance of the observed nonclassical effects. On the one hand, a larger filter width w may increase the negativities in the regularized P function; on the other hand, this will definitely increase the variance. We may tune w in order to optimize the statistical significance S of the negativities, defined via

$$S = \frac{P_\Omega(\alpha)}{\sigma\{P_\Omega(\alpha)\}}. \tag{10}$$

The fourth requirement is of fundamental importance: It ensures that the regularized function $P_\Omega(\alpha)$ still contains the full information on the quantum state. Such P_Ω functions, which fulfill all the four conditions, we refer to as nonclassicality quasiprobabilities.

A proper nonclassicality filter can be constructed by the autocorrelation of a function $\omega(\beta)$,

$$\Omega_1(\beta) = \frac{1}{\mathcal{N}} \int d^2\beta' \omega(\beta')\omega(\beta + \beta'), \tag{11}$$

with the normalization $\mathcal{N} = \int d^2\beta' |\omega(\beta')|^2$. The width parameter is introduced by $\Omega_w(\beta) = \Omega_1(\beta/w)$. The positivity of its Fourier transform is guaranteed by the properties of any autocorrelation function. Furthermore, if $\omega(\beta)$ decays sufficiently fast, as required by condition (1), $\Omega_w(\beta)$ does as well. Therefore, by choosing

$$\omega(\beta) = e^{-|\beta|^4}, \tag{12}$$

and calculating the autocorrelation, we obtain a suitable representative of a nonclassicality filter.

B. Experimental preparation of SPATS

The single-photon-added thermal states are generated in a conditional way by exploiting the parametric amplification at the single-photon level in a nonlinear type-I β-barium borate (BBO) crystal pumped by the second harmonic of a mode-locked picosecond Ti:sapphire laser (see Fig. 1). When no extra field is injected in the crystal, a pump photon can be converted into two spontaneously and simultaneously generated photons (named signal and idler) correlated in frequency and in momentum. The click of the on-off avalanche photodetector D, which is placed in the idler path after narrow spectral and spatial filters (F), is used to conditionally prepare a single photon in a well-defined spatiotemporal mode of the signal channel [13,14].

On the other hand, if the parametric crystal is seeded with some light, described by the operator $\hat{\rho}_{\rm in}$, stimulated emission comes into play, and single-photon excitation of such a state, always converting it into a nonclassical one, is conditionally obtained when one photon is detected in the idler mode [15,16]. Field quadratures of the output signal state are then conditionally measured on a pulse-to-pulse basis using an ultrafast balanced homodyne detection scheme [17].

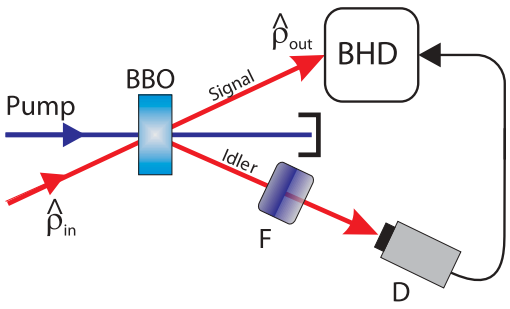

FIG. 1. (Color online) Scheme for the conditional excitation of a thermal light state (denoted by $\hat{\rho}_{\rm in}$) by a single photon. A click in the on-off detector D prepares the photon-added thermal state $\hat{\rho}_{\rm out}$ and triggers its balanced homodyne detection (BHD).

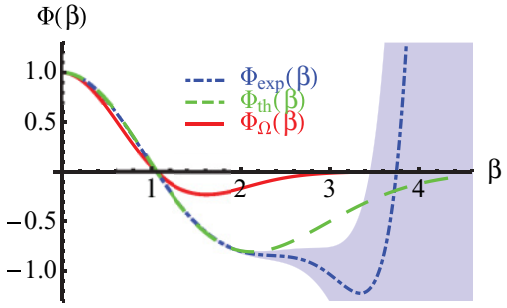

FIG. 2. (Color online) Characteristic functions of a SPATS with $\bar{n} = 0.49$ and $\eta = 0.62$: the experimental result $\Phi_{\rm exp}(\beta)$, the theoretical expectation $\Phi_{\rm th}(\beta)$, and the result $\Phi_\Omega(\beta)$ of filtering for the filter width $w = 1.4$. The shaded area corresponds to one standard deviation.

Here we used a pseudothermal source, obtained by inserting a rotating ground glass disk in a portion of the laser beam (see [10,18,19]), for injecting the parametric amplifier and producing SPATS.

C. Experimental nonclassicality quasiprobabilities

To illustrate the power of nonclassicality quasiprobabilities, let us consider a SPATS with $\bar{n} = 0.49$ and $\eta = 0.62$. In Fig. 2, we show the experimentally reconstructed characteristic function $\Phi_{\rm exp}(\beta)$. Obviously, the Fourier transform of this quantity does not exist as a regular function, since $\Phi_{\rm exp}(\beta)$ does not approach zero for large β as its theoretical expectation $\Phi_{\rm th}(\beta)$ does. This is due to the fact that the uncertainty grows exponentially. Although both the experimental result and the theoretical expectation agree within two standard deviations, the former may even diverge within the divergent noise level. In contrast to the results in [5], it is not obvious just from experimental data, that the characteristic function tends to zero for large β. Moreover, it is not possible to find a reasonable compromise between a low systematic error (requiring a large cutoff parameter $|\beta_c|$), and a statistical uncertainty being sufficiently small to obtain significant negativities in the filtered P function.

The application of the nonclassicality filter with a width $w = 1.4$ leads to an integrable characteristic function $\Phi_\Omega(\beta)$. We emphasize that the shown curve is obtained from the experimental data. We also calculated its standard deviation, which is included in the line thickness. Therefore, this function is suited for deriving the corresponding nonclassicality quasiprobability by Fourier transform. Figure 3 shows the result. We observe a distinct negativity at the origin of phase space, with a significance of 15 standard deviations. By the definition of nonclassicality quasiprobabilities, this negativity is solely due to the nonclassicality of the state.

We may also reconsider the data of the SPATS with $\bar{n} = 1.11$ by our filtering procedure. We obtain a nonclassicality quasiprobability $P_\Omega(\beta)$ which looks similar to the one in Fig. 3. By optimizing the filter width to $w = 1.3$, we get a maximum significance of 7.6 standard deviations, which exceeds that for the rectangular filter. More importantly, the estimation of a systematic error—which was previously needed for the

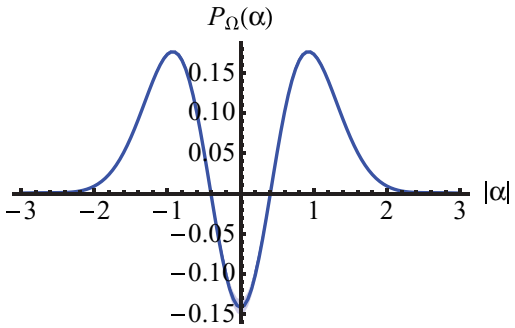

FIG. 3. (Color online) Nonclassicality quasiprobability of a SPATS for the same parameters as in Fig. 2. The blue shaded area corresponds to one standard deviation, which is almost completely hidden by the line thickness.

assessment of nonclassicality and had been based on *a priori* theoretical assumptions—now becomes superfluous.

D. Limits of rectangular filtering

For comparison, let us try to regularize the state with $\bar{n} = 0.49$ and $\eta = 0.62$, whose characteristic function is shown in Fig. 2, with a rectangular filter. Since this is not a nonclassicality filter of the type defined in Sec. III A, we have to consider the systematic error, which comes from the cutoff. From Fig. 2, two possible cutoff parameters may be reasonable: On the one hand, we may choose $|\beta_c| = 2.2$, since from this point the deviations of the theoretical and experimental characteristic functions $\Phi_{\text{th}}(\beta)$ and $\Phi_{\text{exp}}(\beta)$ grow strongly. The corresponding regularized P function with its standard deviation (shaded blue area) and systematic error (dark red area) is shown at the left side of Fig. 4. We clearly see that the statistical uncertainty is negligible, while the systematic error is partly even larger than the P function. Therefore, *a priori* assumptions about the state, which are the basis for the estimation of the systematic error, are crucial. Moreover, the systematic error is larger than the size of the negativity.

On the other hand, we may set $|\beta_c| = 3.8$, where the experimental characteristic function $\Phi_{\text{exp}}(\beta)$ is close to zero. The resulting P function is shown at the right side of Fig. 4.

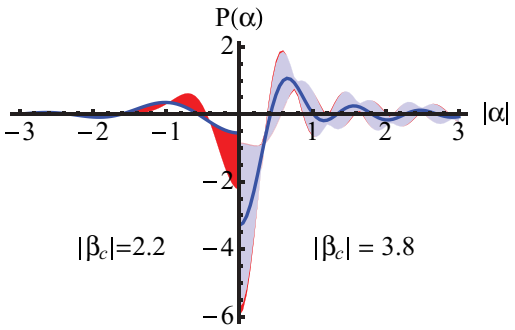

FIG. 4. (Color online) P functions regularized with a rectangular filter. The cutoff parameter at the left side of the figure is rather small, leading to large systematic errors (red shaded). For a larger cutoff parameter, the statistical uncertainty (blue shaded) becomes dominant; see the right side of the figure.

In this case, the systematic error is small, while the statistical uncertainty is dominating. The significance of the negativity of the filtered P function is less than 1.4 standard deviations.

Therefore, we are not able to obtain statistically significant negativities by applying a rectangular filter, if we simultaneously try to achieve low systematic errors due to the regularization. The reason is that the characteristic function of a state with such a small mean photon number approaches zero only for larger β, where the standard deviation is already extremely large. This problem can only be overcome by using suitable nonclassicality filter, which do not require the consideration of systematic errors in order to verify nonclassicality.

IV. INFLUENCE OF THE QUANTUM EFFICIENCY

Let us assume that the characteristic function $\Phi(\beta)$ describes a quantum state, but we measure this state with a nonunit quantum efficiency η. The characteristic function of the measured state is given by

$$\Phi(\beta;\eta) = \Phi(\sqrt{\eta}\beta). \tag{13}$$

Since the corresponding P function is the Fourier transform, this rescaling of β leads to a rescaling of the argument of the P function,

$$P(\alpha;\eta) = \frac{1}{\eta} P\left(\frac{\alpha}{\sqrt{\eta}}\right). \tag{14}$$

Therefore, a nonunit quantum efficiency does not degrade nonclassicality, and removal of losses from experimental data only rescales the P function, but does not affect its course and uncertainty. In contrast, this is not the case for the Wigner function whose negativities more and more disappear with decreasing η values.

How is the situation for nonclassicality quasiprobabilities? For answering this question, we note that the filtered characteristic function of a state, which suffered losses, reads as

$$\Phi_\Omega(\beta;\eta) = \Phi(\beta;\eta)\Omega_w(\beta) = \Phi(\sqrt{\eta}\beta)\Omega_1(\beta/w). \tag{15}$$

We observe that the characteristic function of the lossy state, $\Phi_\Omega(\beta;\eta)$, and the one of the ideal state, $\Phi_\Omega(\beta;1)$, are not connected by simple rescaling. However, they can be easily connected if one allows for rescaling the filter width as well:

$$\Phi_\Omega(\beta;\eta) = \Phi(\sqrt{\eta}\beta)\Omega_1((\sqrt{\eta}\beta)/(\sqrt{\eta}w)). \tag{16}$$

Hence, the characteristic function of a lossy state with some width w, which is on the left side of the equation, is given by the characteristic function of the ideal state with filter width $\sqrt{\eta}w$ by additionally rescaling the argument $\beta \to \sqrt{\eta}\beta$. Removing the losses by postprocessing and simultaneously adapting the width of the nonclassicality filter leads simply to scaled results with no better significance. Therefore, the removal of losses does not uncover nonclassical effects which do not already appear in the nonclassicality quasiprobabilities of the lossy state.

Finally, we note that our method may visualize nonclassicality even for rather small quantum efficiencies. Simulations show that we find for the SPATS with $\bar{n} = 0.49$, for our sample of 10^5 data points, negativities in the nonclassicality

quasiprobability with a significance of at least three standard deviations, if $\eta \geqslant 0.4$. This η value is only limited from below by the size of the sample. In contrast, for $\eta \leqslant 0.5$ the Wigner function is always nonnegative. Therefore, the negativities of the nonclassicality quasiprobabilities are more sensitive to nonclassical effects than negativities of the Wigner function.

V. SUMMARY AND CONCLUSIONS

We have applied the concept of nonclassicality quasiprobabilities to experimental data of single-photon-added thermal states. Even though the Glauber-Sudarshan P function of these states is regular in general, its approximate reconstruction is feasible only for a certain parameter range. Moreover, it requires one to make use of some precognition on the state under study. Our quasiprobability approach does not require such a precognition; it works for any quantum state—even when the P function is strongly singular—and it also suppresses the experimental sampling noise.

We have shown that the nonclassicality filters needed in our procedure suppress the exponential growth of experimentally determined characteristic functions, which yields integrable functions. Hence, Fourier transform delivers nonclassicality quasiprobabilities with finite statistical uncertainties. By optimization of the filter width, significant negativities in the quasiprobabilities are found for nonclassical states. For our chosen example, an approximate reconstruction of the P function was shown to be no longer useful.

With the accessible set of 10^5 data points we could demonstrate negativities in the experimentally determined nonclassicality quasiprobability with a significance of about 15 standard deviations. This result is solely limited by the statistical uncertainties caused by the finite size of the available set of experimental data, it could be further improved by extending this set. We have also considered the role of imperfect detection. In fact, the detection efficiency can be completely eliminated by a proper rescaling of arguments in our functions. Thus, even with a rather small efficiency one can identify all nonclassical effects, provided the sampling noise is sufficiently small.

ACKNOWLEDGMENTS

This work was supported by the Deutsche Forschungsgemeinschaft through SFB 652, and partially supported by Ente Cassa di Risparmio di Firenze and Regione Toscana under project CTOTUS.

[1] U. M. Titulaer and R. J. Glauber, Phys. Rev. **140**, B676 (1965).
[2] R. J. Glauber, Phys. Rev. **131**, 2766 (1963).
[3] E. C. G. Sudarshan, Phys. Rev. Lett. **10**, 277 (1963).
[4] G. S. Agarwal and K. Tara, Phys. Rev. A **46**, 485 (1992).
[5] T. Kiesel, W. Vogel, V. Parigi, A. Zavatta, and M. Bellini, Phys. Rev. A **78**, 021804(R) (2008).
[6] C. K. Hong and L. Mandel, Phys. Rev. Lett. **54**, 323 (1985).
[7] A. Rivas and A. Luis, Phys. Rev. A **79**, 042105 (2009).
[8] E. V. Shchukin and W. Vogel, Phys. Rev. A **72**, 043808 (2005).
[9] T. Richter and W. Vogel, Phys. Rev. Lett. **89**, 283601 (2002).
[10] A. Zavatta, V. Parigi, and M. Bellini, Phys. Rev. A **75**, 052106 (2007).
[11] T. Kiesel and W. Vogel, Phys. Rev. A **82**, 032107 (2010).
[12] G. S. Agarwal and E. Wolf, Phys. Rev. D **2**, 2161 (1970).
[13] A. I. Lvovsky, H. Hansen, T. Aichele, O. Benson, J. Mlynek, and S. Schiller, Phys. Rev. Lett. **87**, 050402 (2001).
[14] A. Zavatta, S. Viciani, and M. Bellini, Phys. Rev. A **70**, 053821 (2004).
[15] A. Zavatta, S. Viciani, and M. Bellini, Science **306**, 660 (2004).
[16] A. Zavatta, V. Parigi, M. S. Kim, and M. Bellini, Science **317**, 1890 (2007).
[17] A. Zavatta, M. Bellini, P. L. Ramazza, F. Marin, and F. T. Arecchi, J. Opt. Soc. Am. B **19**, 1189 (2002).
[18] F. T. Arecchi, Phys. Rev. Lett. **15**, 912 (1965).
[19] V. Parigi, A. Zavatta, and M. Bellini, J. Phys. B **42**, 114005 (2009).

PHYSICAL REVIEW A **83**, 062319 (2011)

Entangled qubits in a non-Gaussian quantum state

T. Kiesel and W. Vogel
Arbeitsgruppe Quantenoptik, Institut für Physik, Universität Rostock, D-18051 Rostock, Germany

B. Hage
ARC Centre of Excellence for Quantum-Atom Optics, Department of Quantum Science, The Australian National University, Canberra, Australian Capital Territory 0200, Australia

R. Schnabel
Institut für Gravitationsphysik, Leibniz Universität Hannover and Max-Planck-Institut für Gravitationsphysik (Albert-Einstein-Institute), Callinstrasse 38, D-30167 Hannover, Germany

(Received 3 December 2010; published 14 June 2011)

We experimentally generate and tomographically characterize a mixed, genuinely non-Gaussian bipartite continuous-variable entangled state. By testing entanglement in 2×2-dimensional two-qubit subspaces, entangled qubits are localized within the density matrix, which, first, proves the distillability of the state and, second, is useful to estimate the efficiency and test the applicability of distillation protocols. In our example, the entangled qubits are arranged in the density matrix in an asymmetric way, i.e., entanglement is found between diverse qubits composed of different photon number states, although the entangled state is symmetric under exchanging the modes.

DOI: 10.1103/PhysRevA.83.062319 PACS number(s): 03.67.Mn, 03.65.Ud, 03.65.Wj

I. INTRODUCTION

Since the early days of quantum mechanics, entanglement has been a topic of great interest [1,2]. Today, it is considered as the key resource for many applications, such as quantum computation, quantum communication, and quantum cryptography—for recent reviews, cf. Refs. [3] and [4]. Last but not least, nowadays the relevance of entanglement is even discussed in the context of life sciences—cf., e.g., Ref. [5]. Traditionally there is a distinct treatment of entanglement in two different regimes, the discrete variable regime being based, for instance, on qubits, and the continuous-variable (CV) regime having either Gaussian or non-Gaussian statistics, respectively. However, both regimes are connected to each other, since qubits can be constructed out of CV states [6], and, vice versa, entangled CV states may be composed of entangled qubits.

A quantum state is referred to as being entangled if it cannot be written as a statistical mixture of factorizable (uncorrelated) quantum states [7]. Although this definition is intuitively clear, it is hard to check in practice for general quantum states. For the case of CV states the Peres condition verifies an important class of entanglement by partial transposition (PT) of the density matrix [8]. The special case of Gaussian entangled states can be fully characterized by moments of second order [9,10]. Gaussian states are easy to prepare and it is easy to identify their entanglement. However, their application in quantum technology is limited. Non-Gaussianity of CV entangled states can be considered as a resource, which is of great interest for various applications in quantum information technologies. A general reformulation of the Peres criterion yields a hierarchy of inequalities in terms of observable moments of arbitrarily high orders [11,12]. Recently, on this basis, *genuine* non-Gaussian entanglement, being invisible in second moments of the field quadratures, could be experimentally demonstrated [13].

PT entanglement tests are necessary and sufficient for bipartite entanglement in very special cases only: for Hilbert spaces of dimension 2×2 and 2×3 and for Gaussian CV quantum states—cf., e.g., Refs. [3] and [4]. Entanglement of general states can be verified by involved generalizations of the PT tests [14], or, based on entanglement witnesses [15], by optimized entanglement conditions [16]. However, it has been proven that for any entangled state there exist subspaces of finite dimension in which the entanglement already exists [17]. A systematic search for these subspaces provides the ability to uncover the structure of the entanglement. In particular, the identification of these entangled subsystems may be helpful for designing protocols for the entanglement distillation, which extracts, in the ideal case, a maximally entangled state from the given mixed state, providing advantages in many quantum information tasks [3].

In the present paper we study the entanglement of a CV quantum state, experimentally created by mixing a fully phase-randomized squeezed vacuum state by a balanced beam splitter with vacuum noise. We analyze the entanglement structure of this decohered nonclassical state by PT tests on two-qubit subsystems. In this way, we extend the completeness of the Peres criterion for bipartite qubit systems to the detection of entanglement in arbitrary CV systems, and establish a link between entanglement in discrete variable and CV systems. Several entangled qubits within the density matrix are identified with an overwhelming statistical significance. Surprisingly, the entanglement is only found between qubits of diverse nature. A closer inspection shows that the entanglement of these qubits can be distilled by the protocol of Bennett *et al.* (BBPSSW) [18].

The paper is structured as follows: In Sec. II, we present the experimental setup and describe the state whose entanglement is analyzed. In Sec. III, we examine the detection of entanglement with Gaussian criteria, showing that they

are not applicable for our states. The search for entangled qubit subsystems is given in Sec. IV, and its use for choosing a suitable distillation protocol is discussed. A summary and some conclusions are given in Sec. V.

II. GENERATION OF A NON-GAUSSIAN ENTANGLED STATE

We start with a Gaussian squeezed-vacuum state being fully characterized by its variances V_x and V_p of the quadratures x and p, respectively, together with its orientation angle φ in phase space. To obtain a phase-independent non-Gaussian state, the orientation is uniformly distributed over a 2π interval. This state is not squeezed anymore, but still exhibits significantly nonclassical properties [19], which are necessary for the generation of entanglement. In the second step, we send the phase-randomized state to a balanced beam splitter where it is mixed with a vacuum mode. For a sketch of the experimental setup, see Fig. 1. The two output modes, which form the entangled state examined in this paper, are measured by joint balanced homodyne detectors. This scenario is equivalent to propagate an entangled two-mode squeezed vacuum through a medium preserving the phase difference but destroying the absolute phase, similar to the experiment in Ref. [20].

The squeezed mode was generated by a degenerate optical parametric amplifier (OPA). The OPA consisted of a type-I noncritically phase-matched second-order nonlinear crystal (7% Mg:$LiNbO_3$) inside a standing-wave optical resonator with a linewidth of 25 MHz. The OPA process was continuously pumped with second harmonic light at 532 nm. The resonator tuning was controlled via the common Pound-Drever-Hall method using phase-modulated fundamental light at 1064 nm. For technical reasons the pump phase was controlled such that the fundamental control field was deamplified, i.e., the OPA generated amplitude quadrature squeezing with respect to this field. With this setup we directly measured a squeezing variance of -4.8 dB and an antisqueezing variance of $+9.0$ dB, both with respect to the unity vacuum noise variance.

The squeezed field propagated in free space from the OPA passing high-reflection mirrors. In order to apply the phase diffusion two of these mirrors were moved by piezoelectric transducers (PZTs) driven by a quasirandom voltage. The

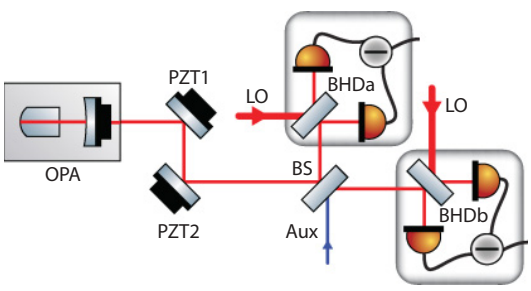

FIG. 1. (Color online) Simplified sketch of the experimental setup. LO: local oscillator; OPA: optical parametric amplifier (squeezed light source); BHD: balanced homodyne detector; PZT: piezoelectrically actuated mirror applying the phase noise. Aux: Frequency shifted weak field providing a readout for the difference of the detection phases of BHDa and BHDb.

driving signal was generated by a high quality PC sound card connected to appropriate filters and amplifiers. The sound card played back a previously generated sound file which was carefully designed to yield the desired phase distribution.

Balanced homodyne detection (BHD) was used to measure the quadrature amplitudes of the two-mode state under consideration. The visibility with the spatially filtered local oscillators were in the range of 98.5%–99%. Regarding the detection phases, the only meaningful figure is the difference between the detection phases of BHDa and BHDb because the state before the beam splitter (BS) is phase randomized. The control of this phase difference was achieved by injecting an auxiliary field into the open port of the beam splitter, which was frequency shifted with respect to the fundamental (LO) frequency. The demodulation of the BHD signal at the beat frequency provided an error signal for locking the detected quadrature angle to the phase of the auxiliary field, with an offset given by the electronic demodulation phase. The signals of the two individual BHD photodetectors were electronically mixed down at 7 MHz and low-pass filtered with a bandwidth of 400 kHz to address a modulation mode of the light showing good squeezing and a high dark noise clearance of the order of 20 dB. The resulting signals were fed into a PC-based data-acquisition system and sampled with one million samples per second and 14-bit resolution. For a more detailed description of the main parts of the setup we refer to Refs. [21] and [22] .

We obtained a set of 10^6 quadrature pairs per detection phase configuration, for ten equally spaced phases per output mode A and B. From these measurements, we estimated the density matrix elements of the state and their full covariance matrix via appropriate pattern functions—see the Appendix for details. Due to the central limit theorem, this yields the full statistical information about the experimental result.

The reconstructed density matrix of the measured state is shown in Fig. 2 for the first 5^4 density matrix elements in the Fock basis. Our reconstruction is restricted to the

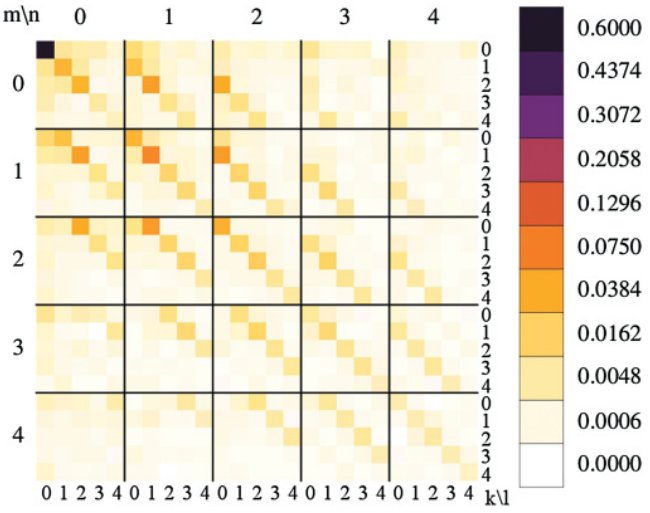

FIG. 2. (Color online) Reconstructed two-mode density matrix of the examined entangled state in the Fock basis. A block mn provides the absolute values of the density matrix elements $\rho_{kl,mn}$, where k,l refers to the photon numbers at BHDa, and m,n to those at BHDb.

seven lowest Fock states for each mode, and thus the full bipartite density matrix has a rank of $7 \times 7 = 49$. The trace of the reconstructed state is equal to 0.9836 ± 0.0002, such that the main information about the state is covered. The standard deviation of the single matrix entries is bounded by 0.0003. It is noteworthy that a higher-dimensional state reconstruction makes no sense for the entanglement test. Already a reconstructed matrix of rank 8×8 would consist of several entries that are no longer significant relative to the statistical error, as it is obtained for our sample. The result of the state reconstruction shows that all significant matrix elements are located on certain lines. Only matrix elements with $k + m = l + n$ contribute, having their origin in the action of the beam splitter on the Fock state $|k + m\rangle$ in the input state. The phase diffusion eliminates all coherences between Fock states in the input state.

III. GAUSSIAN ENTANGLEMENT CRITERIA

Entanglement of Gaussian states can be completely characterized by Simon's inequality [10]. Here we extend the notion of *Gaussian entanglement* to all quantum states for which the entanglement can be identified by the condition of Simon. This can be also the case for non-Gaussian states. Hence entangled states which cannot be identified by this condition will be denoted as *genuinely* non-Gaussian ones.

In the following we prove that Simon's condition for entanglement is equivalent to squeezing of the input state. Let us start from a quadrature covariance matrix of a bipartite state in block form,

$$V = \begin{pmatrix} A & C \\ C^T & B \end{pmatrix}, \tag{1}$$

with A, B being the covariance matrices of the subsystems, and define $J = \left(\begin{smallmatrix} 0 & 1 \\ -1 & 0 \end{smallmatrix}\right)$. The state itself does not have to be a Gaussian one, but we only examine its covariance matrix. A state is entangled if the following inequality is violated:

$$\det A \det B + \left(\tfrac{1}{4} - |\det C|\right)^2 - \mathrm{Tr} A J C J B J C^T J \geqslant \tfrac{1}{4}(\det A + \det B). \tag{2}$$

Let us assume that the covariance matrix of the initial state for the quadratures $\hat{x}_{\mathrm{in}}, \hat{p}_{\mathrm{in}}$ is given by

$$C = \begin{pmatrix} V_x & C_{xp} \\ C_{xp} & V_p \end{pmatrix}. \tag{3}$$

A beam splitter recombines the quadratures of this input field with the quadratures of vacuum to the quadratures of the two-mode output field $\hat{x}_3 = t\hat{x}_{\mathrm{in}} + r\hat{x}_{\mathrm{vac}}$, $\hat{x}_4 = -r\hat{x}_{\mathrm{in}} + t\hat{x}_{\mathrm{vac}}$, where the field transmissivity t and reflectivity r satisfy $|t|^2 + |r|^2 = 1$. Simon's criterion for the resulting covariance matrix leads to the following inequality for entanglement:

$$t^2(1 - t^2)[\left(V_p - \tfrac{1}{2}\right)\left(V_x - \tfrac{1}{2}\right) - C_{xp}^2] < 0. \tag{4}$$

Since $0 \leqslant t^2 \leqslant 1$, the term in square brackets has to be negative. In the following we show that this condition is equivalent to squeezing of the input state. The eigenvalues of the covariance matrix of the latter are the roots of the characteristic polynomial,

$$p(\lambda) = (V_x - \lambda)(V_p - \lambda) - C_{xp}^2. \tag{5}$$

The two roots $\lambda_{1,2}$ are the minimum and maximum quadrature variance of the state. A state is squeezed if for one of these roots we find $\lambda_1 < \frac{1}{2}$, while for the other we have $\lambda_2 > \frac{1}{2}$. This is the case if and only if $p(\lambda)$ is negative between both roots, i.e., $p(\frac{1}{2}) < 0$. This leads to

$$p\left(\tfrac{1}{2}\right) = \left(V_x - \tfrac{1}{2}\right)\left(V_p - \tfrac{1}{2}\right) - C_{xp}^2 < 0, \tag{6}$$

which is equivalent to Simon's condition for entanglement. Therefore, a beam splitter creates Gaussian entanglement if and only if the input state is squeezed. In this sense, one may state that Gaussian entanglement of the split state has its origin in Gaussian *nonclassicality* of the input state. We emphasize that this fact is not restricted to Gaussian states, but holds for arbitrary quantum states.

One can proceed with the analysis of higher-order moments. In Ref. [13], a criterion containing fourth-order moments was sufficient to demonstrate genuine non-Gaussian entanglement. For the studied states the Simon test, based on second-order moments, failed. In our case, one can show that one has to go to sixth-order moments for this purpose, which is a cumbersome task. Therefore, we propose an alternative way to verify non-Gaussian entanglement, which does not only verify the entanglement. In addition, it provides useful insight into the entanglement structure of the state.

IV. ENTANGLED QUBITS

Recently it has been been proven that any entangled quantum state must also be entangled in a finite-dimensional Hilbert space [17]. Therefore, it is sufficient to detect entanglement in a submatrix of the full density matrix. The Peres criterion states that for any separable state the partial transpose of the density matrix, defined by its matrix elements

$$\langle k,m|\rho^{\mathrm{PT}}|l,n\rangle = \langle k,n|\rho|l,m\rangle, \tag{7}$$

is positive semidefinite [8]. Hence, we may start to project the state onto an arbitrary two-qubit subsystem and calculate the eigenvalues of the partially transposed density matrix. If at least one of the latter is negative, the state has a negative partial transposition and entanglement has been verified by the Peres criterion. This test can be implemented efficiently, since a bipartite qubit subsystem can be described by a 4×4 matrix, which has only four eigenvalues. The statistical uncertainty $\sigma(\lambda_{\mathrm{min}})$ of the eigenvalue λ_{min} can be obtained by a Monte Carlo simulation: We draw random matrices, whose entries are chosen by a Gaussian distribution around the reconstructed state, with the covariance matrix as determined from the experimental data. With these simulated density matrices, which are consistent with the reconstructed state within its statistical uncertainties, we calculate the set of least eigenvalues. From the statistics of the results we can estimate the standard deviation of our experimental entanglement test. We note that whenever such a test fails for two-qubit subsystems it may be successful in subsystems of higher dimensions.

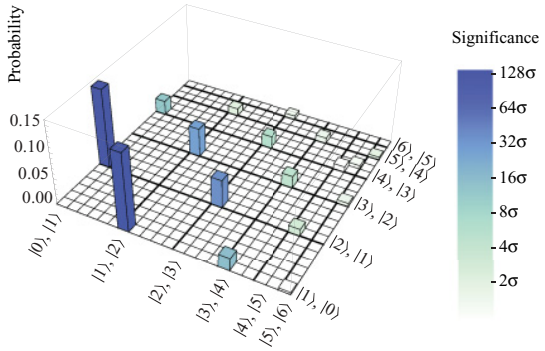

FIG. 3. (Color online) Probabilities for the occurrence of entangled two-qubit subspaces. The statistical significance of the successful entanglement tests is color coded. It represents the smallest (negative) eigenvalue of the partially transposed state in units of the corresponding standard deviation σ.

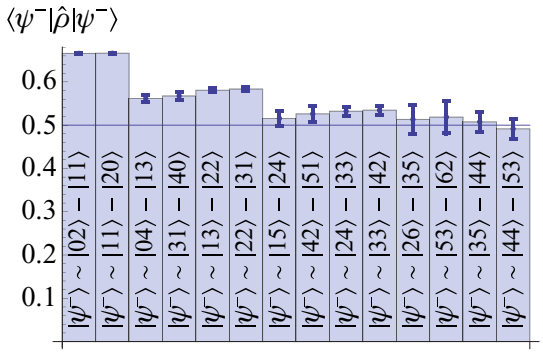

FIG. 4. (Color online) Probability of finding a singlet state $|\psi^-\rangle$ in a specific qubit subsystem.

This test has been performed for all possible qubit subsystems. In Fig. 3, all two-qubit subsystems with negative partial transpose are illustrated by the probability of their occurrence in the state and by the statistical significance, $\frac{\lambda_{\min}}{\sigma(\lambda_{\min})}$, of the smallest eigenvalue. For each mode, the qubit subsystems are ordered from $|0\rangle,|1\rangle$ to $|0\rangle,|6\rangle$, continuing with $|1\rangle,|2\rangle$ to $|1\rangle,|6\rangle$ and so on. Each of the two axes running over subsystem labels refer to one of the two modes. First, it is obvious that there is no symmetric subsystem which displays the entanglement. That is, if both modes are projected onto the same subsystem, no entanglement is indicated. However, projecting on different subsystems, such as the ones composed of the states $|0\rangle,|1\rangle$ in one mode and $|1\rangle,|2\rangle$ in the other, gives states whose entanglement can be verified with significance up to 128 standard deviations. In total, we find ten asymmetric pairs of qubits whose entanglement has a statistical significance of more than two standard deviations. The asymmetry is remarkable, since the state itself is symmetric with respect to both modes. The knowledge of the structure of the entanglement of a given mixed quantum state, in particular the identification of the localization of entangled qubits within a complex CV state, is essential for applications.

Since we find entangled two-qubit subsystems in the state under study, our results clearly show that entanglement distillation is possible. Now the question for a suitable protocol arises. One scheme, which works for any two-qubit state, has been given in Ref. [23]. Our method as presented here identifies appropriate two-qubit Hilbert subspaces. Any subspace in which entanglement is found may be chosen for distillation. The higher the probability of occurrence of the subsystem in the full state, the more efficient is the distillation.

For some entangled qubits, one can directly apply the BBPSSW protocol [18]. Let us have a look at the fidelity of a singlet state with respect to the experimentally generated one within the chosen two-qubit subspace. A singlet in this two-qubit space is defined as $|\psi^-\rangle = \frac{1}{\sqrt{2}}(|i_A,j_B\rangle - |j_A,i_B\rangle)$, where $|i_A\rangle,|j_A\rangle$ and $|i_B\rangle,|j_B\rangle$ are Fock states forming a basis for the qubit systems in the modes A and B, respectively. If the fidelity between the state and the singlet,

$$F = \langle\psi^-|\hat{\rho}|\psi^-\rangle, \tag{8}$$

is greater than $\frac{1}{2}$, the BBPSSW protocol can be directly applied to distill the state. In Fig. 4, the fidelities for the subsystems of interest are shown. Obviously, several subspaces have a fidelity which is significantly larger than $\frac{1}{2}$ being suitable for the application of the BBPSSW protocol.

V. SUMMARY AND CONCLUSIONS

We have demonstrated an efficient method to examine the entanglement structure of CV quantum states using the example of a mixed, genuine non-Gaussian entangled state whose entanglement is invisible for Gaussian entanglement criteria. We have analyzed the two-qubit subsystems and found negative partial transpositions with large statistical significances of up to 128 standard deviations. Our method proves that the CV state under consideration is entangled and distillable.

A remarkable result of our analysis is that the decohered state under consideration *only* shows entanglement in two-qubit subsystems composed of *diverse* qubits, for instance, $|0\rangle,|1\rangle$ and $|2\rangle,|1\rangle$. Such an insight into the entanglement structure might be used to analyze the decoherence process that turned an initially pure entangled state into a mixed entangled one. Moreover, the knowledge of the entanglement structure is important for the development of proper filtering methods for the aim of entanglement distillation.

ACKNOWLEDGMENTS

The authors are grateful to J. Sperling, J. DiGuglielmo, and A. Samblowski for fruitful discussions and their assistance. This work was supported by the Deutsche Forschungsgemeinschaft through SFB 652 and the Centre for Quantum Engineering and Space-Time Research, QUEST.

APPENDIX : RECONSTRUCTION OF THE DENSITY MATRIX

We obtained a set of $N = 10^6$ quadrature pairs $\{x_j(\phi_{j_A}),y_j(\phi_{j_B})\}_{j=1}^N$ data points per phase configuration, for $N_\phi = 10$ equally spaced phases $\phi_{j_{A,B}} = \frac{j_{1,2}\pi}{10}$ per output mode

A,B. From these measurements, we estimated the density matrix of the state via appropriate pattern functions,

$$F^{(r)}_{kl,mn}(j,j_A,j_B) = \mathrm{Re}\{e^{i(k-l)\phi_{j_A}} f_{kl}(x_j(\phi_{j_A})) \times e^{i(m-n)\phi_{j_B}} f_{mn}(y_j(\phi_{j_B}))\}, \quad \text{(A1)}$$

$$F^{(i)}_{kl,mn}(j,j_A,j_B) = \mathrm{Im}\{e^{i(k-l)\phi_{j_A}} f_{kl}(x_j(\phi_{j_A})) \times e^{i(m-n)\phi_{j_B}} f_{mn}(y_j(\phi_{j_B}))\}, \quad \text{(A2)}$$

where $f_{kl}(x)$ has been taken from Ref. [24]. The superscripts (r), (i) indicate the real and imaginary parts of the pattern functions. Then the real and imaginary part of the density matrix elements $\rho_{kl,mn} = \rho^{(r)}_{kl,mn} + i\rho^{(i)}_{kl,mn}$ are estimated as the empirical mean of $F_{kl,mn}(j,j_A,j_B)$:

$$\tilde{\rho}^{(r,i)}_{kl,mn} = \langle F^{(r,i)}_{mn,kl}(j,j_A,j_B)\rangle, \quad \text{(A3)}$$

where the brackets are symbols for

$$\langle F(j,j_A,j_B)\rangle = \frac{1}{N_\phi^2 N}\sum_{j_A=1}^{N_\phi}\sum_{j_B=1}^{N_\phi}\sum_{j=1}^{N} F(j,j_A,j_B). \quad \text{(A4)}$$

Of course, all diagonal elements of the density matrix are real: $\tilde{\rho}^{(i)}_{kk,mm} = 0$. Furthermore, the covariance matrix of all entries can be estimated in the standard way as

$$\mathrm{Cov}\left(\tilde{\rho}^{(r,i)}_{kl,mn}\tilde{\rho}^{(r,i)}_{k'l',m'n'}\right) = \frac{1}{N_\phi^2 N}\left[\left\langle F^{(r,i)}_{mn,kl}(j,j_A,j_B) \times F^{(r,i)}_{m'n',k'l'}(j,j_A,j_B)\right\rangle - \tilde{\rho}^{(r,i)}_{kl,mn}\tilde{\rho}^{(r,i)}_{k'l',m'n'}\right]. \quad \text{(A5)}$$

Since the quadrature pairs are identically and independently distributed for any fixed pair of phases ϕ_{j_A},ϕ_{j_B}, the sums over the pattern functions are Gaussian distributed due to the central limit theorem. Therefore, Eqs. (A3) and (A5) provide the full statistical information about the sampled density matrix.

[1] A. Einstein, B. Podolsky, and N. Rosen, Phys. Rev. **47**, 777 (1935).
[2] E. Schrödinger, Naturwiss. **23**, 807 (1935).
[3] R. Horodecki, P. Horodecki, M. Horodecki, and K. Horodecki, Rev. Mod. Phys. **81**, 865 (2009).
[4] O. Gühne and G. Tóth, Phys. Rep. **474**, 1 (2009).
[5] M. Arndt, T. Juffmann, and V. Vedral, HFSP J. **3**, 386 (2009).
[6] J. S. Neergaard-Nielsen, M. Takeuchi, K. Wakui, H. Takahashi, K. Hayasaka, M. Takeoka, and M. Sasaki, Phys. Rev. Lett. **105**, 053602 (2010).
[7] R. F. Werner, Phys. Rev. A **40**, 4277 (1989).
[8] A. Peres, Phys. Rev. Lett. **77**, 1413 (1996).
[9] L. M. Duan, G. Giedke, J. I. Cirac, and P. Zoller, Phys. Rev. Lett. **84**, 2722 (2000).
[10] R. Simon, Phys. Rev. Lett. **84**, 2726 (2000).
[11] E. Shchukin and W. Vogel, Phys. Rev. Lett. **95**, 230502 (2005).
[12] A. Miranowicz, M. Piani, P. Horodecki, and R. Horodecki, Phys. Rev. A **80**, 052303 (2009).
[13] R. M. Gomes, A. Salles, F. Toscano, P. H. Souto Ribeiro, and S. P. Walborn, Proc. Natl. Acad. Sci. U.S.A. **106**, 21517 (2009).
[14] A. C. Doherty, P. A. Parrilo, and F. M. Spedalieri, Phys. Rev. Lett. **88**, 187904 (2002).
[15] M. Horodecki, P. Horodecki, and R. Horodecki, Phys. Lett. A **223**, 1 (1996).
[16] J. Sperling and W. Vogel, Phys. Rev. A **79**, 022318 (2009).
[17] J. Sperling and W. Vogel, Phys. Rev. A **79**, 052313 (2009).
[18] C. H. Bennett, G. Brassard, S. Popescu, B. Schumacher, J. A. Smolin, and W. K. Wootters, Phys. Rev. Lett. **76**, 722 (1996).
[19] T. Kiesel, W. Vogel, B. Hage, J. DiGuglielmo, A. Samblowski, and R. Schnabel, Phys. Rev. A **79**, 022122 (2009).
[20] A. Fedrizzi *et al.*, Nat. Phys. **5**, 389 (2009).
[21] A. Franzen, B. Hage, J. DiGuglielmo, J. Fiurášek, and R. Schnabel, Phys. Rev. Lett. **97**, 150505 (2006).
[22] B. Hage, A. Samblowski, J. DiGuglielmo, A. Franzen, J. Fiurášek, and R. Schnabel, Nat. Phys. **4**, 915 (2008).
[23] M. Horodecki, P. Horodecki, and R. Horodecki, Phys. Rev. Lett. **78**, 574 (1997); **80**, 5239 (1998).
[24] U. Leonhardt, H. Paul, and G. M. D'Ariano, Phys. Rev. A **52**, 4899 (1995).

Direct Sampling of Negative Quasiprobabilities of a Squeezed State

T. Kiesel and W. Vogel
Arbeitsgruppe Quantenoptik, Institut für Physik, Universität Rostock, D-18051 Rostock, Germany

B. Hage
ARC Centre of Excellence for Quantum-Atom Optics, Department of Quantum Science, The Australian National University, Canberra, Australian Capital Territory 0200, Australia

R. Schnabel
Institut für Gravitationsphysik, Leibniz Universität Hannover and Max-Planck-Institut für Gravitationsphysik (Albert-Einstein-Institute), Callinstrasse 38, 30167 Hannover, Germany

Although squeezed states are nonclassical states, so far, their nonclassicality could not be demonstrated by negative quasiprobabilities. In this work we derive pattern functions for the direct experimental determination of so-called nonclassicality quasiprobabilities. The negativities of these quantities turn out to be necessary and sufficient for the nonclassicality of an arbitrary quantum state and are therefore suitable for a direct and general test of nonclassicality. We apply the method to a squeezed vacuum state of light that was generated by parametric down-conversion in a second-order nonlinear crystal.

PACS numbers: 42.50.Dv, 42.50.Xa, 03.65.Ta, 03.65.Wj

Introduction. In quantum optics and quantum information science, the notion of nonclassicality describes the distinguished difference between classical and quantum physics. Here, a quantum state is referred to as nonclassical, if one is not able to model the outcomes of experimentally measured optical field correlation functions by classical electrodynamics. Considering solely pure states, the famous coherent states $|\alpha\rangle$ are the only classical states according to this notation, which makes them the closest analogue to the classical oscillator [1, 2]. Sudarshan [3] and Glauber [4] showed that the density operator of an arbitrary quantum state can formally be written as a statistical mixture of coherent states,

$$\hat{\rho} = \int d^2\alpha \, P(\alpha) \, |\alpha\rangle \, \langle\alpha| \, . \tag{1}$$

If $P(\alpha)$ resembles the properties of a classical probability function, the state is simply a classical mixture of the (classical) coherent states, e.g. a thermal state. In general, the P function may attain negative values – often in connection with a strongly singular behavior. In such cases the corresponding quantum state is referred to as a nonclassical one [5].

The main problem of this definition of nonclassicality lies in the singularities of the P function, which definitely prevent the experimental reconstruction of $P(\alpha)$. Only for special quantum states one may approximately obtain this quasiprobability [6]. Therefore, different criteria for the detection of nonclassicality have been developed. Some of them are simple, such as squeezing [7], classical limits on probabilities [8] or negativities in the Wigner function [9], but they are only sufficient for nonclassicality. Others are necessary and sufficient, but they consist of an infinite hierarchy of inequalities [10, 11]. Recently, nonclassicality quasiprobabilities have been introduced, which provide a complete and simple method for the verification of nonclassicality [12]: For any nonclassical state, there exists a regular nonclassicality quasiprobability, whose negativities unambiguously reflect its nonclassicality. In [13], the experimental applicability, as a matter of principle, was demonstrate on a nonclassical but less problematic state, which also had a negative Wigner function.

In this Letter, we prove the nonclassicality of a Gaussian squeezed state by reconstructing negative quasiprobabilities from data taken by a balanced homodyne detector. We avoid any Fourier transformation of the data, which was used in [13] and present a method of direct sampling of nonclassicality quasiprobabilities from the measured data. For this purpose, we use the concept of pattern functions [14], which provide an estimate of the quasiprobability together with its variance. This method applies to the experimental characterization of nonclassicality of arbitrary quantum states, the only limitation being statistical uncertainties.

Quasiprobabilities of squeezed states. Squeezed states are prominent examples of nonclassical states, which can be easily generated in the laboratory. Although nonclassicality is defined by negativities of the P function, its general verification by negativities of any commonly used quasiprobability distribution is impossible. For instance, the Wigner function of a squeezed state with quadrature variances V_x and V_p reads as

$$W_{\mathrm{sv}}(x,p;\varphi) = \frac{1}{2\pi\sqrt{V_x V_p}} \exp\left\{ -\frac{x_\varphi^2}{2V_x} - \frac{p_\varphi^2}{2V_p} \right\}, \tag{2}$$

clearly being a Gaussian. In contrast, the P function may formally be written as

$$P_{\mathrm{sv}}(\alpha) = e^{-\frac{V_x - V_p}{8}\left(\frac{\partial^2}{\partial\alpha^2} + \frac{\partial^2}{\partial\alpha^{*2}} - 2\frac{V_x+V_p-2}{V_x-V_p}\frac{\partial}{\partial\alpha}\frac{\partial}{\partial\alpha^*}\right)}\delta(\alpha), \tag{3}$$

representing one of the most singular representations of a quantum state, with infinitely high orders of derivatives of the

δ-distribution. Moreover, the s-parameterized quasiprobabilities [15] of a squeezed state are either Gaussian (and nonnegative) or strongly singular. Based on a simple condition for the characteristic function of the P function [16], the nonclassicality can be easily verified [17]. However, this condition is sufficient only and the question remains if there exists any well-behaved quasiprobability, allowing a complete characterization of the nonclassicality of squeezed states by the failure of being interpreted as a classical probability.

Nonclassicality quasiprobabilities. The starting point of our discussion is the characteristic function of the P function,

$$\Phi(\beta) = \langle : e^{\beta\hat{a}^\dagger - \beta^*\hat{a}} : \rangle = \langle e^{i|\beta|\hat{x}(\arg\beta - \pi/2)} \rangle e^{|\beta|^2/2}, \quad (4)$$

with $\hat{x}(\varphi)$ being the quadrature operator of the optical field at phase φ. In order to obtain a regular phase-space distribution, we filter $\Phi(\beta)$ in the form

$$\Phi_\Omega(\beta) = \Phi(\beta)\Omega_w(\beta). \quad (5)$$

The filter $\Omega_w(\beta)$ has to satisfy the following conditions to be useful for nonclassicality detection [12]:

1. The filtered characteristic function $\Phi_\Omega(\beta)$ should be integrable for an arbitrary quantum state, such that its Fourier transform – the nonclassicality quasiprobability – exists as a regular function.

2. Negativities in the Fourier transform of $\Phi_\Omega(\beta)$ shall unambiguously be due to the nonclassicality of the state. Conversely, the nonclassicality quasiprobability shall be nonnegative for any classical state. This requires that the filter $\Omega_w(\beta)$ has a nonnegative Fourier transform.

3. If the width parameter w approaches infinity, the filtered characteristic function $\Phi_\Omega(\beta)$ should converge to the characteristic function of the P function, $\Phi(\beta)$.

4. The filter should be nonzero everywhere, $\Omega_w(\beta) \neq 0$, such that no information about the quantum state is lost due to the filtering in Eq. (5).

Under these conditions, the nonclassicality quasiprobability is defined as the Fourier transform of the filtered characteristic function,

$$P_\Omega(\alpha) = \frac{1}{\pi^2} \int d^2\beta e^{\alpha\beta^* - \alpha^*\beta} \Phi(\beta)\Omega_w(\beta). \quad (6)$$

In the present work, we construct a filter from the autocorrelation of the function $\omega(\beta) = \exp(-|\beta|^4)$,

$$\Omega_1(\beta) = \frac{1}{\mathcal{N}} \int d^2\beta' \omega(\beta')\omega(\beta' + \beta), \quad (7)$$

the normalization constant $\mathcal{N}$ is chosen to obey $\Omega_1(0) = 1$. The width is introduced via $\Omega_w(\beta) = \Omega_1(\beta/w)$. This filter satisfies all criteria mentioned above, for the proof see [12].

Derivation of a pattern function. Pattern functions provide an efficient technique to directly estimate a physical quantity together with its uncertainty. From balanced homodyne detection, we obtain quadrature values $x_j(\varphi)$ measured for certain phases φ. They obey the quadrature distributions $p(x;\varphi)$, which satisfy $\int p(x;\varphi)dx = 1$. The quadratures are normalized such that the vacuum quadratures have a variance $V_{\rm vac} = 1$. Now the nonclassicality quasiprobability $P_\Omega(\alpha)$ with a certain width parameter w is written as the statistical mean of the pattern function $f_\Omega(x,\varphi;\alpha,w)$, averaged over the quadrature distributions:

$$P_\Omega(\alpha) = \int_{-\infty}^{\infty} dx \int_0^\pi d\varphi \, \frac{p(x;\varphi)}{\pi} f(x,\varphi;\alpha,w). \quad (8)$$

For this purpose, we note that due to Eq. (4), the characteristic function of the P function of the state can be calculated from the quadrature distribution via

$$\Phi(\beta) = \int_{-\infty}^{\infty} dx \, p\left(x; \arg\beta - \tfrac{\pi}{2}\right) e^{i|\beta|x} e^{|\beta|^2/2}. \quad (9)$$

It is convenient to rewrite the integral in Eq. (6) in polar coordinates $\beta = be^{i\varphi}$. Here, we restrict φ to $[0,\pi)$ and extend b to $(-\infty,\infty)$. Then we obtain

$$\begin{aligned} P_\Omega(\alpha) =& \frac{1}{\pi^2} \int_{-\infty}^{\infty} db \int_0^\pi d\varphi |b| e^{2i|\alpha|b\sin(\arg\alpha - \varphi)} \Phi(be^{i\varphi}) \\ &\times \Omega_w(be^{i\varphi}). \end{aligned} \quad (10)$$

The filter is chosen to be independent of the phase, i.e. $\Omega_w(be^{i\varphi}) \equiv \Omega_w(b)$. Now we insert Eq. (9) and obtain

$$\begin{aligned} P_\Omega(\alpha) = & \int_{-\infty}^{\infty} dx \int_0^\pi d\varphi \, \frac{p(x;\varphi)}{\pi} \int_{-\infty}^{\infty} db \, \frac{|b|}{\pi} e^{ibx} e^{b^2/2} \\ &\times e^{2i|\alpha|b\sin(\arg\alpha - \varphi - \frac{\pi}{2})} \Omega_w(b). \end{aligned} \quad (11)$$

This equation defines the pattern function

$$\begin{aligned} f_\Omega(x,\varphi;\alpha,w) = & \int_{-\infty}^{\infty} db \, \frac{|b|}{\pi} e^{ibx} e^{2i|\alpha|b\sin(\arg\alpha - \varphi - \frac{\pi}{2})} \\ &\times e^{b^2/2} \Omega_w(b), \end{aligned} \quad (12)$$

which has to be used in Eq. (8).

Equation (8) gives rise to the following interpretation: Suppose we have measured N quadrature-phase pairs (x_i, φ_i), whose joint probability distribution is $\frac{1}{\pi}p(x;\varphi)$. Here the phases φ are assumed to be uniformly distributed in $[0,\pi)$, while the quadratures obey the quadrature distribution $p(x;\varphi)$, conditioned on the value of the phase φ. Then the quasiprobability $P_\Omega(\alpha)$ can be calculated as the expectation value of the pattern function $f_\Omega(x,\varphi;\alpha,w)$. For experimental data, we replace the expectation value by its empirical estimate,

$$P_\Omega(\alpha) \approx \frac{1}{N} \sum_{i=1}^{N} f_\Omega(x_i, \varphi_i; \alpha, w). \quad (13)$$

Its variance can be obtained naturally as the mean square deviation of the numbers $f_\Omega(x_i, \varphi_i; \alpha, w)$.

If the phases, at which quadratures are measured, are scanned in $[0, \pi]$ or drawn randomly from a uniform distribution, one can calculate the nonclassicality quasiprobability directly as the empirical mean of the sampling function. This mean is taken over all pairs (x_i, φ_i) of quadrature and phase. In our experiment, we only obtained quadratures at 21 fixed phase angles. In this case, one may not simply replace the integral over the phase φ by a sum: This leads to systematic deviations, since the sampling function is varying rapidly with respect to the phase, in particular if $|\alpha|$ becomes large. For a detailed discussion and solution of this problem, we refer to the supplemental material [18].

Experimental set-up. The squeezed vacuum states of light were generated by type-I degenerate parametric down-conversion (optical parametric amplification, OPA) inside an optical resonator. The latter was a standing wave resonator with a line width of 25 MHz containing a non-critically phase matched second-order nonlinear crystal (7% Mg:$LiNbO_3$). The OPA process was continuously pumped by 50 mW of second harmonic light yielding a classical power amplification factor of six. Both, the length (resonance frequency) of the resonator as well as the orientation of the squeezing ellipse were stably controlled by electronic servo loops. With this setup we directly measured a squeezed variance of -4.5 dB and an anti-squeezed variance of +7.2 dB with respect to the unity vacuum variance. From these measurements we inferred an overall efficiency of 75% and an initial squeezing factor of -8.2 dB.

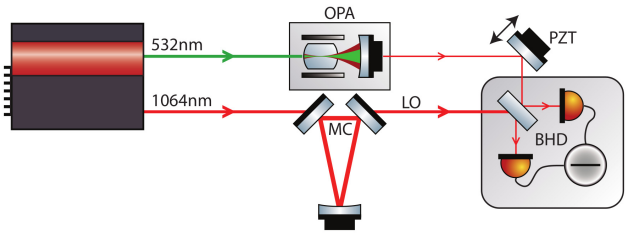

Figure 1. Simplified sketch of the experimental setup. A spatially filtered continuous-wave field at 1064 nm served as a local oscillator (LO) for balanced homodyne detection (BHD) and a phase-locked second harmonic field at 532 nm as the pump for the parametric squeezed light source (OPA). MC: spatial mode cleaner, PZT: piezo-electrically actuated mirror for adjusting the quadrature amplitude phase of the BHD.

The quadrature amplitudes of the squeezed state were measured by balanced homodyne detection (BHD). The visibility of the squeezed field and the spatially filtered (MC, Fig. 1) local oscillator was 98.9% and was limited by OPA crystal inhomogeneities. The quadrature phase of the BHD was adjusted by servo loop controlled micro-positioning of steering mirrors in one of the optical input paths. The photo-electric signals of the two individual BHD-photodiodes were electronically mixed down at 7 MHz and low pass filtered with a bandwidth of 400 kHz to address a mode showing good squeezing and a high detector dark noise clearance of the order of 20 dB. The resulting signals were fed into a PC based data acquisition system and sampled with one million samples per second and 14 bit resolution and finally subtracted yielding the quadrature amplitude data. For a more detailed description of the main parts of the setup we refer to [19, 20].

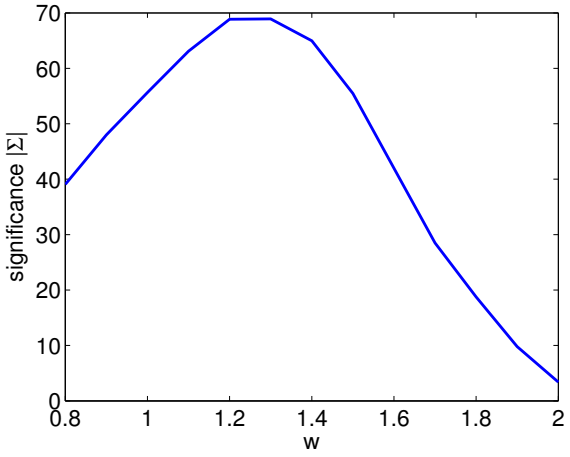

Figure 2. Absolute value of the significance $\Sigma(w)$ of the negativity of the quasiprobability versus the filter width w.

Experimental results. The examined squeezed vacuum state is characterized by the variances $V_x = 0.36$ and $V_p = 5.28$. We acquired 10^5 quadrature values for each of the 21 quadrature phases, the latter being equally spaced in $[0, \pi]$. The values of the quasiprobability $P_\Omega(\alpha)$ as well as their standard deviation $\sigma(P_\Omega(\alpha))$ are estimated from the pattern function as given in Eq. (12). The filter width is chosen such that the significance of the negativity is optimized. Our figure of merit is defined as

$$\Sigma(w) = \min_\alpha \left[\frac{P_\Omega(\alpha)}{\sigma(P_\Omega(\alpha))} \right], \tag{14}$$

with $\Sigma(w)$ being negative if $P_\Omega(\alpha)$ is negative for some α. The larger the absolute value of $\Sigma(w)$, the larger is the significance of the negativity. This quantity can be optimized with respect to w. In Fig 2, we show the dependence of the significance on the filter width w. The larger the filter width, the more nonclassical effects of the state are visible in negativities, but the more also the statistical uncertainty grows. Therefore, an optimum width exists, which is achieved for our data at $w = 1.3$.

Figure 3 shows the nonclassicality quasiprobability obtained from the experimental data. We find that along the axis of $\mathrm{Im}(\alpha)$, the quasiprobability oscillates and becomes clearly negative. This uncovers the nonclassicality of the squeezed state in a general sense, beyond the phase-sensitive reduction of the quadrature variance. It also includes information on other kinds of effects, such as higher-order squeezing of different types [11, 21], see also the experimental results in [17].

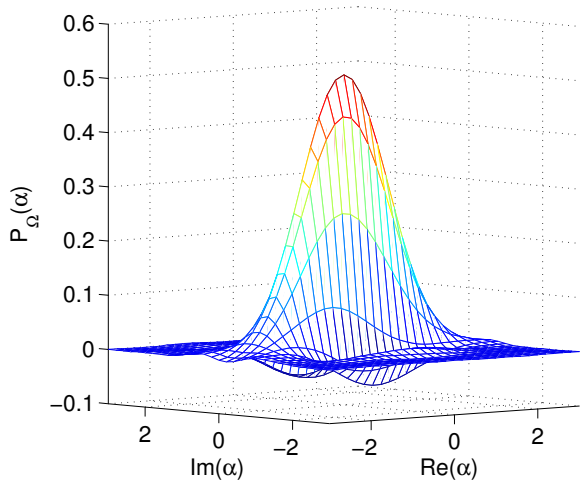

Figure 3. Nonclassicality quasiprobability for a squeezed vacuum state, which is directly sampled from our balanced homodyne data and clearly shows negative values.

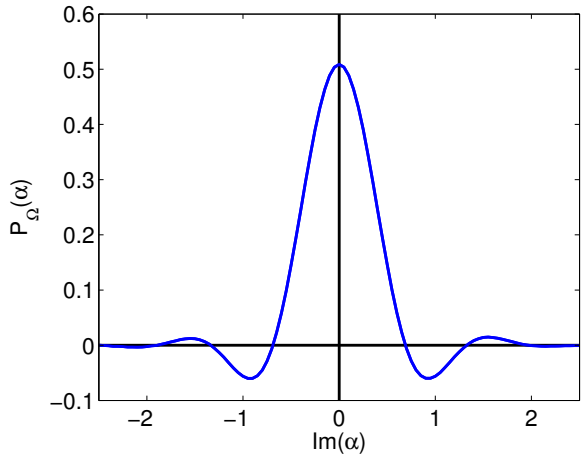

Figure 4. Cross section of the nonclassicality quasiprobability for our squeezed vacuum state. Note, that the uncertainty in the data is less than the line width chosen here.

In Fig. 4, we show a cross-section of Fig. 3 along the $\mathrm{Im}(\alpha)$-axis. We clearly observe distinct negativities. The standard deviation is less than 1.1×10^{-3} for all points and therefore covered by the width of the line. We also calculated a systematic error due to the finite set of examined phases, being less than 3.6×10^{-4} for all points along this axis [18]. $P_\Omega(\alpha)$ attains the minimum at $\alpha = 0.9i$ with $P_\Omega(\alpha_{\min}) = -0.05989$ and $\sigma(P_\Omega(\alpha_{\min})) = 0.9 \times 10^{-3}$, therefore leading to a significance of $|\Sigma| = 69$ standard deviations. Hence, this is a very clear demonstration of the nonclassicality of the examined state by means of negativities of a nonclassicality quasiprobability, which is not possible for commonly used quasiprobabilities such as the Wigner function.

Conclusions. In our work, we introduced a method for the direct sampling of nonclassicality quasiprobabilities of arbitrary quantum states from measured quadrature amplitudes. By applying our method to a squeezed state, whose P function belongs to the most singular ones, we experimentally verified nonclassicality in its general sense, i.e. through negative quasiprobabilities. Our method is not only capable of estimating the significance of the quasiprobability's negativity, but also its statistical uncertainties, in a surprisingly simple manner.

Acknowledgments. T. K. and W. V. gratefully acknowledge financial support by SFB 652.

[1] E. Schrödinger, Naturwiss. **14**, 664 (1926).
[2] M. Hillery, Phys. Lett. A **111**, 409 (1985).
[3] E. C. G. Sudarshan, Phys. Rev. Lett. **10**, 277 (1963).
[4] R. J. Glauber, Phys. Rev. **131**, 2766 (1963).
[5] U. M. Titulaer, and R. J. Glauber, Phys. Rev. **140**, B676 (1965).
[6] T. Kiesel, W. Vogel, V. Parigi, A. Zavatta, and M. Bellini, Phys. Rev. A **78**, 021804(R) (2008).
[7] D. F. Walls, Nature **306**, 141, (1983).
[8] A. Rivas and A. Luis, Phys. Rev. A **79**, 042105 (2009).
[9] A. Kenfack and K. Zyczkowski, J. Opt. B **6**, 396 (2004).
[10] T. Richter, and W. Vogel, Phys. Rev. Lett. **89**, 283601 (2002).
[11] E. V. Shchukin and W. Vogel, Phys. Rev. A **72**, 043808 (2005).
[12] T. Kiesel and W. Vogel, Phys. Rev. A **82**, 032107 (2010).
[13] T. Kiesel, W. Vogel, M. Bellini, and A. Zavatta, Phys. Rev. A **83**,032116 (2011).
[14] G. M. D'Ariano, C. Macchiavello, and M. G. A. Paris, Phys. Rev. A **50**, 4298 (1994).
[15] K. E. Cahill, and R. J. Glauber, Phys. Rev. **177**, 1857 (1969).
[16] W. Vogel, Phys. Rev. Lett. **84**, 1849 (2000).
[17] T. Kiesel, W. Vogel, B. Hage, J. DiGuglielmo, A. Samblowski, and R. Schnabel, Phys. Rev. A **79**, 022122 (2009).
[18] See supplemental material.
[19] A. Franzen, B. Hage, J. DiGuglielmo, J. Fiurášek and R. Schnabel, Phys. Rev. Lett. **97**, 150505 (2006).
[20] B. Hage, A. Franzen, J. DiGuglielmo, P. Marek, J. Fiurášek and R. Schnabel, New J. Phys. **9** 227 (2007).
[21] C. K. Hong and L. Mandel, Phys. Rev. Lett. **54**, 323 (1985).

Lebenslauf

Zur Person

Name:	Thomas Kiesel
Geburtsdatum:	7. Februar 1983
Geburtsort	Wismar
Familienstand:	verheiratet, ein Kind

Bildungsweg

1993 - 2002	Gerhart-Hauptmann-Gymnasium Wismar Leistungskurse Mathematik, Physik Abiturnote 1,0
2002 - 2003	Zivildienst bei der Wismarer Werkstätten GmbH, einer gemeinnützigen Einrichtung für Menschen mit Behinderung
2003 - 2008	Studium der Physik auf Diplom an der Universität Rostock Nebenfächer Mathematik sowie Informatik UNICERT III-Kurs Englisch mit Prädikat "Gut" Diplomabschluss nach neun Semestern mit Gesamtnote 1,0
2008-2011	Promotion in der AG Quantenoptik an der Universität Rostock über Nachweis nichtklassischer Effekte mit Hilfe von Quasiverteilungen

Forschungserfahrungen

Seit 2005	Mitarbeit in der Arbeitsgruppe Quantenoptik bei Prof. W. Vogel, Projektarbeit zur Zustandsrekonstruktion und Nichtklassizität, Zusammenarbeit mit Gruppen in Kopenhagen, Florenz und Hannover
Sommer 2006	sechswöchiges Praktikum am Max-Planck-Institut für Plasmaphysik in Greifswald, Aufbau und Justage eines Spektrometersystems zur Plasmadiagnostik
März 2007	vierwöchiger Forschungsaufenthalt bei Prof. E. Polzik am Niels-Bohr-Institut in Kopenhagen, Arbeit zur Zustandsrekonstruktion mit experimentellen Daten

Erklärung

Hiermit erkläre ich, dass ich die vorliegende Arbeit selbständig und ohne fremde Hilfe angefertigt, andere als die von mir angegebenen Quellen und Hilfsmittel nicht benutzt und die den benutzten Werken wörtlich oder inhaltlich entnommenen Stellen als solche kenntlich gemacht habe.

Rostock, 29. Juni 2011 Thomas Kiesel